國立台灣師範大學生命科學系碩士論文

以 SCA3 誘導細胞模式進行潛力新藥之篩選

Screening Novel Potential Therapeutic Drugs for Spinocerebellar Ataxia Type 3 through Inducible Cell system

研 究 生：陳 星 蓉

Hsing-Jung Chen

指導教授：謝 秀 梅 博士

Hsiu-Mei Hsieh

中 華 民 國 一 百 年 六 月

國立臺灣師範大學生命科學系碩士論文通過簽名表

系所別：生命科學系

姓名： 陳星蓉　　學號：699430096

碩士論文題目：Screening Novel Potential Therapeutic Drugs for Spinoerebellar Ataxia Type 3 through Inducible Cell system

經審查合格，特予證明

論文口試委員

王桂馨　博士
中央研究院生醫所助理研究員

林炎壽　博士
國立臺灣師範大學生命科學系助理教授

謝秀梅　博士
國立臺灣師範大學生命科學系副教授
論文指導教授

系主任（所長）簽章：

中 華 民 國 一百 年 六 月 十 日

致謝

這本論文的順利完成，真的受到了許多人的幫助，仔細回想起來，要感謝的名單真的太多太多了，只能用這篇小小的致謝來傳達我對曾經幫助我的所有人的大大感激。

首先要謝謝陪伴著我實驗生涯，抽許多時間與我討論實驗、給予我研究方向、資源、帶領我成為一個研究生的謝秀梅老師。謝謝您在這段時間為我所付出的一切，給我許多機會將我的實驗結果設計成海報參加大大小小的研討會，很多的修改再修改，討論再討論，因為有您的付出，我才能夠在這兩年有許多的學經歷和成長，也讓我更堅定我的研究目標。當然還有與老師如朋友般的聊天、嘻笑、B 計畫擂台賽一起的咖啡聊天聚會，也成為我碩士生涯中很難忘的回憶。真的很謝謝老師。

感謝帶領我從稚嫩到能獨當一面的孝修學長，從我什麼都不懂，每次報告前的推盤操演，實驗規劃設計，以及在大學時課業實驗兩頭燒時總會帶來意外的宵夜驚喜以及加油打氣，好友之間的玩樂談心，在你身上我學到了什麼叫做瘋狂忙碌瘋狂玩。看著在台下的你彷彿比我在台上還要緊張，以及我成功達到目標你比我還要開心的樣子，很感謝你在我身上所花的心思，我能順利的走到今天，真的也要好好地謝謝你這個後浪推手。

感謝所有 D309 的成員陪伴，讓我在實驗上有同伴能夠討論進步。謝謝雅津學姊平常對於實驗上給我的意見，很喜歡與您討論實驗以及論文，您總能給我許多不同的想法和做實驗的技巧。謝謝阿達學長總是幫助我們往返中研院以及每次提供我實驗上很有幫助的方法和技巧，當然還要感謝您高超的攝影技巧，實驗室在您的加入後，大家的照片都變得超級美麗的！謝謝蕙婷、高妹學姊在離開實驗室之後仍然給我許多實驗上的建議，讓我在 construct 實驗中能夠順利進行下來。謝謝君宇與峻緯在實驗上以及報告上給予我的建議以及支援。謝謝天駿、婉君、偉毅、興杰、智剛等學長姐們的陪伴以及許多建議，平常的你們也帶給實驗室許多的笑聲以及在實驗上所樹立的好榜樣。謝謝振銘平常在實驗上的陪伴、支援以及一起度過的每一個被報告壓迫的日子，回想起來總讓人會心一笑，當然還要感謝每次實驗做得很晚的夜晚，你貼心地幫我們大家買晚餐讓我們不用挨餓。謝謝玄峰、志長在 construct 實驗上給我的幫助以及在實驗上的建議，和課餘的聚餐。尤其要特別謝謝玄峰，在我實驗卡住許久都沒有結果時，常常關心我的困難和問題，幫助我在步驟上的修正，讓我的實驗可以順利進行。感謝我的同學：志謙以及彥旭一起修課討論報告應付考試的日子，以及一起參加研討會貼海報和報告的時光。以及感謝大學部的學弟妹：執中、紫綾、會妤、皇芹、賀強、健博、育晨，平常帶給

實驗室的歡樂以及給我實驗上的支援，因為有你們，我忙碌的時間也得以有稍微的喘息。貼心的會妤和健博也是我完成這本論文的大助力幫手，在這裡也要特別大力地感謝他們兩個！希望之後你們實驗路上可以順利。

最後要感謝我的爸爸媽媽，得忍耐長時間見不到孩子的孤單，也因為你們的支持和體諒，我才能有今天的榮耀，謝謝你們！

Abbreviations

Ac	acetylation
AD	Alzheimer's disease
ADCAs	autosomal dominant cerebella ataxias
AT3	ataxin 3
BDNF	brain-derived neurotrophic factor
CBP	cAMP response element-binding protein
DAPI	4,6-diamidino-2-phenylindole
DRPLA	dentatorubropallidoluysian atrophy
EcR	ecdysone receptor
EcRE	ecdysone-responsive element
FBS	fetal bovine serun
FDA	Food and Drug Administration
H_2O_2	Hydrogen peroxide
HAT	histone acetyltransferase
HD	Huntington's diaease
HDAC	histone deacetylases
HDACi	histone deacetylase inhibitors
HS	horse serum
Hsp	heat shock protein
htt	huntingtin
IC_{50}	half maximal inhibitory concentration
LDH	Lactate dehydrogenase
MCS	multiple cloning sites
MJD	Machado-Joseph disease

MTT	3-(4,5-Dimethylthiazol-2-yl)-2,5-diphenyltetrazolium-bromide
NAM	Nicotinamide
NGF	nerve growth factor
NIs	nuclear inclusions
nNOS	nitric oxide synthase
OD	absorbance density
polyQ	poly glutamine
ponA	ponastrone A
PVDF	polyvinylidene difluoride
ROS	reactive oxygen species
RXR	retinoid-X-receptor
SAHA	Suberoylanilide hydroxamic acid
SBMA	spinobulbar muscular atrophy
SCA3	spinocerebellar ataxia type 3
STAGA	SPT3-TAF9-ADA-GCN5 acetyltransferase
TBH	Tert-Butylhydroperoxide
TSA	Trichostatin A
UIM	ubiquitin interaction motifs
UPS	ubiquitin proteasome system
USP	ultraspiracle

INDEX

摘要

小腦脊髓運動失調症第三型(spinocerebellar ataxia type 3; SCA3)，亦稱 Machado–Joseph disease (MJD)，為小腦脊髓運動失調症眾多亞型中最常見的一型，屬於晚發性自體顯性遺傳的神經退化性疾病。主要是因為座落於 14q24.3-q32 的 MJD1 基因發生 CAG 三核苷酸過度擴增的現象，這些擴增的 CAG 序列會轉譯出含多麩醯胺酸(polyglutamine; polyQ)序列的蛋白質產物 ataxin3 (AT3)，突變的 AT3 會在細胞內聚集，透過蛋白質水解機制切割後，在細胞核內形成包含體(nuclear inclusions; NIs)產生細胞毒性使得細胞死亡。目前 SCA3 實際的致病機轉尚未明瞭，為了解 AT3 與 SCA3 病程中的致病機制，我們建立 AT3 誘導表現的 PC12 細胞模式。我們發現 75Q 細胞在氧化壓力以及蛋白質酶抑制劑處理過後會比 27Q 細胞更容易產生蛋白質聚集在細胞核以及細胞和周圍的現象，對於壓力藥物的耐受性也比 27Q 細胞要低許多。因此我們藉由建立的 SCA3 細胞模式做一系列新穎組蛋白去乙醯酶抑制劑(histone deacetylase inhibitors; HDACi)藥物篩選，結果發現某些抑制劑藥物確實能保護 SCA3 細胞，提升細胞存活率以及神經細胞分支生長，降低氧化壓力以及蛋白質聚集的現象，並增加組蛋白(histone)乙醯化及活化許多具神經保護性的訊息傳遞路徑例如 Hsp27、ERK、 MnSOD 和 NF-κB 等。因此，組蛋白去乙醯酶抑制劑藥物或許可成為治療 SCA3 的良好候選療法。

關鍵字：第三型脊髓小腦運動共濟失調症, 去乙醯化抑制劑, 氧化壓力, 神經退化性疾病

Abstract

Spinocerebellar ataxia type 3 (SCA3), also called Machado–Joseph disease (MJD), is an autosomal dominant neurodegenerative disease results from expanded CAG repeat of MJD1 gene. The CAG repeat expansion encodes polyglutamine (polyQ) stretch in mutant ataxin-3 protein and causes protein cleaved, insoluble, accumulated and aggregated in the neurons. These inclusions further elevate cellular oxidative stress and lead to cell death. We established inducible cell system expressing human full length ataxin-3 containing 27Q or 75Q in PC12 cells. Cells with 75Q ataxin-3 showed lower viability and more nuclear/peri-nuclear aggregation in stress environments. We tested several novel HDAC inhibitor (HDACi) compounds in the inducible SCA3 cells. Our results show that some HDACi could elevate cell viability, reduce aggregation and promote neurite outgrowth. We also observed that HDACi could increase histone acetylation and activate neuroprotective proteins, such as Hsp27, ERK pathway regulators, MnSOD and NF-κB. These findings indicate that some novel HDACi compounds might be potential for SCA3 treatment.

Keywords: Spinocerebellar Ataxia Type 3, HDACi, oxidative stress, neurodegenerative disease

Introduction

Spinocerebellar ataxias

Spinocerebellar ataxias (SCAs) or also named autosomal dominant cerebella ataxias (ADCAs) are groups of progressive hereditary and late onset neurodegenerative diseases. The prevalence of SCAs is three cases per 100,000 people and the average of diseases onset is approximate 39.19±11.88 years old (from 13 to 70 years old) (Harding, 1982; van de Warrenburg et al., 2002). The general clinical feature includes ataxia of gait and stance, dysmetria, oculomotor disturbances, facial impassivity, ophthalmoplegia, optic atrophy, cognitive impairment, sphincter disturbances and epilepsy (Harding, 1982; Schols et al., 2004). The age of disease onset and symptoms for children who suffer from SCAs are earlier and more severe than their parent. This phenomenon is called anticipation (Rosenberg, 1995). Based on the multiple types of gene mutation and clinical symptom, there are 31 types of SCAs have been found so far (Sato et al., 2009a), and could be classified into three major groups. The first group is caused by the expansion of CAG trinucleotide which encodes abnormal length of glutamine stretch in its protein product. These group diseases are called poly-glutamine (polyQ) diseases which include SCA1, 2, 3, 6, 7, 8 and 17. Besides SCAs, there are other polyQ neurodegenerative disorders, include Huntington's disease (HD), spinobulbar muscular atrophy (SBMA), and dentatorubropallidoluysian atrophy (DRPLA) (Trottier et al., 1995). The second group is caused by nucleotide expansion in noncoding region, which contain SCA8, 10 and 12. The other SCAs are not due to coding or noncoding region expansion,

but caused by gene missense/deletion/duplication/insertion or splice site mutations (Rosenberg, 1995; Manto, 2005; Sato et al., 2009a). There are various clinical feature and pathogenesis in each distinct subtype of SCAs.

PolyQ-mediated neurodegenerative disorder

SBMA is the first identified neurodegenerative disorder that caused by CAG trinucleotide expansion (La Spada et al., 1991). During these years, other nine associated neurodegenerative disorders have been discovered (HD, SCA1, 2, 3, 6, 7, 8, 17, and DRPLA) (Trottier et al., 1995). They are all autosomal dominance disorders. These diseases' progression and the age of onset mostly are depends on the length of polyQ tract, the more repeat number, the earlier onset and the more severe disease process. These polyQ mediate neurodegenerative disease showed repeat instability and anticipation as well, with increasing repeat numbers and disease severity in successive affected generations(Orr and Zoghbi, 2007; Netravathi et al., 2009; Sato et al., 2009b; Swami et al., 2009). The mechanism of polyQ repeat instability is still poorly understood. Some evidence indicated that the longer CAG repeat in DNA the higher instability in repeat numbers (Ranen et al., 1995; Rasmussen et al., 2007). There are many possibilities contribute to CAG repeat instability, one of the reasons is related to DNA metabolism. The CAG repeat number could be amplified during DNA replication, repair and recombination process (Pearson et al., 2005). In SCA1 transgenic mouse model, the intergeneration of CAG repeat transmission occurred after

meiosis but before fertilization. It's possible that the older age material DNA might accumulate higher DNA damage need to be repaired so that the higher possibility to influence the CAG repeat size then transmitted to the offspring (Kaytor et al., 1997). Therefore, the offspring inherited the more CAG repeat number than their parents, which lead to a more severe disease symptom in the later generations. This phenomenon is called anticipation.

The misfolded proteins which contain expansion polyQ stretch might be cleaved by caspase family or other proteases. After cleavage, the polyQ protein will recruit other protein to form insoluble aggregation in cytosome or nuclear inclusion (NI) (Kubodera et al., 2003; LaFevre-Bernt and Ellerby, 2003; Nucifora et al., 2003; Goti et al., 2004; Cong et al., 2006; Young et al., 2007). Several researches have indicated that those neuron cells which involve mutant polyQ expansion protein under higher oxidative stress, and further lead to cell death (Cowan et al., 2003; Kim et al., 2003; Miyata et al., 2008; Reina et al., 2010; Ryu et al., 2010). However, the pathogenesis of those polyQ diseases was still poorly understood, but there is a well known hypothesis indicated that mutant expansion protein aggregation or NI would produce reactive oxygen species (ROS) to elevate cells oxidative stress which will further induce cell apoptosis (Goswami et al., 2006b; Pandolfo, 2008). These finding indicated that there might be a tight relationship between oxidative stress and protein aggregated neurodegenerative disease. Thus, defining the correlation between polyQ-mediated protein aggregation disease and oxidative stress could be potential in developing of effective therapeutic

strategy to cure these diseases.

Spinocerebellar ataxia type 3 (SCA3)

Spinocerebellar ataxia type 3 (SCA3) or also called Machado–Joseph disease (MJD) is the most frequent type of SCAs in the worlds (Silveira et al., 1996;Jardim et al., 2001; Schols et al., 2004). The disease results from expanded CAG repeat in chromosome 14q32.1 at the MJD1 gene which encodes polyQ stretch in ataxin-3 (AT3) protein. SCA3 is a late onset progressive neurodegenerative disorder with a mean of age of onset 39.7±11.7 years old (van de Warrenburg et al., 2002). The clinical features included cerebella ataxia, spasticity, dystonia, ophthalmoplegia, sensory loss, muscle atrophy, faciolingual fasciculation, pyramidal and extrapyramidal dysfunctions and sleep disturbances. In neuron pathology, neuron loss in substantianigra, dentate nucleus, basal nuclei, pallidum, subthalamic and Purkinje cell layer in the cerebellum were found in SCA3 patients. However, there is wild-range variation in the disease phenotype of each SCA3 patient (Barbeau et al., 1984; Fowler, 1984; Rosenberg, 1992; Durr et al., 1996).As the general phenotype in polyQ disease, SCA3 is also experience anticipation and repeat instability, disease onset and process is highly relative to polyQ stretches (Limprasert et al., 1996). The normal polyQ repeat number in AT3 is 12 to 41, but it was found more than 41 polyQ repeat in SCA3 patients (Naito and Oyanagi, 1982; Kawaguchi et al., 1994). It has been reported that the repeat instability of SCA3 contributed to the loss of function of cAMP response element-binding protein (CBP)(Jung and Bonini, 2007). CBP is

a protein which could regulate DNA repair and also functions as a histone acetyltransferase (HAT) (Chan and La Thangue, 2001). The overexpansion of polyQ tract causes CBP loss of its normal function in DNA repair and HAT activity in transcriptional regulation. It might cause the impairment in DNA repair mechanism which further results in a higher repeat instability and more severe anticipation (Fortini, 2007). Thus it was suggested that the CAG expansions in SCA3 causes CBP loss of function that contributes to intergeneration polyQ toxicity cycle.

The function of AT3 has not been clearly understood, nevertheless, immunostaining from normal human's brain and in vitro model indicated that AT3 was distributed equally in whole neuron cells, especially in cytoplasm, but only mutant AT3 with expanded polyQ has aggregation formation in nuclear and cytosol (Paulson et al., 1997; Perez et al., 1998; Haacke et al., 2006; Rub et al., 2006). There are three domains in AT3 protein (appendix Fig. 1). The N terminal Josephin domain has ubiquitin protease activity which could remove the polyubuquitin chain on the ubiquitinated protein, and prevent the degradation of that protein (Burnett et al., 2003; Chai et al., 2004; Berke et al., 2005; Mao et al., 2005). The coiled-coil domain of AT3 is a common amino acid structure in protein. The third domain is poly-ubiquitin binding domain, which contained ubiquitin interaction motifs (UIM) so that AT3 could be recognized by ubiquitin. There are more than two UIM domains in AT3 (Berke et al., 2005). These structure characteristics of AT3 reveal that activity of ubiquitin proteasome system (UPS) was tightly associated with SCA3 pathology

UPS and SCA3

UPS played the central role in protein degradation; therefore, ubiquitinated proteins and proteasome components were detected in aggregation and NI (Chai et al., 1999;Burnett and Pittman, 2005;Bichelmeier et al., 2007; Wang et al., 2007a). It seems that the accumulated protein in cells might due to UPS dysfunction so that they could not be degraded successfully, this hypothesis could be supported by expression of dominant-negative mutant E4B, an UPS enzyme, and then AT3 aggregation was induced. On the other hand, overexpression of E4B colocalized with AT3 and promoted its clearance, ameliorated disease's progression (Matsumoto et al., 2004). These findings indicated that SCA3 patients possibly loss the normal function in UPS that induce SCA3 disease progression.

Oxidative and proteasomal stress

Many report mentioned that expanded polyQ tract could elevate cell's oxidative stress and ROS production. Also, cells with mutant polyQ expansion shows lower tolerance with oxidative stress. HD cells treated with oxidative drug such as H_2O_2 could accelerate aggregation formation (Goswami et al., 2006b). SCA3 cells were detected to have lower antioxidative enzyme expression, leading to mitochondria mediated apoptosis (Tsai et al., 2004; Yu et al., 2009). Oxidative drug treatment would promote AT3 aggregation and stimulate it enter nuclear, which resulted in cell toxicity (Reina et al., 2010). Base on these findings, we plan to use oxidative stress and proteasomal stress to induce a more

severe pathological condition or accelerate disease progression on our SCA3 cell model so we could use this system to screen several potential drugs.

Tert-Butylhydroperoxide (TBH)

TBH is a useful oxidative drug, it was wildly used in oxidative related research because of it could produce ROS and induce mitochondria depolarization, which further active cell apoptosis pathway (Maher and Hanneken, 2005; Zhao et al., 2005). Moreover, TBH would induct antioxidant enzyme expression, in order to protect itself from apoptosis (Pias et al., 2003).

Hydrogenperoxide (H_2O_2)

As TBH, H_2O_2 is also a long used oxidative stress drug. The molecular pathway of H_2O_2 was well understood, it could active lysosomal protease pathway and upregulate ERK1/2, JNK and several related protein levels (Crossthwaite et al., 2002; Lee et al., 2007; Veal et al., 2007). In SCA3 animal model, treat with H_2O_2 might make AT3 accumulate to form NI (Reina et al., 2010). Not only in SCA3, but also in other polyQ diseases such as SCA1 and HD, aggregation formation and neurodegeneration were also observed after H_2O_2 treatment (Kim et al., 2003; Du et al., 2009; Ryu et al., 2010).

MG-132

MG-132, a reversible proteasome inhibitor, could raise nitric oxide synthase (nNOS) level, cause ubiqutinated protein accumulation, and active caspase-3 mediated apoptosis pathway (Sun et al., 2006; Lam and Cadenas, 2008). In both HD and SCA3 animal and cell models, MG-132 would lead to aggregation and cell death (Wang et al., 2007a; Mishra et al., 2009). Overall, MG-132 would be a useful drug used to study the relationship of UPS and protein aggregation disease in our SCA3 cell model

Lactacystin

Lactacystin is also a proteasome inhibitor, but different from MG-132, Lactacystin is an irreversible proteasome inhibitor. Like MG-132, it was wildly utilized to study the relationship between protein aggregation disease and UPS (Ravikumar et al., 2002; Kim et al., 2004). Especially in SCA3, evidence indicated that full length AT3 needed longer time to be cleavaged by protease protein to fragment so that it could form aggregation and NI, but after treated lactacystin, AT3 could accumulated in the nucleus in a short time (Chai et al., 1999). Lactacystin might accelerate disease progression, could be a good stress drug used in our cell model.

Proteaolytics and transcriptional regulation of AT3

Besides ubiquitin, AT3 also interacts with caspase and histone associated protein, like HDAC3, CBP and p300 (Li et al., 2002; Berke et

al., 2004; Evert et al., 2006). It was reported that AT3 has caspase catalysis sequence and could be cut by caspase or other proteases (Berke et al., 2004). Compared to full length AT3, fragmented AT3 with expanded polyQ tract has higher toxicity to cells (Goti et al., 2004; Haacke et al., 2006). It was observed AT3 fragment presented in aggregation both *in vitro* and *in vivo* (Yoshizawa et al., 2000; Goti et al., 2004; Haacke et al., 2006). If inhibit mutant AT3 proteolysis by mutated the caspase interaction sequence or treated with caspase inhibitor, zVAD-fmk could retard neurodegeneration(Jung et al., 2009). According to these findings, inhibition of AT3 fragment formation would be a potential strategy to rescue neurodegeneration.

Additionally, AT3 could interact with HAT enzyme such as CREB-binding protein and p300 and HDAC3 which response for histone acetylation/deacetylation in order to regulate the gene expression (Li et al., 2002; Evert et al., 2006). The development in SCA3 disease progression might also contribute to that mutant AT3 caused the impairment in gene regulation.

Neuroprotective pathways in polyglutamine disease

Cells might do many responses in stress conditions in order to survive. For instance, misfolded protein would be recognized by ubiquitin molecular and targeted to proteasome for degradation (Goldberg, 2003), but before these proteins are degraded, heat shock protein (Hsp) family and several chaperones would tried to refold its conformation. If Hsp and chaperones failed to make the misfolded protein reorganized, USP

pathway will be activated to degrade the misfolded protein (Cashikar et al., 2005). PolyQ disease showed UPS dysfunction and lower Hsp family protein expression so that these misfolded proteins neither be refolded nor be degraded (Zourlidou et al., 2007; Chang et al., 2009; Williams et al., 2009; Yamagishi et al., 2010). Other evidences also supported this hypothesis; overexpressed Hsp family could protect neuron from degeneration and prevent protein aggregation in polyQ disease models. (Cashikar et al., 2005; Firdaus et al., 2006; Jorgensen et al., 2007; Lee do and Goldberg, 2010; Yamagishi et al., 2010).

Besides UPS, there is another protein clearance pathway called autophagy pathway. UPS depends on proteasome and autophagy relies on lysosome for protein degradation. When UPS failed to clean the aggregation protein, UPS would active autophagosome formation, the aggregation will be recruited and sent to lysosome (Iwata et al., 2005). In polyQ cell model, protein aggregation would active Atg12 and autophagosome to clean aggregation so cell death could be avoided (Kouroku et al., 2007). Rapamycin treatment could stimulate autophagy pathway by mTOR activation. HD mice and fly showed aggregation reduction and disease symptom improvement after Rapamycin treatment (Ravikumar et al., 2002; Ravikumar et al., 2004).

There was a research indicated that HD-accociated protein huntingtin (htt) could enhance brain-derived neurotrophic factor (BDNF) transport in microtubules (Gauthier et al., 2004). The mutant htt with expanded polyQ tract reduced BDNF level in several brain regions. The BDNF transcription would also be disrupted (Zuccato et al., 2001).

Overexpression of BDNF in HD brain could rescue HD disease progression (Xie et al., 2010). The hallmark of these polyQ mediated neurodegenerative disease was neuron loss in affected brain region. So that activation of cell survival pathway could also be a strategy against cell death from polyQ toxicity. The activation of ERK pathway was associated to cell survival. Cells with expanded polyQ tract in htt would activate ERK pathway in order to protect cell from polyQ toxicity (Apostol et al., 2006).

These observations suggest that there are several neuroprotective approaches could against polyQ mediate cell toxicity.

Histone deacetylase inhibitor (HDACi)

Histone acetyltransferases (HATs) and histone deacetylases (HDACs) perform a homeostasis in gene expression control. HAT enzyme functions in histone acetylation so that the gene's expression could be turned on. Different to HAT, HDAC would remove acetyl group from histone. Both HAT and HDAC played an important role in neuron cells; it could lead to neurodegenerative disease if the homeostasis was disrupted (Saha and Pahan, 2006). According to the sequence and structure homology, HDAC are classified into four classes (Gao et al., 2002). Class I HDACs include HDAC 1, 2, 3, and 8, which are expressed in most cell nuclei and control gene transcription (Butler and Bates, 2006). Class II HDACs are HDAC 4, 5, 6, 7, 9, and 10, which are tissue specific expression and show dynamic localization in cells. Class III HDACs are Sirt 1 to Sirt 7, and Class IV are HDAC11 (Gao et al., 2002).The interaction of HAT and HDAC regulates histone acetylation and chromatin structure, which lead to

influence on gene activity (Mathis et al., 1978; Grunstein, 1997).HDAC inhibitors (HDACi) are compounds could inhibit histone deacetylation. There are several researches support that HDACi compounds could be potential compounds in neurodegenerative disease. The first HDACi drug used to treat polyQ disease was Suberoylanilidehydroxamic acid (SAHA). It could rescue motor dysfunction, enter blood-brain barrier, turn on gene expression and retard HD symptom in both mice and fly models (Steffan et al., 2001; Hockly et al., 2003). Beside SAHA, there were many HDACi compounds discovered to have neuroprotective effect in polyQ disease, including Sodium Butyrate, Phenylbutyrate, Trichostatin A (TSA),Nicotinamide (NAM) (Ferrante et al., 2003; Dompierre et al., 2007; Jeong et al., 2009). TSA could improve CBP mediate repeat stability in SCA3 fly model (Jung and Bonini, 2007). HDACi treatment was also reported to elevate BDNF expression level and ease disease progression in HD (Dompierre et al., 2007). HDACi might function in protein posttranslational modification, too. The mutant htt was acetylated and autophagy degradation pathway was stimulated in the TSA and NAM treated cells (Jeong et al., 2009). HDACi also turned on many other neuroprotective gene expressions like MnSOD, Bcl-2, and Hsp family, and inhibited apoptosis pathway (Saha and Pahan, 2006; Uo et al., 2009). In SCA7, ataxin-7 is included in SPT3-TAF9-ADA-GCN5 acetyltransferase (STAGA) transcription coactivatior complex (Palhan et al., 2005). Mutant ataxin-7 which contained expansion polyQ region would inhibit HAT activity in STAGA and suppress the transcription (Palhan et al., 2005). SAHA and sodium butyrate could rescue HAT

activity and active gene transcription. (Palhan et al., 2005). Based on these evidences, HDACi compounds could be used as a potential drug in our SCA3 disease cell model and other polyQ mediate neurodegenerative diseases.

Rat adrenal pheochromocytoma (PC12) and SCA3 inducible cell system

PC12 is one of the common model cells used in neuron associated research. After nerve growth factor (NGF) treatment, PC12 had neurite extension (Greene and Tischler, 1976), dopamine and norephineprine neurotransmitters secretation, and MAP2, βⅢ-tubulin, and Tau expression (Esmaeli-Azad et al., 1994; Aletta, 1996; Davis and Johnson, 1999; Fontaine-Lenoir et al., 2006). These biochemical and morphological features were similar to neuron cells, and the pathway of NGF treated cell was extensively studied, so PC12 could be a suitable cell model for us to study neurodegenerative diseases.

In order to investigate how AT3 contributed to SCA3 and develop a platform for therapic potential compounds screen, we established an inducible AT3 expression PC12 cell model. The Complete Control Inducible Mammalian Expression System (Stratagene) was used to establish our SCA3 inducible system. The system contains two vectors, pERV3 and pEGSH. Plasmid pERV3 includes a gene encoding insect ecdysone hormone receptor, VgEcR and DNA response element, RXR. VgEcR would bind to RXR to form heterodimer and recognize E/GRE sequence in pEGSH. In lack of induction material, ecdysones, VgEcR binds to corepressor and inhibit downstream gene transcription. When

ecdysone's analog, ponastroneA (ponA) is applied, ponA could bind to VgEcR and change its structure so that corepressor becomes the bridge between VgEcR and other transcription factors, which could turn on the gene expression in pEGSH. We have human full length AT3 with normal (27Q) or expanded (75Q) polyQ tract inducible expressed by this system.

Truncated AT3 protein constructs in this study

As previously described, from the protein structure and amino acid sequence of AT3, it was suggested that AT3 might interact with UPS, caspase and HDAC6 proteins. Based upon the basis of the hypothesis that fragment AT3 is more toxic to cells (Goti et al., 2004; Haacke et al., 2006), we further generated inducible expression system in PC12 cell model with three truncated AT3 to compare to the full length AT3. We deleted N terminal 69, 219 and 257 amino acid of AT3 (c69, c219 and c257 represent for these three N terminal deletion construct) respectively, to investigate whether shorter form of AT3 could cause more toxic to PC12 cell. We could also examine the role of UIM motif, realize the function of Josephin domain and indentify the relationship of AT3 and UPS from these constructs. Moreover, we could also screen potential drugs with these truncated SCA3 cell model and accelerate the development of potential drugs for SCA3.

Materials and Methods

Cell culture

PC12 cells with inducible expression SCA3 constructs were maintained in 85% RPMI1640 (Gibco, Carlsbad, CA, USA) supplemented with 5% fetal bovine serum (FBS) and 10% horse serum (HS), containing 2 mM L-glutamine, 1% penicillin/streptomycin, 1 mM sodium pyruvate (Gibco), 4.5 g/L D-glucose, 1.5 g/L sodium bicarbonate, 1 M HEPES (Sigma, St. Louis, MO, USA), 100 μM/ml G418 (Gibco) and 50 μM/ml hygromycin B (Sigma), and were incubated in 5% CO_2 atmosphere at 37℃. Cells were grown in 0.01% poly-L-lysine (Sigma) coated dish and the culture media was changed every 48-72 hr.

Characterization of SCA3 inducible cell system

Complete Control® Inducible Mammalian Expression System (Strategene, Santa Clara, CA, USA) was applied to establish the SCA3 inducible cell model. The ecdysone receptor (EcR) is a member of the retinoid-X-receptor (RXR) family of nuclear receptors. In insect, EcR gather with nuclear receptor ultraspiracle (USP) to form heterdimer in order to regulate gene transcription. The receptor heterodimer binds to corepressors if absence of ecdysone, so that repressed gene expression. In the other words, the gene will be active transcribed only if ecdysone bounds to EcR, and the corepressor will release, then the coactivators will be recruited to the complex. EcR bound to RXR, the homologue of USP in mammalian cells to form heterodimer. The EcR–RXR heterodimer binds to multiple copies of the ecdysone-responsive element (EcRE).

PonA is the analog of ecdysone, such as the regulatory system in insect; in the absence of ponA, the gene will not activate its transcription (appendix Fig. 2).

Complete Control® Inducible Mammalian Expression System has two vectors. One is pERV3 receptor vector, which contains VgEcR and RXR under CMV promotor. VgEcR is the complex of EcR with VP16 activation domain. pERV3 also has G418 selection site (appendix Fig. 3A). Another is pEGSH expression vector, which contains five copies of the E/GRE recognition sequence and ponA-inducible expression cassette, multiple cloning sites (MCS) for insertion of interested DNA, flag epitope and hygromysin andampicillin antibiotics selection sites (appendix Fig. 3B). As previous described mechanism, after ponA treatment, the interested insert DNA will be activated for transcription.

Generation of truncated SCA3 constructs

The human full length SCA3 with 27Q and 75Q constructs were generated previously (Wang, 2007). We use the full length AT3 contained 27Q or 75Q DNA as a template to generate three different truncated AT3 by GC-RICH PCR System (Roche, South San Francisco, CA, USA). We could get different length of AT3 DNA fragments by coupled variant primers (Table 1). All of the forward primers contain Kozak sequence and *Bam*H1 cutting site. The backward primer includes*Xba*I cutting site. After PCR amplification, these DNA fragments were then subsequently subcloned into PGEM-T easy vector (Promega,

San Luis Obispo, CA, USA) and sequenced to check the enzyme junction and CAG repeat numbers. The 27Q and 75Q truncated AT3 fragments were then isolated from the pGEM-AT3 plasmids after digested with *Bam*H1 and *Xba*I and then subcloned to pEGSH vector. The pEGSH-AT3 constructs were then transfected into pERV3-bearing PC12 cells by Lipofectamine 2000 (Invitrogen, Carlsbad, CA, USA). 4 hrafter transfection, the culture medium was then changed from serum free to 5% HSand 10% FBS contained medium. The next day, transfected cells were selected by 100 μM/ml of G418 and 50 μM/ml of hygromycin B for one week and then single-cell seeded to 96 well poly-L-lysine coated culture plates to select stable cell line. The selected stable SCA3 inducible cells were examined by western blot in the presence of 1 mM of ponA (Merck, Whitehouse Station, NJ, USA).

Genotyping of SCA3 cells

Genomic DNA was extracted from SCA3cells by lysis solution (1 mg/ml proteinase K, 0.2% SDS, 0.2 M NaCl, 5 mM EDTA (pH 8.0), 0.1 M Tris (pH 7.4)) and incubated in 65℃ for 30 min to lyse cells and 75℃ for 20 min to stop proteinase K activity. Potassium acetate (2 M, Sigma) was then added to the extract and incubated at 4℃ for 30 min to precipitate protein, DNA was then eluted by 99.5% ethanol. The genotyping of our SCA3 cells was identified by PCR. After PCR amplification each DNA polyQ repeat fragment, 27Q was 252 bp and 75Q was 396 bp in the agarose gel electrophoresis results.

Stress drug treatment of SCA3 cells

Cells were seeded in 12-well plate or 6 cm dish at the density of 4×10^4 cells/ml (12-well plate) and 1×10^6 (6 cm dish). After 24 hr, cells were differentiated by treated with 50 ng/mL NGF (Millipore, Billerica, MA, USA) for 48 hr. The AT3 expression was induced by ponA (1 mM) and incubated with thefollowing stress drug at different concentration: TBH (20, 40 and 80 μM, Sigma); MG-132 (20, 40 and 80 nM, Sigma);lactacistin(1, 2, 2.5 and 3 μM, Calbiochem, Whitehouse Station, NJ, USA) and H_2O_2 (100, 200, 300 and 400 μM, Sigma) for 8 hr. Cell viability was examined by MTT assay and protein ubiquitination was identified by western blot.

Screening of novel HDACi compounds

Cells were seeded in 12-well plate, after differentiation by NGF (50 ng/mL) for 48 hr, AT3 expression was induced by ponA (1 mM) and oxidative stress drug TBH (40 μM) cotreatment was applied to the cells to accelerate disease progression. SAHA and 8 different HDAC inhibitors (L-BMX, L-1027, L-1209, TP extract, 0225, 0311, 0312, 0319; Nature Wise Biotech and Medicals Corporation; NBM, Taipei, Taiwan) were used individually to treat cells with the following concentration (0.25, 0.5, 1, 5 and 10 μM, respectively) for 48 hr (Figure 1). IC_{50} and related signaling pathways of each compound were characterized by MTT assay and western blot.

Cell viability and cell death assay

Cell viability was determined by 3-(4,5-Dimethylthiazol-2-yl)-2,5-

diphenyltetrazolium-bromide (MTT) assay (Sigma), which could change yellow MTT to purple formazan product in viable cells by the mitochondria enzyme succinate dehydrogenase. After culture, MTT reagent was added to the 12-well cells to a final concentration of 0.5 mg/ml and the reaction was then incubated at 37℃ for 20 min. The cell medium was removed and the purple crystallized formazan was dissolved by DMSO (Sigma). Finally, the absorbance density (OD) value at 570 nm of the reaction was observed on a multiwell scanning spectrophotometer.

Cell death was observed by Lactate dehydrogenase (LDH) assay. In general condition, LDH is a soluble enzyme which localizes in cytosol. It will be released from cells when plasma is damaged or lysed. The assay was performed by CytoTox-ONE^{TM} assay kit (Promega), based on the activity of LDH worked on its substrate lactate. The equations are: Lactate $^{+}$ + NAD^{+} → pyruvate + NADH; NADH + tetrazolium → NAD^{+} + formazan. 50 μl of cell culture medium (cell free medium was used as a blank, and total LDH release level in cells was measured with the culture medium treated with 9% Triton-X-100) was mixed with the same volumeof CytoTox-ONE^{TM}reagent and vortexed for 30 sec in 96-well plate. After incubation 10 min in room temperature, 25 μl of stop solution was added in each well and vortexed for 10 sec. Finally, the fluorescence with the excitation wavelength of 560 nm and an emission wavelength of 590 nm was detected by fluorescent microplate reader (Molecular Devices Gemini XPS, Molecular Devices, Orleans Drive Sunnyvale, CA, USA). And calculate the LDH release ratio of total cells over TBH treated cells.

Filter retardation assay

Cells were lysed in RIPA buffer (5 mM EDTA (pH 8.0), 10 mM Tris (pH 7.4), 150 mMNaCl, 0.1% SDS, 1% DOS, 1% NP40) with protease inhibitor cocktail (Halt™ Protease Inhibitor, Single-Use Cocktail EDTA-Free, Thermo) and incubated on ice for 30 min, the protein concentration was then quantified by BCA assay kit (Thermo, Waltham, MA, USA). Proteins (0, 10, 20, 30 μg) was diluted with0.1% SDS (in PBS) to a final volume of 200 μl. Each protein soultion was applied to 0.2 μmcellulose acetate membrane on a 96-well dot blot apparatus (BioRad, Hercules, CA, USA). The membrane was incubated with 0.1% SDS before the experiment. The membrane was then washed with 0.1% SDS twice by 96-well dot blot apparatus and blocked in 5% skim milk (in 0.05% TBST) for 2 hr at room temperature. After several washes in 0.05% TBST, the membrane was hybridized with 1C2 antibody at 4℃ overnight. The next day, membrane was incubated with secondary antibody at room temperature for 1 h and stained by ECL reagent (Millipore). The chemiluminescence was detected by LAS3000 (Fuji Corporation, Japan) and quantified by Multi Gauge software (Fuji Photo Film, Japan).

Western blot

Cells were lysed in RIPA buffer (5 mM EDTA (pH 8.0), 10 mM Tris (pH 7.4), 150 mMNaCl, 0.1% SDS, 1% DOS, 1% NP40) with protease

inhibitor cocktail (Halt™ Protease Inhibitor, Single-Use Cocktail EDTA-Free,Thermo) and phosphatase inhibitor (phosphatase inhibitor cocktail 1, Sigma) for 30 min on ice, centrifuged at 16000 g for 30 min and then collected the supernatant as the protein sample. Protein samples were separated by SDS- polyacrylamine gels (Bio-Rad) and transfered to 0.45 μm polyvinylidenedifluoride membrane (PVDF; Millipore). Membranes were blocked by 1% BSA or 0.05% skim milk in 0.05% TBST at room temperature for 2 hr. After three times washed in TBST, blot was incubated with the following primary antibodies (Table 2) at 4℃ overnight. The next day, the membrane was then probed with secondary antibody at room temperature for 1 hr after several washed in TBST, and visualized target protein by ECL reagent mix (Millipore), the chemiluminescence was detected by LAS3000 (Fuji Corporation). Western blot data were quantified by Multi Gauge (Fuji Photo Film).

Neurite outgrowth assays

PC12 cells were seeded on poly-L-lysine coated coverslips in six-well plates. 24 hr later, cells were treated with 50 ng/mL NGF for 48 hr to induce neurite extension. After drug treatment, the cells were washed by PBS, fixed with cold 4% paraformaldehyde (in PBS) for 5 min. After washed three times with 0.1% Triton X-100 in PBS for 10 min, we then permeabilized these cells with PBS containing 0.1% Triton-X-100 at 37℃ for 1 hr or 4℃ overnight. Subsequently, cells were incubated at 37 ℃ with Rhodamine-Phalloidin (1:100; Invitrogen) containing 0.1%

Triton-X-100 (in PBS) with light protection for 30 min to label the F-actin. 30 min later, we washed each cell contained coverslips by 0.1% Triton-X-100 in PBS and counterstained with 4,6-diamidino-2-phenylindole (DAPI) (1:10000; Sigma). After several wash, each coverslips was mounted by 50% glycerol in PBS, and visualized with confocal spectral microscope imaging system (Leica TCS SP2, Germany). The length of neurite was quantification by NeuronJ software (www.imagescience.org/meijering/software/neuronj/).

Immunocytochemistry

PC12 cells were grown on poly-L-lysine coated 25 mm coverslips in six-well plates. After differentiation and drug treatment as previously described, the cells were washed by PBS, fixed with cold 4% paraformaldehyde for 10 min, and washed three times with 0.1% Triton X-100 in PBS for 10 min. The cells were then blocked and permeabilized with PBS containing 5% FBS and 0.1% Triton X-100 at 37℃ for 1 hr or overnight at 4℃. Subsequently, cells were incubated at 4℃ overnight with primary antibody. After washed with 0.2% PBST 10 min for three times, the cells were incubated at 37℃ for 2 hr with fluorescent secondary antibody or dye under light protection. After extensive washing with 0.2% PBST, each coverslip was counterstained with DAPI (1:10000) and mounted with 50% glycerol in PBS. Images were observed with confocal spectral microscope imaging system (Leica TCS SP2) and High Content Micro-Imaging Acquisition and Screening System (Molecular

Devices), and image were captured on separate fluorescence channels, processed and assembled by Photoshop software (Adobe). The quantification of the aggregation was performed with Molecular Devices ImageXpress (Molecular Devices).

Mitochondria morphology analysis

Cells were treated withMitotracker green (1:1000, Invitrogen) and incubated at 37℃ for 30 min. After several washes with PBS, cell images were captured by confocal microscope imaging system (Leica TCS SP2). The quantification of mitochondria distribution and fluorescent intensity were perfrmed by using Molecular Devices ImageXpress (Molecular Devices).

Results

Maintaining inducible SCA3 cell lines

Inducible SCA3 cell models containing normal (27Q) and expanded (75Q) human full length AT3 was previously established in our lab (王, 2007).In order to check the CAG repeat number in each SCA3 cell lines, we used SCA3 repeat forward and reverse primers (Table 1) to amplify the DNA fragment containingthe CAG_nregion by PCR. The amplified products for cells with 27Q and 75Q are 252 and396 bp respectively (Figure 2A).

To analyzethe SCA3 inducible system, ponA was added to turn on the expression of human full length AT3. After 48 hr, each cells were lysed and examined the AT3 expression by western blot (Figure 2B). Rat endogenous AT3 was shown at 43 KD and inducible expressed human AT3 with 27Q and 75Q was observed at 48 and 60 KD only after ponA treatment.

These results indicated that our inducible SCA3 cell lines were not leaky and with correct CAG repeat numbers, which should be applicable models for us to process the following experiments.

SCA3-75Q cellshave lower tolerance to oxidative stress

SCA3 cells have been reported that they have lower antioxidative enzyme activity (Yu et al., 2009). Elevated oxidative stress in fibroblast cell isolated from SCA3 patient could promote AT3 nuclear inclusion body formation (Reina et al., 2010). To test the relationship between SCA3 pathogenesis and oxidative stress, we used H_2O_2 and TBH as

oxidative drugs and test cell viability by MTT and LDH assays after drug treatment. Cells with SCA3 27Q, 75Q or control vector (V) were seeded to 12-well plate, after differentiated by NGF and induced AT3 expression by ponA, oxidative stress was stimulated by 40 or 80 μM TBH for 48 hr. The cell viability was determined by MTT assay and the results showed that 75Q cells have lower cell viability than 27Q and V cells after TBH treatment (Figure 3A). We also used LDH assay to confirm the result of cell viability, as the result of MTT assay, 75Q cell showed higher LDH release amount than cells with 27Q or V (Figure 3B). To support this finding, we applied another oxidative drug, H_2O_2 to more clarify whether oxidative stress could accelerate SCA3 75Q cell disease progression. Cells were exposed to 100-400 μM H_2O_2 for 8 hr and their viability was then tested by MTT assay. We found the similar tendency which was observed in cells treated with TBH, 75Q cells decreased their cell viability after exposed to different concentration of H_2O_2 (Figure 3C).

Taken together, these data indicated that 75Q cell line was more sensitive to oxidative stress than 27Q and V cell lines, oxidative stress might be involved in SCA3 pathogenesis.

Proteasome inhibitor cause viability loss and UPS dysfunction in SCA3 75Q cells

Protein aggregation is a hallmark in SCA3 pathogenesis. Ubiquitin proteasome system (UPS) is a major mechanism to degrade abnormal proteins. In order to test whether proteasome stress could accelerate SCA3 progression, we applied MG-132 and lactacystin as proteasomal

stress drugs to SCA3 cells. Cell aggregation, ubuquitination and viability after proteasomal stress treatment were characterized. After differentiated by NGF, cells were treated with 20-80 nM of MG-132 for 24 hr and then cell viability was determined by MTT assay. We observed that 75Q cells showed lower tolerance to proteasomal stress (Figure 4A). Compared to V and 27Q cells, 75Q cells decreased cell viability with 40 nM of MG-132 and reached a significant reduction with 80 nM of MG-132 treatment. We also applied another proteasome inhibitor, lactacystion to the cells to confirm our result. 75Q cells showed a significant reduction in cell viability after 1 and2 μM of lactacystin treatment (Figure 4B). 27Q and V cell didn't show any significant change after lactacystin treatment. We analyzed SCA3 cell protein aggregation and ubiquitination level after proteasomal stress. SCA3 75Q cells were more ubiquitinated than 27Q and showed dose dependence to MG-132 for 24 hr (Figure 5). The same result was also found in cells treated with 2 μM of lactacystin for 8 hr, 75Q cells were more polyubitinated than 27Q cells, and form high molecular weight aggregation (Figure 6A). In order to understand whether proteasome stress could promote aggregation formation, we used immunofluorescence staining to detect aggregation after 2 μM lactacystin treatment for 24 hr. Compared to 27Q cell; 75Q cells showed perinuclear aggregation after exposed to lactacystin (Figure 6B).

Put together, these data indicate that SCA3 75Q cells were more sensitive to proteasomal stress, and showed lower cell viability and more aggregation formation than 27Q cells after exposed to proteasomal stress drugs.

Screening potential HDACi for SCA3 therapy using the inducible SCA3 cell model

It has been reported that HDACi could reduce polyQ toxicity and retard motor dysfunction in many polyQ diseases (Steffan et al., 2001; Ferrante et al., 2003; Hockly et al., 2003; Dompierre et al., 2007; Jeong et al., 2009). In order to know whether HDCAi was a candidate therapeutic drug forSCA3, we used our SCA3 cell model to screen several HDACi compounds which were synthesized by NBM. There were 8 HDACi compounds modified from SAHA. SAHA was reported that it could reduce polyQ toxicity in HD fly model, and it also was Food and Drug Administration (FDA) available drug in cancer therapy (Mann et al., 2007). We therefore tested whether SAHA and other 8 novel HDACi could work on our SCA3 cells. HDACi drug screening condition was conducted as previously described in material and method, we using TBH as the stress drug to accelerate our SCA3 cell disease progression to speed up the drug screen efficiency.

From cell viability result, SAHA showed slightly effective to our SCA3 cells, but cause high cell toxicity (Figure 7A). Next, we test the 8 novel HDACi compounds modified from SAHA. These drugs could be classified into three groups according to their effect on cell viability. The first group was specific to SCA3 75Q cells; these drugs could specially and significantly increase cell viability in 75Q cells, included L-1027, L-BMX, 0225 and 0319 (Figures 7B-E). The effective dosage of L-1027 and L-BMX were higher than 0225 and 0319, which suggests that L-1027 and L-BMX have lower toxicity to our cells. Compounds of the second

group could elevate survival generally. 0312 was classified to this group and it could significantly promote cell viability of all the cells with 27Q, 75Q or V (Figure 7F). The last group of compounds showed limited effect to our SCA3 model. Compounds 0311, 1029 and TP are belong to this group and couldn't improve viability of all the 3 cell lines (Figures 7G-I).

We also calculated the half maximal inhibitory concentration (IC_{50}) of these compounds from the cell viability data. We found the IC_{50} of these 8 HDACi were all lower than SAHA (Table 3). It indicated that these compounds were less toxic than SAHA on our SCA3 cells. According to the information provided by NBM that L-1027 and L-BMX are HDAC8 inhibitor and L-BMX also could inhibit HDAC3 activity (Appendix Table 1).

These data indicated that HDACi could be a potential neural therapeutic drug to SCA3 with lower cell toxicity than SAHA. We were interested in L-BMX and used it for further study for it could specifically elevate 75Q cell viability in oxidative environment and inhibit HDAC3/8 activity.

Both T-BMX and L-BMX could elevate SCA3 75Q cell neurite outgrowth

In addition to cell viability, we further examined whether the potential HDACi L-BMX influence on cell morphology. In this study, we first tested T-BMX which was previously shown increased cell viability by MTT assay (顏, 2009). T-BMXhas the same chemical structure but not

in lithium salt as L-BMX. We stained cells with Rhodamine-Phalloidin to observe their morphology. SCA3 75Q cells gathered and showed poorly neurite outgrowth without T-BMX treatment (Figure 8A). However, 75Q cells with T-BMX treatment for 48 hr showed significant improvement in neurite outgrowth and increased neurite length (Figures 8A-C), and these phenomenon were not observed in V and 27Q cells (Figures 8A-C). Among these results, we found that some 75Q cells showed very distinct neurite outgrowth under the T-BMX treatment (Figure 8D). We also investigate cell morphology of SCA3 cells after L-BMX treatment. Similar to the effect of T-BMX, L-BMX could significant promote neurite outgrowth and length (Figures 8E-G).

These data indicate that both T-BMX and L-BMX could promote 75Q cell neurite outgrowth and length and might be potential in SCA3 treatment.

Both T-BMX and L-BMX could reduce AT3 aggregation in 75Q cells

We previously showed that both T-BMX and L-BMX could elevate SCA3 75Q cell viability and neurite outgrowth. We then used immunocytochemistry to analyze AT3 aggregation after T-BMX and L-BMX treatment in the SCA3 cells. We found that SCA3 27Q cells exhibited higher AT3 expression and distributed in whole cell evenly without aggregation formation after drug treatment (Figure 9A), while 75Q cells with lower AT3 expression level but aggregated in the cytosome or nuclear without treatment (Figure 9B). After T-BMX or L-BMX treatment, SCA3 75Q showed significantly reduction in AT3

aggregation compared to DMSO treated cells (Figures 9B-C).

Furthermore, we also used 1C2 antibody, which specifically targeted to polyQ epitope of AT3, to confirm the treatment effect of L-BMX. As the results previously shown in AT3 immunostaining with AT3 antibody, we didn't observe protein aggregation in SCA3 27Q cell (Figures 10A-B). However, some punctual and spherical 1C2aggregats were identified in SCA3 75Q cells (Figures 10C-D). After L-BMX treatment, the number of 1C2 positive aggregation was reduced (Figure 10E). In addition to characterization the aggregation with immunostaining, we also conducted filter trap assay to observe the effect of L-BMX on aggregation. Using 1C2 antibody to probe the membrane, we hardly found 1C2 positive signal in 27Q cell lysate but found dose-dependent 1C2 positive signal in 75Q cell lysate. The 1C2 positive aggregation was decreased in 75Q cells after L-BMX treatment (Figure 10F). Taken together; these data indicate that both T-BMX and L-BMX could suppress SCA3 polyQ-expandedaggregation.

Several neuroprotected pathways might be activated by L-BMX treatment

We have shown that both T-BMX and L-BMX could elevated 75Q cell viability, neurite outgrowth and reduced AT3 aggregation. We further tried to elucidate the molecular mechanism of the L-BMX effect. We first examined Hsp27 and Hsp70 levels after L-BMX treatment (Figure 11A). We found that L-BMX could elevate Hsp27 expression level in SCA3 75Q cell (Figure 11B), but had limited effect on Hsp70 (Figure 11C). Furthermore, several reports suggested that expanded polyQ would

decrease the expression or transportation of NF-κB (Goswami et al., 2006a; Wang et al., 2007b; Marcora and Kennedy, 2010; Reijonen et al., 2010). The downregulation of NF-κB might decrease the antioxidative ability and lead to cell death (Reijonen et al., 2010). In order to investigate the relationship between NF-κB and antioxidative ability, we thus examined the expression level of NF-κB and antioxidative enzyme, MnSOD (Figure 11A). Our results indicate that L-BMX could significantly elevate the level of NF-κB and MnSOD in both 27Q and 75Q cells (Figures 11D-E). Taken together, L-BMX treatment would elevate several neuroprotected factors, such as heat shock proteins and antioxidative factor; furthermore, it could also rescue NF-κBdownregulation in our SCA3 cell model.

L-BMX reduced the activated GSK3β

The phosphorylation of GSK3β (P- GSK3β) was reported to correlate to neurodegeneration and neural death (Bhat et al., 2000). Inhibition of GSK3β activation would be a potential therapeutic strategy for neurodegenerative diseases, such as HD and Alzheimer's disease (AD) (Carmichael et al., 2002; Leng et al., 2008; Bolos et al., 2010). AKT is the upstream protein of GSK3β and plays an important role in neuroprotection(Humbert et al., 2002). Also, the phosphorylation of AKT could eliminate the cell toxicity in HD and SBMA (Humbert et al., 2002; Palazzolo et al., 2007).We examined the levels of AKT and GSK3β were affected after L-BMX treatment by western blot analyses. We observed that L-BMX treatment did not affect the ratio of P-AKT/AKT (Figures

12A-B), but reduced the ratio of P-GSK3β/ GSK3β. These data indicated that L-BMX could reduce activation of GSK3β.

ERK pathway was activated after L-BMX treatment

We previously showed that the elevation of SCA3 cell viability by L-BMX treatment. To understand whether the increase of 75Q cell viability by L-BMX was through the MAPK pathway, we examined the activation of ERK pathway. Our western blot results showed that L-BMX could active ERK pathway, the cell survival pathway (Figures 13A-B). Compared to SCA3 27Q cell, 75Q cell exhibited lower activation of ERK pathway. However, after L-BMX treatment, we found P-c-RAF, the upstream of ERK was elevated slightly (Figure 12B), the P-ERK and P-MEK was significant upregulated in SCA3 75Q cells (Figure 12C). P-90RSK, one of P-ERK downstream regulator, which could activate cell growth related transcription factor showed slightly increase after L-BMX treatment (Figure 12D). Despite cell survival pathway, we also examined cell death pathway, JNK pathway (Figure 13A). We found that L-BMX would inhibit P-JNK and the downstream protein, P-p38 (Figures 13B-C). These data indicate that L-BMX could activate ERK cell survival pathway cascade and inhibit JNK pathway, which in turn to promote the cell survival in our SCA3 cell model.

L-BMX amerliorated the dysregulated autophagy activity in SCA3 cells

We previously showed that L-BMX would reduce SCA3 protein accumulation. It was reported that HDACi treatment could clearance

mutant htt aggregation by autophagy induction (Jeong et al., 2009).We therefore tried to elucidate whether L-BMX treatmentcould induce autophagy pathway to clear AT3 aggregation. During the autophagosome formation, LC3 I would be cleaved into a smaller fragment, LC3 II (Tanida et al., 2004). Our result showed the ratio of LC3 I (uncleaved LC3) and LC3 II (autophagy formation) was reduced in 75Q cells, and it was recovered by L-BMX treatment (Figures 15A-B).These data suggest that L-BMX could activate autophagy formation, which further reduced the SCA3 aggregation in our SCA3 cell model.

L-BMX elevalated the acetylation of H2A

Next, we investigated the level of histone acetylation (Ac) in SCA3 cells after L-BMX treatment. Our observation of the acetylation on H2A, H2B, H3 and H4 in SCA3 cells treated with L-BMX showed that L-BMX would significantly elevate the acetylation level of H2A (Figures 16A-B). We also found that the ratio of Ac-H2B/ H2B in SCA3 75Q cells was lower than 27Q cells. However, L-BMX was failed to rescue the hypoacetylation on H2B in 75Q cells (Figure 16B). L-BMX could also elevate Ac-H3 in 27Q cells but had limit effect in 75Q cells (Figure 16C). The expression level of Ac-H4 was slightly affected by L-BMX treatment (Figure 16D). These data indicated that L-BMX increased H2A acetylation in SCA3 75Q cells. H2A might be one of the candidate acetylation targets of L-BMX.

The mitochondria area and Mitotracker distribution pattern was

rescued in SCA3 75Q cell after L-BMX treatment

There are several reports pointed out that many polyQ-mediated neurodegenerative diseases were tightly related to mitochondrial function (Panov et al., 2002; Ranganathan et al., 2009; Costa et al., 2010; Song et al., 2011). We used Mitotracker to stain the mitochondria in our SCA3 cells. The staining results showed that mitochondria in 27Q cells were more strongly stained and accumulated distributedaround the nuclei (Figure 17A), which is similar to the mitochondrial pattern under a stress environment (Buckman et al., 2001)). The pattern which mitochondria highly accumulated around cell nuclei in 27Q DMSO cells was ameliorated by L-BMX treatment (Figures 17A-D). On the other hand, the mitochondria in75Q DMSO cells showed irregular and diffused pattern (Figure 17A). L-BMX could rescue the abnormal mitochondria distribution in 75Q cell (Figure 17A). We quantitated the mitochondria distribution area and total Mitotracker positive intensity in SCA3 cells (Figures 17B-D). Compared to the 27Q DMSO cells, Mitotracker staining intensity was reduced in 27Q L-BMX treatment cells (Figure 17B). In contrast, L-BMX elevated the total Mitotracker intensity in 75Q cells (Figure 17B). The diffused distributed pattern of 75Q DMSO cells highly raised the total mitochondria area, and which was also ameliorated by L-BMX treatment (Figure 17C). Furthermore, we calculated the ratio of total Mitotracker signal intensity/area and found that L-BMX reduced the ratio in 27Q cells but increased the ratio in 75Q cells (Figure 17D). Taken together, L-BMX could alter mitochondria distribution in polyQ-expanded stress environment in our SCA3 cell model.

L-BMX pretreatment protected SCA3 cells against the decrease of cell viability induced by TBH

Different from the previous treatment condition, in this study, we applied L-BMX to the cells prior to TBH treatment. After L-BMX treatment for 48 hr, we applied TBH to induce the cell stress for 72 hr and then analyzed cell viability by MTT assay (Figure 18A). The results show all the 3 SCA3 cell line viability were reduced after TBH treatment for 72 hr (Figure 18B). L-BMX could rescue the reduced cell viability caused by the elevation of cellular oxidative stress by TBH in 75Q SCA3 cells (Figure 18C).These data indicate that the neuroprotective effect of L-BMX could decrease TBH induced cell toxicity in SCA3 cells.

Generation of inducible truncatedAT3 cell lines

We planned to introduce truncate AT3 inducible expression in PC12 cells to accelerate the disease progression in our cell model. We generated N-terminal deleted 69, 219 and 257 amino acid DNA fragments in pEGSH vector (Figure 19A). The truncated AT3 fragments were PCR amplified and subcloned into the pEGSH vector. We examined the truncated AT3 construct by *Bam*HI and *Xba*I enzyme double digestion (Figure 19B). After the digest map and DNA sequences were validated, we transfected each construct into PC12 cells. The expression of truncated AT3 were then induced by ponA and analyzed by western blot. We have successfully established C69 and C219 27Q inducible expression in PC12 cells (Figure 19C).

Discussion

HDACi had been used in several polyQ-mediated neurodegenerative diseases. We have summarized the HDACi therapeutic effects in molecular and functional aspects in polyQ diseases (Table 4). We found that several HDACi compounds could reverse polyQ caused neurodegeneration, motor dysfunction, body weight loss and active several neuroprotected pathways. However, these HDACi compounds had limited effect in aggregation reduction. In our study, we used SCA3 inducible cell model to screen novel HDACi compounds (provided by NBM) for potential SCA3 therapy. SAHA is an FDA approved HDACi, and could rescue many polyQ caused neurodegeneration (Table 4). The novel HDACi compounds used in this study were modified from SAHA and the drug effect on cell survival, neurite outgrowth, protein aggregation, anti-oxidative stress, the ability to suppress HDAC enzyme and downstream related neuroprotective pathways were analyzed.

SCA3-75Q cells have lower tolerance to oxidative stress

Oxidative stress was tightly related to polyQ disorders. In our result, we found the SCA3-75Q cells showed lower viability under oxidative stress condition. This result is consistent with many neurodegeneration disease researches (Taylor et al., 2002; Bossy-Wetzel et al., 2004; Sayre et al., 2008). Several studies of SCA3 have reported that antioxidative enzyme was reduced in SCA3 cells and stress environment could cause AT3 to enter cell nuclear (Yu et al., 2009; Reina et al., 2010). Mutant htt containing expanded polyQ track induced higher oxidative stress included

DNA damage, abnormal mitochondria morphology and mitochondria membrane potential (Perez-Severiano et al., 2002; Giuliano et al., 2003; Firdaus et al., 2006; Puranam et al., 2006). HD cells with expanded polyQ tract under oxidative stress drug H_2O_2 treatment underwent cell death, aggregation formation and mitochondria fragmentation earlier (Goswami et al., 2006b; Wang et al., 2009). The similar results were also observed in SCA1, SCA2, SBMA and DRPLA studies (Cowan et al., 2003; Giuliano et al., 2003; Kim et al., 2003; Miyata et al., 2008). TBH and H_2O_2 treatment in our SCA3 cell model could accelerate the disease progress in order to provide as a quick platform for drug screen.

Proteasome inhibitor cause viability loss and UPS dysfunction in SCA3 75Q cells

PolyQ aggregation was highly related to UPS dysfunction (Bence et al., 2001). In SCA3 and HD models, proteasome were included in protein aggregation (Chai et al., 1999; Wyttenbach et al., 2000; Waelter et al., 2001; Wang et al., 2007a). That polyQ caused protein aggregation could be due to UPS impairment. There are many researches indicated that proteasome inhibitor MG-132 or lactacystin applied on polyQ models would accelerate aggregation formation. In HD cell model, MG-132 treatment would promote aggregation formation, and the effect of MG-132 was dose-dependent (van Tijn et al., 2007). Similar observations were also described for lactacystin treatment of polyQ models: lactacystin could promote AT3, HD and other polyQ expanded protein aggregated in the cell (Wyttenbach et al., 2000; Bence et al., 2001; Waelter et al., 2001).

Further supporting the correlation between UPS and polyQ caused protein aggregation, overexpression ubiquitin could reverse the protein aggregation in HD model (Wang et al., 2006). Our SCA3 inducible cell model is concurred with these finding. SCA3 75Q cells showed lower tolerance in MG-132 and lactacystin, the proteasome inhibitor and exhibited decreasing in cell survival, highly insoluble polyubiquitinated protein aggregation and AT3 aggregation at peri-nuclear. The effect of lactacystin was stronger than MG-132 for lactacystin is an irreversible proteasomal inhibitor. Our cell model displayed similar results which were seen in previous reports, so it could be a suitable model for studying the SCA3 pathogenesis and screening candidate therapeutic drugs for SCA3.

Screening potential HDACi for SCA3 therapy using the inducible SCA3 cell model

We applied SAHA and 8 SAHA derived HDACi compounds on our inducible cell model to evaluate their potential in SCA3 therapy. We analyzed the effect of these HDACi on cell survival, the ability to suppress aggregation formation, neurite outgrowth promotion and downstream related pathways. Several HDACi compounds such as SAHA, TSA, NAM, sodium butyrate, phenyl butyrate, HDACi-4b were reported to have the potential in sustaining cell and animal life span of polyQ disease models *in vitro* and *in vivo* (Table 4). From the cell model screen, we also identified many candidate drugs, such as L-1027, L-BMX, 0225, 0312, 0319, could elevated SCA3 cell viability. L-1027, L-BMX,

0225 and 0319 could specifically improve SCA3 75Q cell viability. These finding was consistent with previous study of HDACi compounds used in polyQ therapy. The HDAC enzyme inhibition activity of these HDACi was further identified. L-1027 was identified to be a HDAC8inhibitor, and L-BMX was identified to be HDAC3 and HDAC8 inhibitor. They both exhibited higher effect on inhibition of HDAC enzyme than TSA (Appendix Table 1). Most of HDACi were inhibitors of multiple HDAC inhibitors (Dokmanovic et al., 2007). For instance, SAHA was used to suppress class I and class II enzymes, include HDAC 1, 2, 3, 4, 5, 7, 8, 9 (Dokmanovic et al., 2007). Application of SAHA in HD mice caused HDAC7 downregulation and showed neuroprotective effect; on the other hand, the protective effect was abolished when HDAC7 was specifically knock-down (Benn et al., 2009). It's hard to define the correlation between HDAC enzyme and disease progression by use of multiple HDACi drug. Compared to SAHA, L-BMX and L-1027 are more specific HDAC3 and HDAC8 inhibitors, these HDACi might provide more clear relationship between HDAC3 and 8 and SCA3 pathogenesis.

Both T-BMX and L-BMX could elevate SCA3 75Q cell neurite outgrowth

With our SCA3 cell model, we found that HDACi, T-BMX and L-BMX elevated 75Q cell neurite number and length. The finding is consistent with the following researches. HDACi could elevate neurite outgrowth through transcription regulation, for instance, TSA was reported to promote neurite outgrowth in rat neuron primary culture

through transcription regulation of prepronociceptin gene (Zaveri et al., 2006). Prepronociceptin gene was tightly related to regulation of neurite outgrowth (Ring et al., 2006); TSA would promote the recruitment of cAMP at the promoter region of prepronociceptin and enhance its mRNA expression (Zaveri et al., 2006). In mouse cortical and cerebellum neuron primary culture, TSA also could promote neurite outgrowth by regulation of CBP/p300 and P-CAF (Gaub et al., 2010); valproic acid promoted ERK pathway activation and neurite outgrowth in primary neuron culture and promote neurogenesis in adult mouse hippocampus (Hao et al., 2004). The neurite outgrowth was inhibited if the activation of ERK pathway was blocked (Hao et al., 2004). In our study, we also observed that ERK pathway was activated after L-BMX treatment. Inhibition of P-GSK3β increased the expression level of P-ERK (Hao et al., 2004). We also observed the decrease of P- GSK3β in 75Q cell after L-BMX treatment. The induction of neurite outgrowth by NGF in PC12 was disrupted by expanded mutant htt (Song et al., 2002). A similar research also indicated that sodium butyrate could also promote neurite outgrowth in PC12 through enhancing the NGF effect (Suzuki-Mizushima et al., 2002). In our cell model, we found the elevation of the neurite outgrowth after HDACi treatment only in 75Q- but not in 27Q- or vector-bearing cells. The possible reason might be that the NGF pathway has already applied good protection for V and 27Q cells, the protective effect of L-BMX was not strong enough to be observed in these cells . Also, AT3 has been reported to be involved in stabilization of cytoskeleton.The organization of cytoskeleton was disordered in AT3 knock down cells (Rodrigues et al.,

2010). In our SCA3 cell, we also found abnormal cell morphology by using F-actin staining analysis. The HDACi treatment could rescue the abnormal phenotype in our 75Q cells.

Both T-BMX and L-BMX could reduce AT3 aggregation in 75Q cells

Our result shows that L-BMX treatment could decrease polyQ protein aggregation. We also found autophagosome formation might be elevated by L-BMX through upregulation of autophagosome marker, LC3 II. Autophagy-lysosomal degradation pathway plays essential role in protein degradation. The mutant htt protein aggregation and cellular toxicity were raised if autophagy pathway was blocked in HD cell model (Qin et al., 2003). It was also suggested autophagy is a major degradation pathway of polyQ expansion htt (Ravikumar et al., 2002; Heng et al., 2010). In a recent study, autophagy was suggested to be a self-protected effect toward htt toxicity and used to clean the aggregation protein (Martinez-Vicente et al., 2010). The therapeutic effect in polyQ mediated protein aggregation model was raised throughinducing or enhancing autophagy pathway (Qin et al., 2003). Treatment with mTOR inhibitor, such as rapamycin and CCI-779, could activate autophagy pathway to clear polyQ mediated protein aggregation (Ravikumar et al., 2004; Sarkar et al., 2008; Menzies et al., 2010). Beside mTOR inhibitor, lithium could also induce autophagy pathway, but the molecular mechanism was mTOR-independent and through inhibition of IP_3 and P-GSK3β (Sarkar et al., 2005; Sarkar et al., 2008). The structure of L-BMX contained lithium and it could also decrease P-GSK3β and raised the expression level of

LC3 II. We therefore suggest that the possible mechanism of L-BMX in the clearance of protein aggregation is through induction of autophagy in our SCA3 cell model.

Several neuroprotective pathways might be activated by L-BMX treatment.

Several HDACi such as TSA, valproic acid, and sodium butyrate, were reported to reduce cellular oxidative stress and elevate cell viability in oxidative environment by transcription regulation mechanism (Ryu et al., 2003; Huuskonen et al., 2004; Kanai et al., 2004; Peng et al., 2005; Chen et al., 2007; Langley et al., 2008). Our finding is consistent to these studies, L-BMX treatment could promote 75Q cell viability, elevate antioxidant enzyme, MnSOD and rescue abnormal mitochondria morphology in oxidative environment. Overexpression of MnSOD could decrease oxidative stress and improve protein aggregation in AD mouse model (Dumont et al., 2009). The elevation of MnSOD in 75Q cell might increase the cellular antioxidative activity so that 75Q cells exhibit higher cell viability at oxidative stress condition after L-BMX treatment. We found L-BMX could also rescue the downregulation of Hsp27 in 75Q cells. Hsp27 was reduced in SCA3 and SCA7 cells and patients (Wen et al., 2003; Tsai et al., 2005). Hsp27 played a very important role in neuron protection and prevention of oxidative stress mediate apoptosis (Gorman et al., 2005; Stetler et al., 2008; Friedman et al., 2009). In HD, Hsp27 decreased oxidative stress produced by mutant htt and promote HD cell survival (Wyttenbach et al., 2002). The similar result was also observed

in our study; L-BMX could retrieve Hsp27 expression and promote cell survival under an oxidative stress environment.

Moreover, we found L-BMX treatment decreased the expression levels of cellular stress markers, P-JNK and P-p38 accompanied the activation of cell survival pathway, ERK pathway. Mutant htt and ataxin1 would elevate P-JNK and P-p38 expression level and disrupt ERK pathway and lead to cell death in both *in vitro* and *in vivo* model (Apostol et al., 2006; Varma et al., 2007; Roze et al., 2008; Tsirigotis et al., 2008). Activation of ERK pathway protected cell from htt toxicity-caused cell death (Apostol et al., 2006; Varma et al., 2007).

Furthermore, we discovered that L-BMX rescued the downregulation of NF-κB in 75Q cells. The downregulation of NF-κB was also identified in HD and SCA7 (Goswami et al., 2006a; Wang et al., 2007b; Reijonen et al., 2010). NF-κB was reported as a crucial factor involved in cerebellar granule neuron survival (Koulich et al., 2001). The reduction of NF-κB activation would lead to elevation of oxidative stress and granule neuron apoptosis (Piccioli et al., 2001). Our findings are similar to these studies, L-BMX could rescue NF-κB activation in 75Q cells and provide higher ability to resist oxidative stress.

Studieshave indicated that HDACi treatment could activate several neuroprotected pathway (Saha and Pahan, 2006). In our study, we showed that L-BMX pretreatment could improve SCA3 cell viability against TBH challenge. The neuroprotective effect of L-BMX might through the activation of several neuroprotected pathways and could last for at least three days.

In conclusion, L-BMX treatment in our SCA3 cells could elevate cell viability and neurite outgrowth, reduce protein aggregation, activate several neuroprotected pathways and promote the acetylation of H2A. We suggest that L-BMX could be a potential drug for SCA3 therapy.

Reference

Aletta JM (1996) Phosphorylation of type III beta-tubulin PC12 cell neurites during NGF-induced process outgrowth. J Neurobiol 31:461-475.

Apostol BL, Illes K, Pallos J, Bodai L, Wu J, Strand A, Schweitzer ES, Olson JM, Kazantsev A, Marsh JL, Thompson LM (2006) Mutant huntingtin alters MAPK signaling pathways in PC12 and striatal cells: ERK1/2 protects against mutant huntingtin-associated toxicity. Hum Mol Genet 15:273-285.

Barbeau A, Roy M, Cunha L, de Vincente AN, Rosenberg RN, Nyhan WL, MacLeod PL, Chazot G, Langston LB, Dawson DM, et al. (1984) The natural history of Machado-Joseph disease. An analysis of 138 personally examined cases. Can J Neurol Sci 11:510-525.

Bence NF, Sampat RM, Kopito RR (2001) Impairment of the ubiquitin-proteasome system by protein aggregation. Science 292:1552-1555.

Benn CL, Butler R, Mariner L, Nixon J, Moffitt H, Mielcarek M, Woodman B, Bates GP (2009) Genetic knock-down of HDAC7 does not ameliorate disease pathogenesis in the R6/2 mouse model of Huntington's disease. PLoS One 4:e5747.

Berke SJ, Schmied FA, Brunt ER, Ellerby LM, Paulson HL (2004) Caspase-mediated proteolysis of the polyglutamine disease protein ataxin-3. J Neurochem 89:908-918.

Berke SJ, Chai Y, Marrs GL, Wen H, Paulson HL (2005) Defining the role of ubiquitin-interacting motifs in the polyglutamine disease

protein, ataxin-3. J Biol Chem 280:32026-32034.

Bhat RV, Shanley J, Correll MP, Fieles WE, Keith RA, Scott CW, Lee CM (2000) Regulation and localization of tyrosine216 phosphorylation of glycogen synthase kinase-3beta in cellular and animal models of neuronal degeneration. Proc Natl Acad Sci U S A 97:11074-11079.

Bichelmeier U, Schmidt T, Hubener J, Boy J, Ruttiger L, Habig K, Poths S, Bonin M, Knipper M, Schmidt WJ, Wilbertz J, Wolburg H, Laccone F, Riess O (2007) Nuclear localization of ataxin-3 is required for the manifestation of symptoms in SCA3: in vivo evidence. J Neurosci 27:7418-7428.

Bolos M, Fernandez S, Torres-Aleman I (2010) Oral administration of a GSK3 inhibitor increases brain insulin-like growth factor I levels. J Biol Chem 285:17693-17700.

Bossy-Wetzel E, Schwarzenbacher R, Lipton SA (2004) Molecular pathways to neurodegeneration. Nat Med 10 Suppl:S2-9.

Buckman JF, Hernandez H, Kress GJ, Votyakova TV, Pal S, Reynolds IJ (2001) MitoTracker labeling in primary neuronal and astrocytic cultures: influence of mitochondrial membrane potential and oxidants. J Neurosci Methods 104:165-176.

Burnett B, Li F, Pittman RN (2003) The polyglutamine neurodegenerative protein ataxin-3 binds polyubiquitylated proteins and has ubiquitin protease activity. Hum Mol Genet 12:3195-3205.

Burnett BG, Pittman RN (2005) The polyglutamine neurodegenerative protein ataxin 3 regulates aggresome formation. Proc Natl Acad Sci

U S A 102:4330-4335.

Butler R, Bates GP (2006) Histone deacetylase inhibitors as therapeutics for polyglutamine disorders. Nat Rev Neurosci 7:784-796.

Carmichael J, Sugars KL, Bao YP, Rubinsztein DC (2002) Glycogen synthase kinase-3beta inhibitors prevent cellular polyglutamine toxicity caused by the Huntington's disease mutation. J Biol Chem 277:33791-33798.

Cashikar AG, Duennwald M, Lindquist SL (2005) A chaperone pathway in protein disaggregation. Hsp26 alters the nature of protein aggregates to facilitate reactivation by Hsp104. J Biol Chem 280:23869-23875.

Chai Y, Berke SS, Cohen RE, Paulson HL (2004) Poly-ubiquitin binding by the polyglutamine disease protein ataxin-3 links its normal function to protein surveillance pathways. J Biol Chem 279:3605-3611.

Chai Y, Koppenhafer SL, Shoesmith SJ, Perez MK, Paulson HL (1999) Evidence for proteasome involvement in polyglutamine disease: localization to nuclear inclusions in SCA3/MJD and suppression of polyglutamine aggregation in vitro. Hum Mol Genet 8:673-682.

Chan HM, La Thangue NB (2001) p300/CBP proteins: HATs for transcriptional bridges and scaffolds. J Cell Sci 114:2363-2373.

Chang WH, Tien CL, Chen TJ, Nukina N, Hsieh M (2009) Decreased protein synthesis of Hsp27 associated with cellular toxicity in a cell model of Machado-Joseph disease. Neurosci Lett 454:152-156.

Chen PS, Wang CC, Bortner CD, Peng GS, Wu X, Pang H, Lu RB, Gean

PW, Chuang DM, Hong JS (2007) Valproic acid and other histone deacetylase inhibitors induce microglial apoptosis and attenuate lipopolysaccharide-induced dopaminergic neurotoxicity. Neuroscience 149:203-212.

Cong SY, Pepers BA, Roos RA, van Ommen GJ, Dorsman JC (2006) Small N-terminal mutant huntingtin fragments, but not wild type, are mainly present in monomeric form: Implications for pathogenesis. Exp Neurol 199:257-264.

Costa V, Giacomello M, Hudec R, Lopreiato R, Ermak G, Lim D, Malorni W, Davies KJ, Carafoli E, Scorrano L (2010) Mitochondrial fission and cristae disruption increase the response of cell models of Huntington's disease to apoptotic stimuli. EMBO Mol Med 2:490-503.

Cowan KJ, Diamond MI, Welch WJ (2003) Polyglutamine protein aggregation and toxicity are linked to the cellular stress response. Hum Mol Genet 12:1377-1391.

Crossthwaite AJ, Hasan S, Williams RJ (2002) Hydrogen peroxide-mediated phosphorylation of ERK1/2, Akt/PKB and JNK in cortical neurones: dependence on Ca(2+) and PI3-kinase. J Neurochem 80:24-35.

Davis PK, Johnson GV (1999) The microtubule binding of Tau and high molecular weight Tau in apoptotic PC12 cells is impaired because of altered phosphorylation. J Biol Chem 274:35686-35692.

Dokmanovic M, Clarke C, Marks PA (2007) Histone deacetylase inhibitors: overview and perspectives. Mol Cancer Res 5:981-989.

Dompierre JP, Godin JD, Charrin BC, Cordelieres FP, King SJ, Humbert S, Saudou F (2007) Histone deacetylase 6 inhibition compensates for the transport deficit in Huntington's disease by increasing tubulin acetylation. J Neurosci 27:3571-3583.

Du Y, Wooten MC, Wooten MW (2009) Oxidative damage to the promoter region of SQSTM1/p62 is common to neurodegenerative disease. Neurobiol Dis 35:302-310.

Dumont M, Wille E, Stack C, Calingasan NY, Beal MF, Lin MT (2009) Reduction of oxidative stress, amyloid deposition, and memory deficit by manganese superoxide dismutase overexpression in a transgenic mouse model of Alzheimer's disease. FASEB J 23:2459-2466.

Durr A, Stevanin G, Cancel G, Duyckaerts C, Abbas N, Didierjean O, Chneiweiss H, Benomar A, Lyon-Caen O, Julien J, Serdaru M, Penet C, Agid Y, Brice A (1996) Spinocerebellar ataxia 3 and Machado-Joseph disease: clinical, molecular, and neuropathological features. Ann Neurol 39:490-499.

Esmaeli-Azad B, McCarty JH, Feinstein SC (1994) Sense and antisense transfection analysis of tau function: tau influences net microtubule assembly, neurite outgrowth and neuritic stability. J Cell Sci 107 (Pt 4):869-879.

Evert BO, Araujo J, Vieira-Saecker AM, de Vos RA, Harendza S, Klockgether T, Wullner U (2006) Ataxin-3 represses transcription via chromatin binding, interaction with histone deacetylase 3, and histone deacetylation. J Neurosci 26:11474-11486.

Ferrante RJ, Kubilus JK, Lee J, Ryu H, Beesen A, Zucker B, Smith K, Kowall NW, Ratan RR, Luthi-Carter R, Hersch SM (2003) Histone deacetylase inhibition by sodium butyrate chemotherapy ameliorates the neurodegenerative phenotype in Huntington's disease mice. J Neurosci 23:9418-9427.

Firdaus WJ, Wyttenbach A, Diaz-Latoud C, Currie RW, Arrigo AP (2006) Analysis of oxidative events induced by expanded polyglutamine huntingtin exon 1 that are differentially restored by expression of heat shock proteins or treatment with an antioxidant. FEBS J 273:3076-3093.

Fontaine-Lenoir V, Chambraud B, Fellous A, David S, Duchossoy Y, Baulieu EE, Robel P (2006) Microtubule-associated protein 2 (MAP2) is a neurosteroid receptor. Proc Natl Acad Sci U S A 103:4711-4716.

Fortini ME (2007) Medicine. Anticipating trouble from gene transcription. Science 315:1800-1801.

Fowler HL (1984) Machado-Joseph-Azorean disease. A ten-year study. Arch Neurol 41:921-925.

Friedman MJ, Li S, Li XJ (2009) Activation of gene transcription by heat shock protein 27 may contribute to its neuronal protection. J Biol Chem 284:27944-27951.

Gao L, Cueto MA, Asselbergs F, Atadja P (2002) Cloning and functional characterization of HDAC11, a novel member of the human histone deacetylase family. J Biol Chem 277:25748-25755.

Gaub P, Tedeschi A, Puttagunta R, Nguyen T, Schmandke A, Di Giovanni

S (2010) HDAC inhibition promotes neuronal outgrowth and counteracts growth cone collapse through CBP/p300 and P/CAF-dependent p53 acetylation. Cell Death Differ 17:1392-1408.

Gauthier LR, Charrin BC, Borrell-Pages M, Dompierre JP, Rangone H, Cordelieres FP, De Mey J, MacDonald ME, Lessmann V, Humbert S, Saudou F (2004) Huntingtin controls neurotrophic support and survival of neurons by enhancing BDNF vesicular transport along microtubules. Cell 118:127-138.

Giuliano P, De Cristofaro T, Affaitati A, Pizzulo GM, Feliciello A, Criscuolo C, De Michele G, Filla A, Avvedimento EV, Varrone S (2003) DNA damage induced by polyglutamine-expanded proteins. Hum Mol Genet 12:2301-2309.

Goldberg AL (2003) Protein degradation and protection against misfolded or damaged proteins. Nature 426:895-899.

Gorman AM, Szegezdi E, Quigney DJ, Samali A (2005) Hsp27 inhibits 6-hydroxydopamine-induced cytochrome c release and apoptosis in PC12 cells. Biochem Biophys Res Commun 327:801-810.

Goswami A, Dikshit P, Mishra A, Nukina N, Jana NR (2006a) Expression of expanded polyglutamine proteins suppresses the activation of transcription factor NFkappaB. J Biol Chem 281:37017-37024.

Goswami A, Dikshit P, Mishra A, Mulherkar S, Nukina N, Jana NR (2006b) Oxidative stress promotes mutant huntingtin aggregation and mutant huntingtin-dependent cell death by mimicking proteasomal malfunction. Biochem Biophys Res Commun

342:184-190.

Goti D, Katzen SM, Mez J, Kurtis N, Kiluk J, Ben-Haiem L, Jenkins NA, Copeland NG, Kakizuka A, Sharp AH, Ross CA, Mouton PR, Colomer V (2004) A mutant ataxin-3 putative-cleavage fragment in brains of Machado-Joseph disease patients and transgenic mice is cytotoxic above a critical concentration. J Neurosci 24:10266-10279.

Greene LA, Tischler AS (1976) Establishment of a noradrenergic clonal line of rat adrenal pheochromocytoma cells which respond to nerve growth factor. Proc Natl Acad Sci U S A 73:2424-2428.

Grunstein M (1997) Histone acetylation in chromatin structure and transcription. Nature 389:349-352.

Haacke A, Broadley SA, Boteva R, Tzvetkov N, Hartl FU, Breuer P (2006) Proteolytic cleavage of polyglutamine-expanded ataxin-3 is critical for aggregation and sequestration of non-expanded ataxin-3. Hum Mol Genet 15:555-568.

Hao Y, Creson T, Zhang L, Li P, Du F, Yuan P, Gould TD, Manji HK, Chen G (2004) Mood stabilizer valproate promotes ERK pathway-dependent cortical neuronal growth and neurogenesis. J Neurosci 24:6590-6599.

Harding AE (1982) The clinical features and classification of the late onset autosomal dominant cerebellar ataxias. A study of 11 families, including descendants of the 'the Drew family of Walworth'. Brain 105:1-28.

Heng MY, Duong DK, Albin RL, Tallaksen-Greene SJ, Hunter JM, Lesort

MJ, Osmand A, Paulson HL, Detloff PJ (2010) Early autophagic response in a novel knock-in model of Huntington disease. Hum Mol Genet 19:3702-3720.

Hockly E, Richon VM, Woodman B, Smith DL, Zhou X, Rosa E, Sathasivam K, Ghazi-Noori S, Mahal A, Lowden PA, Steffan JS, Marsh JL, Thompson LM, Lewis CM, Marks PA, Bates GP (2003) Suberoylanilide hydroxamic acid, a histone deacetylase inhibitor, ameliorates motor deficits in a mouse model of Huntington's disease. Proc Natl Acad Sci U S A 100:2041-2046.

Humbert S, Bryson EA, Cordelieres FP, Connors NC, Datta SR, Finkbeiner S, Greenberg ME, Saudou F (2002) The IGF-1/Akt pathway is neuroprotective in Huntington's disease and involves Huntingtin phosphorylation by Akt. Dev Cell 2:831-837.

Huuskonen J, Suuronen T, Nuutinen T, Kyrylenko S, Salminen A (2004) Regulation of microglial inflammatory response by sodium butyrate and short-chain fatty acids. Br J Pharmacol 141:874-880.

Iwata A, Riley BE, Johnston JA, Kopito RR (2005) HDAC6 and microtubules are required for autophagic degradation of aggregated huntingtin. J Biol Chem 280:40282-40292.

Jardim LB, Silveira I, Pereira ML, Ferro A, Alonso I, do Ceu Moreira M, Mendonca P, Ferreirinha F, Sequeiros J, Giugliani R (2001) A survey of spinocerebellar ataxia in South Brazil - 66 new cases with Machado-Joseph disease, SCA7, SCA8, or unidentified disease-causing mutations. J Neurol 248:870-876.

Jeong H, Then F, Melia TJ, Jr., Mazzulli JR, Cui L, Savas JN, Voisine C,

Paganetti P, Tanese N, Hart AC, Yamamoto A, Krainc D (2009) Acetylation targets mutant huntingtin to autophagosomes for degradation. Cell 137:60-72.

Jorgensen ND, Andresen JM, Pitt JE, Swenson MA, Zoghbi HY, Orr HT (2007) Hsp70/Hsc70 regulates the effect phosphorylation has on stabilizing ataxin-1. J Neurochem 102:2040-2048.

Jung J, Bonini N (2007) CREB-binding protein modulates repeat instability in a Drosophila model for polyQ disease. Science 315:1857-1859.

Jung J, Xu K, Lessing D, Bonini NM (2009) Preventing Ataxin-3 protein cleavage mitigates degeneration in a Drosophila model of SCA3. Hum Mol Genet 18:4843-4852.

Kanai H, Sawa A, Chen RW, Leeds P, Chuang DM (2004) Valproic acid inhibits histone deacetylase activity and suppresses excitotoxicity-induced GAPDH nuclear accumulation and apoptotic death in neurons. Pharmacogenomics J 4:336-344.

Kawaguchi Y, Okamoto T, Taniwaki M, Aizawa M, Inoue M, Katayama S, Kawakami H, Nakamura S, Nishimura M, Akiguchi I, et al. (1994) CAG expansions in a novel gene for Machado-Joseph disease at chromosome 14q32.1. Nat Genet 8:221-228.

Kaytor MD, Burright EN, Duvick LA, Zoghbi HY, Orr HT (1997) Increased trinucleotide repeat instability with advanced maternal age. Hum Mol Genet 6:2135-2139.

Kim SJ, Kim TS, Hong S, Rhim H, Kim IY, Kang S (2003) Oxidative stimuli affect polyglutamine aggregation and cell death in human

mutant ataxin-1-expressing cells. Neurosci Lett 348:21-24.

Kim WY, Horbinski C, Sigurdson W, Higgins D (2004) Proteasome inhibitors suppress formation of polyglutamine-induced nuclear inclusions in cultured postmitotic neurons. J Neurochem 91:1044-1056.

Koulich E, Nguyen T, Johnson K, Giardina C, D'Mello S (2001) NF-kappaB is involved in the survival of cerebellar granule neurons: association of IkappaBbeta [correction of Ikappabeta] phosphorylation with cell survival. J Neurochem 76:1188-1198.

Kouroku Y, Fujita E, Tanida I, Ueno T, Isoai A, Kumagai H, Ogawa S, Kaufman RJ, Kominami E, Momoi T (2007) ER stress (PERK/eIF2alpha phosphorylation) mediates the polyglutamine-induced LC3 conversion, an essential step for autophagy formation. Cell Death Differ 14:230-239.

Kubodera T, Yokota T, Ohwada K, Ishikawa K, Miura H, Matsuoka T, Mizusawa H (2003) Proteolytic cleavage and cellular toxicity of the human alpha1A calcium channel in spinocerebellar ataxia type 6. Neurosci Lett 341:74-78.

La Spada AR, Wilson EM, Lubahn DB, Harding AE, Fischbeck KH (1991) Androgen receptor gene mutations in X-linked spinal and bulbar muscular atrophy. Nature 352:77-79.

LaFevre-Bernt MA, Ellerby LM (2003) Kennedy's disease. Phosphorylation of the polyglutamine-expanded form of androgen receptor regulates its cleavage by caspase-3 and enhances cell death. J Biol Chem 278:34918-34924.

Lam PY, Cadenas E (2008) Compromised proteasome degradation elevates neuronal nitric oxide synthase levels and induces apoptotic cell death. Arch Biochem Biophys 478:181-186.

Langley B, D'Annibale MA, Suh K, Ayoub I, Tolhurst A, Bastan B, Yang L, Ko B, Fisher M, Cho S, Beal MF, Ratan RR (2008) Pulse inhibition of histone deacetylases induces complete resistance to oxidative death in cortical neurons without toxicity and reveals a role for cytoplasmic p21(waf1/cip1) in cell cycle-independent neuroprotection. J Neurosci 28:163-176.

Lee DC, Mason CW, Goodman CB, Holder MS, Kirksey OW, Womble TA, Severs WB, Palm DE (2007) Hydrogen peroxide induces lysosomal protease alterations in PC12 cells. Neurochem Res 32:1499-1510.

Lee do H, Goldberg AL (2010) Hsp104 is essential for the selective degradation in yeast of polyglutamine expanded ataxin-1 but not most misfolded proteins generally. Biochem Biophys Res Commun 391:1056-1061.

Leng Y, Liang MH, Ren M, Marinova Z, Leeds P, Chuang DM (2008) Synergistic neuroprotective effects of lithium and valproic acid or other histone deacetylase inhibitors in neurons: roles of glycogen synthase kinase-3 inhibition. J Neurosci 28:2576-2588.

Li F, Macfarlan T, Pittman RN, Chakravarti D (2002) Ataxin-3 is a histone-binding protein with two independent transcriptional corepressor activities. J Biol Chem 277:45004-45012.

Limprasert P, Nouri N, Heyman RA, Nopparatana C, Kamonsilp M,

Deininger PL, Keats BJ (1996) Analysis of CAG repeat of the Machado-Joseph gene in human, chimpanzee and monkey populations: a variant nucleotide is associated with the number of CAG repeats. Hum Mol Genet 5:207-213.

Maher P, Hanneken A (2005) The molecular basis of oxidative stress-induced cell death in an immortalized retinal ganglion cell line. Invest Ophthalmol Vis Sci 46:749-757.

Mann BS, Johnson JR, Cohen MH, Justice R, Pazdur R (2007) FDA approval summary: vorinostat for treatment of advanced primary cutaneous T-cell lymphoma. Oncologist 12:1247-1252.

Manto MU (2005) The wide spectrum of spinocerebellar ataxias (SCAs). Cerebellum 4:2-6.

Mao Y, Senic-Matuglia F, Di Fiore PP, Polo S, Hodsdon ME, De Camilli P (2005) Deubiquitinating function of ataxin-3: insights from the solution structure of the Josephin domain. Proc Natl Acad Sci U S A 102:12700-12705.

Marcora E, Kennedy MB (2010) The Huntington's disease mutation impairs Huntingtin's role in the transport of NF-kappaB from the synapse to the nucleus. Hum Mol Genet 19:4373-4384.

Martinez-Vicente M, Talloczy Z, Wong E, Tang G, Koga H, Kaushik S, de Vries R, Arias E, Harris S, Sulzer D, Cuervo AM (2010) Cargo recognition failure is responsible for inefficient autophagy in Huntington's disease. Nat Neurosci 13:567-576.

Mathis DJ, Oudet P, Wasylyk B, Chambon P (1978) Effect of histone acetylation on structure and in vitro transcription of chromatin.

Nucleic Acids Res 5:3523-3547.

Matsumoto M, Yada M, Hatakeyama S, Ishimoto H, Tanimura T, Tsuji S, Kakizuka A, Kitagawa M, Nakayama KI (2004) Molecular clearance of ataxin-3 is regulated by a mammalian E4. EMBO J 23:659-669.

Menzies FM, Huebener J, Renna M, Bonin M, Riess O, Rubinsztein DC (2010) Autophagy induction reduces mutant ataxin-3 levels and toxicity in a mouse model of spinocerebellar ataxia type 3. Brain 133:93-104.

Mishra A, Godavarthi SK, Maheshwari M, Goswami A, Jana NR (2009) The ubiquitin ligase E6-AP is induced and recruited to aggresomes in response to proteasome inhibition and may be involved in the ubiquitination of Hsp70-bound misfolded proteins. J Biol Chem 284:10537-10545.

Miyata R, Hayashi M, Tanuma N, Shioda K, Fukatsu R, Mizutani S (2008) Oxidative stress in neurodegeneration in dentatorubral-pallidoluysian atrophy. J Neurol Sci 264:133-139.

Naito H, Oyanagi S (1982) Familial myoclonus epilepsy and choreoathetosis: hereditary dentatorubral-pallidoluysian atrophy. Neurology 32:798-807.

Netravathi M, Pal PK, Purushottam M, Thennarasu K, Mukherjee M, Jain S (2009) Spinocerebellar ataxias types 1, 2 and 3: age adjusted clinical severity of disease at presentation correlates with size of CAG repeat lengths. J Neurol Sci 277:83-86.

Nucifora FC, Jr., Ellerby LM, Wellington CL, Wood JD, Herring WJ,

Sawa A, Hayden MR, Dawson VL, Dawson TM, Ross CA (2003) Nuclear localization of a non-caspase truncation product of atrophin-1, with an expanded polyglutamine repeat, increases cellular toxicity. J Biol Chem 278:13047-13055.

Orr HT, Zoghbi HY (2007) Trinucleotide repeat disorders. Annu Rev Neurosci 30:575-621.

Palazzolo I, Burnett BG, Young JE, Brenne PL, La Spada AR, Fischbeck KH, Howell BW, Pennuto M (2007) Akt blocks ligand binding and protects against expanded polyglutamine androgen receptor toxicity. Hum Mol Genet 16:1593-1603.

Palhan VB, Chen S, Peng GH, Tjernberg A, Gamper AM, Fan Y, Chait BT, La Spada AR, Roeder RG (2005) Polyglutamine-expanded ataxin-7 inhibits STAGA histone acetyltransferase activity to produce retinal degeneration. Proc Natl Acad Sci U S A 102:8472-8477.

Pandolfo M (2008) Drug Insight: antioxidant therapy in inherited ataxias. Nat Clin Pract Neurol 4:86-96.

Panov AV, Gutekunst CA, Leavitt BR, Hayden MR, Burke JR, Strittmatter WJ, Greenamyre JT (2002) Early mitochondrial calcium defects in Huntington's disease are a direct effect of polyglutamines. Nat Neurosci 5:731-736.

Paulson HL, Perez MK, Trottier Y, Trojanowski JQ, Subramony SH, Das SS, Vig P, Mandel JL, Fischbeck KH, Pittman RN (1997) Intranuclear inclusions of expanded polyglutamine protein in spinocerebellar ataxia type 3. Neuron 19:333-344.

Pearson CE, Nichol Edamura K, Cleary JD (2005) Repeat instability: mechanisms of dynamic mutations. Nat Rev Genet 6:729-742.

Peng GS, Li G, Tzeng NS, Chen PS, Chuang DM, Hsu YD, Yang S, Hong JS (2005) Valproate pretreatment protects dopaminergic neurons from LPS-induced neurotoxicity in rat primary midbrain cultures: role of microglia. Brain Res Mol Brain Res 134:162-169.

Perez-Severiano F, Escalante B, Vergara P, Rios C, Segovia J (2002) Age-dependent changes in nitric oxide synthase activity and protein expression in striata of mice transgenic for the Huntington's disease mutation. Brain Res 951:36-42.

Perez MK, Paulson HL, Pendse SJ, Saionz SJ, Bonini NM, Pittman RN (1998) Recruitment and the role of nuclear localization in polyglutamine-mediated aggregation. J Cell Biol 143:1457-1470.

Pias EK, Ekshyyan OY, Rhoads CA, Fuseler J, Harrison L, Aw TY (2003) Differential effects of superoxide dismutase isoform expression on hydroperoxide-induced apoptosis in PC-12 cells. J Biol Chem 278:13294-13301.

Piccioli P, Porcile C, Stanzione S, Bisaglia M, Bajetto A, Bonavia R, Florio T, Schettini G (2001) Inhibition of nuclear factor-kappaB activation induces apoptosis in cerebellar granule cells. J Neurosci Res 66:1064-1073.

Puranam KL, Wu G, Strittmatter WJ, Burke JR (2006) Polyglutamine expansion inhibits respiration by increasing reactive oxygen species in isolated mitochondria. Biochem Biophys Res Commun 341:607-613.

Qin ZH, Wang Y, Kegel KB, Kazantsev A, Apostol BL, Thompson LM, Yoder J, Aronin N, DiFiglia M (2003) Autophagy regulates the processing of amino terminal huntingtin fragments. Hum Mol Genet 12:3231-3244.

Ranen NG, Stine OC, Abbott MH, Sherr M, Codori AM, Franz ML, Chao NI, Chung AS, Pleasant N, Callahan C, et al. (1995) Anticipation and instability of IT-15 (CAG)n repeats in parent-offspring pairs with Huntington disease. Am J Hum Genet 57:593-602.

Ranganathan S, Harmison GG, Meyertholen K, Pennuto M, Burnett BG, Fischbeck KH (2009) Mitochondrial abnormalities in spinal and bulbar muscular atrophy. Hum Mol Genet 18:27-42.

Rasmussen A, De Biase I, Fragoso-Benitez M, Macias-Flores MA, Yescas P, Ochoa A, Ashizawa T, Alonso ME, Bidichandani SI (2007) Anticipation and intergenerational repeat instability in spinocerebellar ataxia type 17. Ann Neurol 61:607-610.

Ravikumar B, Duden R, Rubinsztein DC (2002) Aggregate-prone proteins with polyglutamine and polyalanine expansions are degraded by autophagy. Hum Mol Genet 11:1107-1117.

Ravikumar B, Vacher C, Berger Z, Davies JE, Luo S, Oroz LG, Scaravilli F, Easton DF, Duden R, O'Kane CJ, Rubinsztein DC (2004) Inhibition of mTOR induces autophagy and reduces toxicity of polyglutamine expansions in fly and mouse models of Huntington disease. Nat Genet 36:585-595.

Reijonen S, Kukkonen JP, Hyrskyluoto A, Kivinen J, Kairisalo M, Takei N, Lindholm D, Korhonen L (2010) Downregulation of

NF-kappaB signaling by mutant huntingtin proteins induces oxidative stress and cell death. Cell Mol Life Sci 67:1929-1941.

Reina CP, Zhong X, Pittman RN (2010) Proteotoxic stress increases nuclear localization of ataxin-3. Hum Mol Genet 19:235-249.

Ring RH, Alder J, Fennell M, Kouranova E, Black IB, Thakker-Varia S (2006) Transcriptional profiling of brain-derived-neurotrophic factor-induced neuronal plasticity: a novel role for nociceptin in hippocampal neurite outgrowth. J Neurobiol 66:361-377.

Rodrigues AJ, do Carmo Costa M, Silva TL, Ferreira D, Bajanca F, Logarinho E, Maciel P (2010) Absence of ataxin-3 leads to cytoskeletal disorganization and increased cell death. Biochim Biophys Acta 1803:1154-1163.

Rosenberg RN (1992) Machado-Joseph disease: an autosomal dominant motor system degeneration. Mov Disord 7:193-203.

Rosenberg RN (1995) Autosomal dominant cerebellar phenotypes: the genotype has settled the issue. Neurology 45:1-5.

Roze E, Betuing S, Deyts C, Marcon E, Brami-Cherrier K, Pages C, Humbert S, Merienne K, Caboche J (2008) Mitogen- and stress-activated protein kinase-1 deficiency is involved in expanded-huntingtin-induced transcriptional dysregulation and striatal death. FASEB J 22:1083-1093.

Rub U, de Vos RA, Brunt ER, Sebesteny T, Schols L, Auburger G, Bohl J, Ghebremedhin E, Gierga K, Seidel K, den Dunnen W, Heinsen H, Paulson H, Deller T (2006) Spinocerebellar ataxia type 3 (SCA3): thalamic neurodegeneration occurs independently from thalamic

ataxin-3 immunopositive neuronal intranuclear inclusions. Brain Pathol 16:218-227.

Ryu H, Lee J, Olofsson BA, Mwidau A, Dedeoglu A, Escudero M, Flemington E, Azizkhan-Clifford J, Ferrante RJ, Ratan RR (2003) Histone deacetylase inhibitors prevent oxidative neuronal death independent of expanded polyglutamine repeats via an Sp1-dependent pathway. Proc Natl Acad Sci U S A 100:4281-4286.

Ryu J, Cho S, Park BC, Lee do H (2010) Oxidative stress-enhanced SUMOylation and aggregation of ataxin-1: Implication of JNK pathway. Biochem Biophys Res Commun 393:280-285.

Saha RN, Pahan K (2006) HATs and HDACs in neurodegeneration: a tale of disconcerted acetylation homeostasis. Cell Death Differ 13:539-550.

Sarkar S, Krishna G, Imarisio S, Saiki S, O'Kane CJ, Rubinsztein DC (2008) A rational mechanism for combination treatment of Huntington's disease using lithium and rapamycin. Hum Mol Genet 17:170-178.

Sarkar S, Floto RA, Berger Z, Imarisio S, Cordenier A, Pasco M, Cook LJ, Rubinsztein DC (2005) Lithium induces autophagy by inhibiting inositol monophosphatase. J Cell Biol 170:1101-1111.

Sato N, Amino T, Kobayashi K, Asakawa S, Ishiguro T, Tsunemi T, Takahashi M, Matsuura T, Flanigan KM, Iwasaki S, Ishino F, Saito Y, Murayama S, Yoshida M, Hashizume Y, Takahashi Y, Tsuji S, Shimizu N, Toda T, Ishikawa K, Mizusawa H (2009a) Spinocerebellar ataxia type 31 is associated with "inserted"

penta-nucleotide repeats containing (TGGAA)n. Am J Hum Genet 85:544-557.

Sato T, Miura M, Yamada M, Yoshida T, Wood JD, Yazawa I, Masuda M, Suzuki T, Shin RM, Yau HJ, Liu FC, Shimohata T, Onodera O, Ross CA, Katsuki M, Takahashi H, Kano M, Aosaki T, Tsuji S (2009b) Severe neurological phenotypes of Q129 DRPLA transgenic mice serendipitously created by en masse expansion of CAG repeats in Q76 DRPLA mice. Hum Mol Genet 18:723-736.

Sayre LM, Perry G, Smith MA (2008) Oxidative stress and neurotoxicity. Chem Res Toxicol 21:172-188.

Schols L, Bauer P, Schmidt T, Schulte T, Riess O (2004) Autosomal dominant cerebellar ataxias: clinical features, genetics, and pathogenesis. Lancet Neurol 3:291-304.

Silveira I, Lopes-Cendes I, Kish S, Maciel P, Gaspar C, Coutinho P, Botez MI, Teive H, Arruda W, Steiner CE, Pinto-Junior W, Maciel JA, Jerin S, Sack G, Andermann E, Sudarsky L, Rosenberg R, MacLeod P, Chitayat D, Babul R, Sequeiros J, Rouleau GA (1996) Frequency of spinocerebellar ataxia type 1, dentatorubropallidoluysian atrophy, and Machado-Joseph disease mutations in a large group of spinocerebellar ataxia patients. Neurology 46:214-218.

Song C, Perides G, Liu YF (2002) Expression of full-length polyglutamine-expanded Huntingtin disrupts growth factor receptor signaling in rat pheochromocytoma (PC12) cells. J Biol Chem 277:6703-6707.

Song W, Chen J, Petrilli A, Liot G, Klinglmayr E, Zhou Y, Poquiz P, Tjong J, Pouladi MA, Hayden MR, Masliah E, Ellisman M, Rouiller I, Schwarzenbacher R, Bossy B, Perkins G, Bossy-Wetzel E (2011) Mutant huntingtin binds the mitochondrial fission GTPase dynamin-related protein-1 and increases its enzymatic activity. Nat Med 17:377-382.

Steffan JS, Bodai L, Pallos J, Poelman M, McCampbell A, Apostol BL, Kazantsev A, Schmidt E, Zhu YZ, Greenwald M, Kurokawa R, Housman DE, Jackson GR, Marsh JL, Thompson LM (2001) Histone deacetylase inhibitors arrest polyglutamine-dependent neurodegeneration in Drosophila. Nature 413:739-743.

Stetler RA, Cao G, Gao Y, Zhang F, Wang S, Weng Z, Vosler P, Zhang L, Signore A, Graham SH, Chen J (2008) Hsp27 protects against ischemic brain injury via attenuation of a novel stress-response cascade upstream of mitochondrial cell death signaling. J Neurosci 28:13038-13055.

Sun F, Anantharam V, Zhang D, Latchoumycandane C, Kanthasamy A, Kanthasamy AG (2006) Proteasome inhibitor MG-132 induces dopaminergic degeneration in cell culture and animal models. Neurotoxicology 27:807-815.

Suzuki-Mizushima Y, Gohda E, Okamura T, Kanasaki K, Yamamoto I (2002) Enhancement of NGF- and cholera toxin-induced neurite outgrowth by butyrate in PC12 cells. Brain Res 951:209-217.

Swami M, Hendricks AE, Gillis T, Massood T, Mysore J, Myers RH, Wheeler VC (2009) Somatic expansion of the Huntington's disease

CAG repeat in the brain is associated with an earlier age of disease onset. Hum Mol Genet 18:3039-3047.

Tanida I, Ueno T, Kominami E (2004) Human light chain 3/MAP1LC3B is cleaved at its carboxyl-terminal Met121 to expose Gly120 for lipidation and targeting to autophagosomal membranes. J Biol Chem 279:47704-47710.

Taylor JP, Hardy J, Fischbeck KH (2002) Toxic proteins in neurodegenerative disease. Science 296:1991-1995.

Trottier Y, Lutz Y, Stevanin G, Imbert G, Devys D, Cancel G, Saudou F, Weber C, David G, Tora L, et al. (1995) Polyglutamine expansion as a pathological epitope in Huntington's disease and four dominant cerebellar ataxias. Nature 378:403-406.

Tsai HF, Tsai HJ, Hsieh M (2004) Full-length expanded ataxin-3 enhances mitochondrial-mediated cell death and decreases Bcl-2 expression in human neuroblastoma cells. Biochem Biophys Res Commun 324:1274-1282.

Tsai HF, Lin SJ, Li C, Hsieh M (2005) Decreased expression of Hsp27 and Hsp70 in transformed lymphoblastoid cells from patients with spinocerebellar ataxia type 7. Biochem Biophys Res Commun 334:1279-1286.

Tsirigotis M, Baldwin RM, Tang MY, Lorimer IA, Gray DA (2008) Activation of p38MAPK contributes to expanded polyglutamine-induced cytotoxicity. PLoS One 3:e2130.

Uo T, Veenstra TD, Morrison RS (2009) Histone deacetylase inhibitors prevent p53-dependent and p53-independent Bax-mediated

neuronal apoptosis through two distinct mechanisms. J Neurosci 29:2824-2832.

van de Warrenburg BP, Sinke RJ, Verschuuren-Bemelmans CC, Scheffer H, Brunt ER, Ippel PF, Maat-Kievit JA, Dooijes D, Notermans NC, Lindhout D, Knoers NV, Kremer HP (2002) Spinocerebellar ataxias in the Netherlands: prevalence and age at onset variance analysis. Neurology 58:702-708.

van Tijn P, de Vrij FM, Schuurman KG, Dantuma NP, Fischer DF, van Leeuwen FW, Hol EM (2007) Dose-dependent inhibition of proteasome activity by a mutant ubiquitin associated with neurodegenerative disease. J Cell Sci 120:1615-1623.

Varma H, Cheng R, Voisine C, Hart AC, Stockwell BR (2007) Inhibitors of metabolism rescue cell death in Huntington's disease models. Proc Natl Acad Sci U S A 104:14525-14530.

Veal EA, Day AM, Morgan BA (2007) Hydrogen peroxide sensing and signaling. Mol Cell 26:1-14.

Waelter S, Boeddrich A, Lurz R, Scherzinger E, Lueder G, Lehrach H, Wanker EE (2001) Accumulation of mutant huntingtin fragments in aggresome-like inclusion bodies as a result of insufficient protein degradation. Mol Biol Cell 12:1393-1407.

Wang H, Lim PJ, Karbowski M, Monteiro MJ (2009) Effects of overexpression of huntingtin proteins on mitochondrial integrity. Hum Mol Genet 18:737-752.

Wang H, Lim PJ, Yin C, Rieckher M, Vogel BE, Monteiro MJ (2006) Suppression of polyglutamine-induced toxicity in cell and animal

models of Huntington's disease by ubiquilin. Hum Mol Genet 15:1025-1041.

Wang H, Jia N, Fei E, Wang Z, Liu C, Zhang T, Fan J, Wu M, Chen L, Nukina N, Zhou J, Wang G (2007a) p45, an ATPase subunit of the 19S proteasome, targets the polyglutamine disease protein ataxin-3 to the proteasome. J Neurochem 101:1651-1661.

Wang HL, He CY, Chou AH, Yeh TH, Chen YL, Li AH (2007b) Polyglutamine-expanded ataxin-7 decreases nuclear translocation of NF-kappaB p65 and impairs NF-kappaB activity by inhibiting proteasome activity of cerebellar neurons. Cell Signal 19:573-581.

Wang H-H (2007) Evaluation of therapeutic effect of valproic acid in polyglutamine-expanded cell and animal models. Dept of LifeScience, NTNU, Taiwan, Taipei, Master's thesis

Wen FC, Li YH, Tsai HF, Lin CH, Li C, Liu CS, Lii CK, Nukina N, Hsieh M (2003) Down-regulation of heat shock protein 27 in neuronal cells and non-neuronal cells expressing mutant ataxin-3. FEBS Lett 546:307-314.

Williams AJ, Knutson TM, Colomer Gould VF, Paulson HL (2009) In vivo suppression of polyglutamine neurotoxicity by C-terminus of Hsp70-interacting protein (CHIP) supports an aggregation model of pathogenesis. Neurobiol Dis 33:342-353.

Wyttenbach A, Sauvageot O, Carmichael J, Diaz-Latoud C, Arrigo AP, Rubinsztein DC (2002) Heat shock protein 27 prevents cellular polyglutamine toxicity and suppresses the increase of reactive oxygen species caused by huntingtin. Hum Mol Genet

11:1137-1151.

Wyttenbach A, Carmichael J, Swartz J, Furlong RA, Narain Y, Rankin J, Rubinsztein DC (2000) Effects of heat shock, heat shock protein 40 (HDJ-2), and proteasome inhibition on protein aggregation in cellular models of Huntington's disease. Proc Natl Acad Sci U S A 97:2898-2903.

Xie Y, Hayden MR, Xu B (2010) BDNF overexpression in the forebrain rescues Huntington's disease phenotypes in YAC128 mice. J Neurosci 30:14708-14718.

Yamagishi N, Goto K, Nakagawa S, Saito Y, Hatayama T (2010) Hsp105 reduces the protein aggregation and cytotoxicity by expanded-polyglutamine proteins through the induction of Hsp70. Exp Cell Res 316:2424-2433.

Yen H-H (2010) Establishment of and inducible cell model system for spinocerebellar ataxia type 3 potential drug screen. Dept of LifeScience, NTNU, Taiwan, Taipei, Master's thesis

Yoshizawa T, Yamagishi Y, Koseki N, Goto J, Yoshida H, Shibasaki F, Shoji S, Kanazawa I (2000) Cell cycle arrest enhances the in vitro cellular toxicity of the truncated Machado-Joseph disease gene product with an expanded polyglutamine stretch. Hum Mol Genet 9:69-78.

Young JE, Gouw L, Propp S, Sopher BL, Taylor J, Lin A, Hermel E, Logvinova A, Chen SF, Chen S, Bredesen DE, Truant R, Ptacek LJ, La Spada AR, Ellerby LM (2007) Proteolytic cleavage of ataxin-7 by caspase-7 modulates cellular toxicity and transcriptional

dysregulation. J Biol Chem 282:30150-30160.

Yu YC, Kuo CL, Cheng WL, Liu CS, Hsieh M (2009) Decreased antioxidant enzyme activity and increased mitochondrial DNA damage in cellular models of Machado-Joseph disease. J Neurosci Res 87:1884-1891.

Zaveri NT, Waleh N, Toll L (2006) Regulation of the prepronociceptin gene and its effect on neuronal differentiation. Gene 384:27-36.

Zhao K, Luo G, Giannelli S, Szeto HH (2005) Mitochondria-targeted peptide prevents mitochondrial depolarization and apoptosis induced by tert-butyl hydroperoxide in neuronal cell lines. Biochem Pharmacol 70:1796-1806.

Zourlidou A, Gidalevitz T, Kristiansen M, Landles C, Woodman B, Wells DJ, Latchman DS, de Belleroche J, Tabrizi SJ, Morimoto RI, Bates GP (2007) Hsp27 overexpression in the R6/2 mouse model of Huntington's disease: chronic neurodegeneration does not induce Hsp27 activation. Hum Mol Genet 16:1078-1090.

Zuccato C, Ciammola A, Rigamonti D, Leavitt BR, Goffredo D, Conti L, MacDonald ME, Friedlander RM, Silani V, Hayden MR, Timmusk T, Sipione S, Cattaneo E (2001) Loss of huntingtin-mediated BDNF gene transcription in Huntington's disease. Science 293:493-498.

Appendix Table 1.HDAC targets of the HDACi used in this study.

HDAC		L-BMX	L-1027	Trichostatin A[1]
HDAC-1	HILLSLOPE			-0.96
	IC50 (M)			3.37E-09
HDAC-2	HILLSLOPE			-0.85
	IC50 (M)			7.14E-09
HDAC-3	HILLSLOPE	-0.88		-0.93
	IC50 (M)	2.73E-05		5.55E-09
HDAC-4	HILLSLOPE			-0.30
	IC50 (M)			9.51E-08
HDAC-5	HILLSLOPE			-0.88
	IC50 (M)			6.99E-09
HDAC-6	HILLSLOPE			-1.22
	IC50 (M)			9.96E-10
HDAC-7	HILLSLOPE			-0.65
	IC50 (M)			2.46E-08
HDAC-8	HILLSLOPE	-1.09	-1.20	-1.01
	IC50 (M)	8.31E-07	1.60E-06	1.31E-07
HDAC-9	HILLSLOPE			-0.88
	IC50 (M)			1.39E-08
HDAC-10	HILLSLOPE			-0.88
	IC50 (M)			1.14E-08
HDAC-11	HILLSLOPE			-0.96
	IC50 (M)			6.15E-09

[1]Trichostatin A was used as a pan-HDACi positive control.

Table 1. Primer list in this study

Primer name	sequence	Tm	Product size (bp)
SCA3 c69 F’	5’-GGATCCCCACCATGGATGA		856 (27Q)
	CAGTGTTTTTTCTC-3’		1000 (75Q)
SCA3 c219 F’	5’-GGATCCCCACCATGTTAGA		427 (27Q)
	AGCAAATATGCTC-3’		571 (75Q)
SCA3 c257 F’	5’-GGATCCCCACCATGCAAGG	65℃	292 (27Q)
	TAGTTCCAGAAACATATC-3’		430 (75Q)
SCA3 R’	5’- TCTAGACCTAGATCACT		
	CCAAGTGCTCCTG-3’		
SCA3	5’-CCAGAAACATATCTCAAGA	55℃	252 (27Q)
Repeat F’	TATG-3’		396 (75Q)

Table 2. Antibody list in this study

Protein	Manufacturer	Titer	Source	MW (kDa)
Ataxin-3	Chemicon	1:2000	mouse	43/48/60
β-actin	Millipore	1:2000	mouse	43
AKT	Epitomics	1:1000	rabbit	60
P-AKT (Ser473)	Epitomics	1:1000	rabbit	60
GSK3β	Santa Cruz Biotechnology	1:1000	goat	47
P-GSK-3β (Ser9)	Santa Cruz Biotechnology	1:1000	rabbit	47
ERK1/2	Cell signaling	1:1000	rabbit	42/44
P-ERK1/2 (Thr202/204)	Cell signaling	1:2000	rabbit	42/44
P-MEK1/2 (Ser217/221)	Cell signaling	1:1000	rabbit	45
P-c-RAF (Ser338)	Cell signaling	1:1000	rabbit	74
P-90RSK (Ser380)	Cell signaling	1:1000	rabbit	90
Hsp27	Santa Cruz Biotechnology	1:1000	mouse	27
Hsp70	Cell signaling	1:1000	rabbit	70
AcH4/H4	Cell signaling	1:2000	rabbit	11

Protein	Manufacturer	Titer	Source	MW (kDa)
AcH3/H3	Cell signaling	1:2000	rabbit	17
AcH2A/H2A	Cell signaling	1:2000	rabbit	14
AcH2B/H2B	Cell signaling	1:2000	rabbit	14
LC-3	MBL	1:1000	rabbit	16/18
JNK	Cell signaling	1:1000	rabbit	46/54
P-JNK (Thr183/185)	Cell signaling	1:1000	rabbit	46/54
NFκB	Millipore	1:2000	rabbit	65
p38	Cell signaling	1:1000	rabbit	38
P-p38 (Thr180/182)	Cell signaling	1:1000	rabbit	38
MnSOD	Upstate Biotechnologies	1:1000	rabbit	26
Ubiquitin	Santa Cruz Biotechnology	1:500	goat	

Table 3.IC_{50} of SAHA and 8 novelHDACi compounds on SCA3 cells.

	IC_{50}(μM)		
HDACi	V	27Q	75Q
SAHA	5.1	5.1	4.8
L-1027	12.9	13.8	11.8
1209	28.3	40.8	18.0
L-BMX	19.4	13.8	11.1
TP	——	84.5	25.0
0225	9.2	11.6	9.9
0311	15.2	15.0	9.4
0312	15.1	17.9	9.2
0319	6.7	9.1	8.7

Table 4. HDACi therapy in polyQ disease

polyQ disease	model	HDACi	molecular mechanism	survival	motor function	aggregation	weight	effect on neuropathology or other	reference
HD	Drosophila	SAHA, Sodium butyrate	Ac-H4 ↑	↑		no effect		correct no. of ommatidia ↑	(Steffan et al., 2001)
HD	R6/2	SAHA	Ac-H4 ↑ Ac-H2B ↑	↑	↑	no effect	↑		(Hockly et al., 2003)
HD	R6/2	Sodium butyrate	Ac-H3 ↑ Ac-H4 ↑ HAT: Sp1 ↑ Ac-Striatal tissue ↑ mRNA ↑	↑	↑	no effect	↑	striatal neuron area ↑	(Ferrante et al., 2003)
HD	N171-82Q transgene mouse	Phenylbu-tyrate	Caspase 3 ↓ Caspase 9 ↓ UPS protein ↑ Glutathione-S-transferase ↑ Ac-H3 ↑ Ac-H4 ↑ Ac-Striatal tissue ↑	↑				size of neostriatum ↑ neuron atrophy ↓	(Gardian et al., 2005)
HD	HEK293, COS7, Hdh 109Q mouse	SAHA, TSA	BDNF ↑ Ac-tubulin ↑ Ac-H3 ↑ HDAC6 ↑					mortor complex protein ↑ BNDF transport ↑ Improve Microtubule dynamics	(Dompierre et al., 2007)

polyQ disease	model	HDACi	molecular mechanism		survival	motor function	aggregation	weight	effect on neuropathology or other	reference
HD	R6/2, STHdh cell, ST14a cell	Phenylbuty-rate, sodium butyrate	mRNA Ac-H3	↑ ↑					Rescue transcription dysfunction in HD	(Sadri-Vakili et al., 2007)
HD	R6/2, HD-yeast 103Q	SAHA, sodium butyrate	3-HK	↓					protect neuron after LPS challenge rescue abnormal increase of 3-HK in HD	(Giorgini et al., 2008)
HD	R6/2	HDACi-4b	Ac-H3 mRNA	↑ ↑		↑	No effect	↑	Striatum volume ↑ Reverse mRNA abnormalities Clasping ↓	(Thomas et al., 2008)
HD	Drosophila	Inhibition of HDAC: Sir2 and Rpd3 HDACi drug: NAM, niacin	Sir2 Rpd3	↓ ↓	↑				correct no. of ommatidia ↑ eclosion ↑	(Pallos et al., 2008)
HD	c-elegant, Htt571-72 mouse, COS7	TSA+NAM	Ac-Htt CBP P300 Caspase3/7 LC-3	↑ ↑ ↑ ↓ ↑			↓		no neurodegeneration clearance mutant Htt active autophagy pathway	(Jeong et al., 2009)
HD	YAC128 STHdh Q111	TSA, sodium butyrate	Ac-H3 NMDAR	↑ ↑					rescue early neuron dysfunction Ca^{2+} homeostasis	(Oliveira et al., 2006)

polyQ disease	model	HDACi	molecular mechanism	survival	motor function	aggregation	weight	effect on neuropathology or other	reference
HD	c-elegant	Knock down HDAC3						degeneration ↓	(Bates et al., 2006)
HD	R6/2	SAHA, knock down HDAC7	HDAC7 ↓					Knock down HDAC7: no effect	(Benn et al., 2009)
HD	R6/1	NAM	PGC-1α ↑ BNDF ↑		↑	no effect	↑		(Hathorn et al., 2011)
SCA3	SCA3-Q79 mouse	Sodium butyrate	Ac-H3 ↑ Ac-H4 ↑ Hsp family ↑ neuroprotected mRNA ↑	↑	↑		↑	abnormalities of neurite morphology ↓	(Chou et al., 2011)
SBMA	AR-Q79 mouse, MN-1	TSA, SAHA, sodium butyrate	Ac-H3 ↑ CBP ↑	↑				Overexpression CBP as the same result which was seen in HDACi drug treatment	(McCampbell et al., 2001)
SBMA	AR-Q97 mouse	sodium butyrate	Ac-H3	↑	↑	↑	no effect	↑	muscle fiber diameter ↑	(Minamiya ma et al., 2004)
DRPLA			Ac-H3	↑	↑	↑			(Ying et al., 2006)

Table 5. The neuroprotective pathways examined after L-BMX treatment in the SCA3 cell model.

	Neuroprotected effect	27Q L-BMX	75Q L-BMX
Hsp27	neuron protection and prevention of oxidative stress mediate apoptosis *(Gorman et al., 2005; Stetler et al., 2008; Friedman et al., 2009)*	—	↑
NF-κB	cerebellar granule neuron survival, decrease oxidative stress *(Koulish et al.,2001; Piccioli et al.,2001)*	↑	↑
MnSOD	decrease oxidative stress and improve protein aggregation *(Dumont et al., 2009)*	↑	↑
P-GSK3β	Increased ERK, autophage *(Hao et al., 2004; Sarkar et al., 2005; Sarkar et al., 2008)*	—	↓
ERK pathway	Improve neurite outgrowth , cell survival *(Apostol et al., 2006; Hao et al., 2004)*	—	↑
JNK pathway	disrupt ERK pathway and lead to cell death in SCA1 and HD *(Apostol et al., 2006; Varma et al., 2007; Roze et al., 2008; Tsirigotis et al., 2008)*	—	↓
LC3 II	clean the aggregation protein *(Martinez-Vicente et al., 2010)*	↑	↑
Ac-H2A		—	↑

level was —, expression retained after L-BMX treatment; ↑ , expression level was upregulated after L-BMX treatment; ↓ , expression level was downregulated after L-BMX treatment.

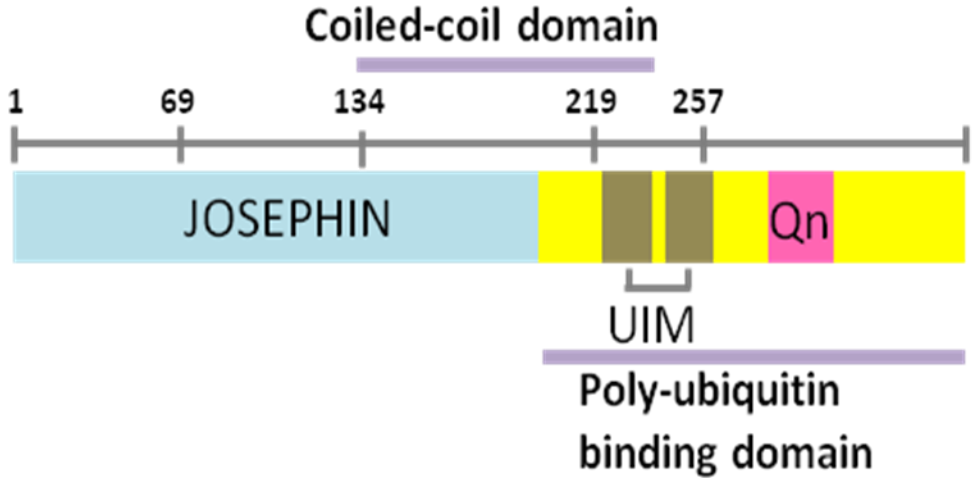

Appendix figure 1. Schematic diagram of AT3 protein structure

There are three domains in AT3 protein. Blue, the Josephin domain.Yellow, the poly-ubiquitin domain.Brown, the UIM motif.Pink, the CAG coding region. (modified form Berke et al., 2005)

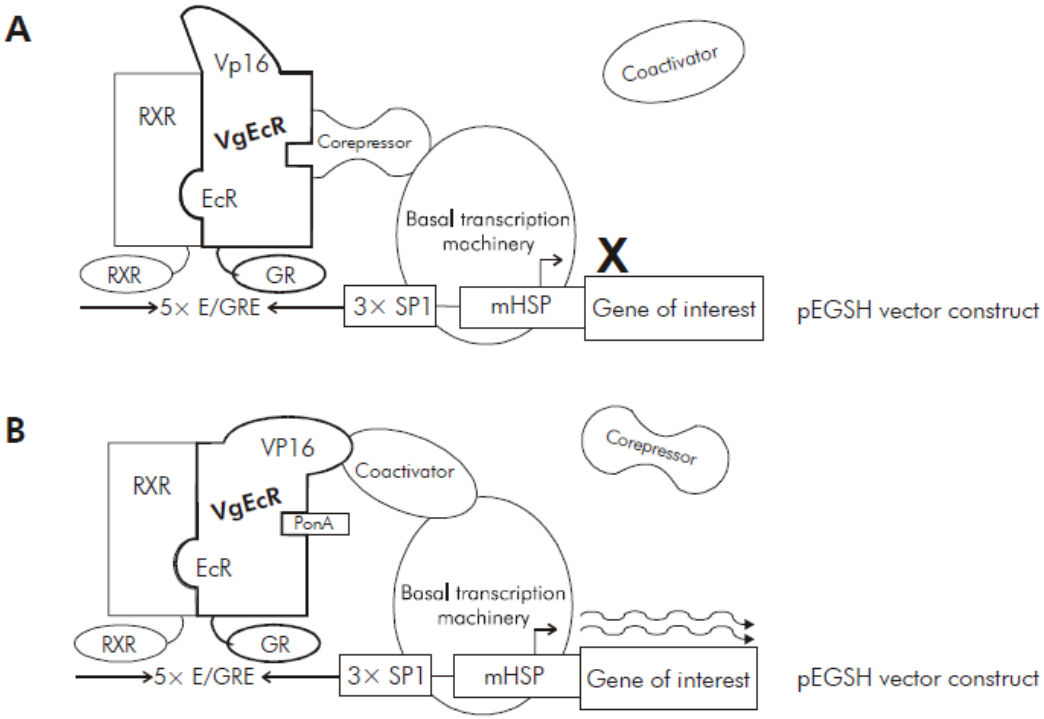

Appendix figure 2. Complete Control Inducible Mammalian Expression System® overview

A. The corepressor bound to VgEcR so that gene of interest in pEGSH vector construct couldn't be transcribed in the absence of ponA.

B. Gene of interest in pEGSH could be turned on in the presence of ponA. The corepressor was released from VgEcR, and the coactivator would bind to VgEcRto active the gene expression.

A

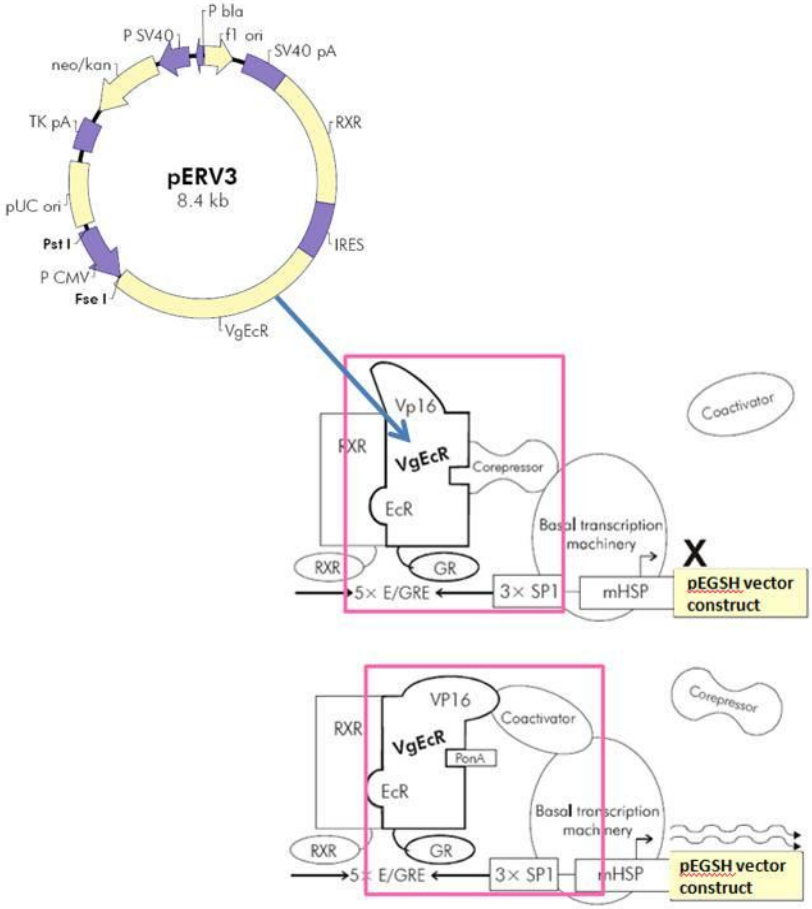
P bla
P SV40
f1 ori
SV40 pA
neo/kan
RXR
TK pA
pERV3
8.4 kb
pUC ori
IRES
Pst I
P CMV
Fse I
VgEcR
Vp16
RXR
VgEcR
Coactivator
Corepressor
EcR
Basal transcription machinery
X
RXR
GR
5× E/GRE
3× SP1
mHSP
pEGSH vector construct
VP16
Coactivator
Corepressor
RXR
VgEcR
PonA
EcR
Basal transcription machinery
RXR
GR
5× E/GRE
3× SP1
mHSP
pEGSH vector construct

B

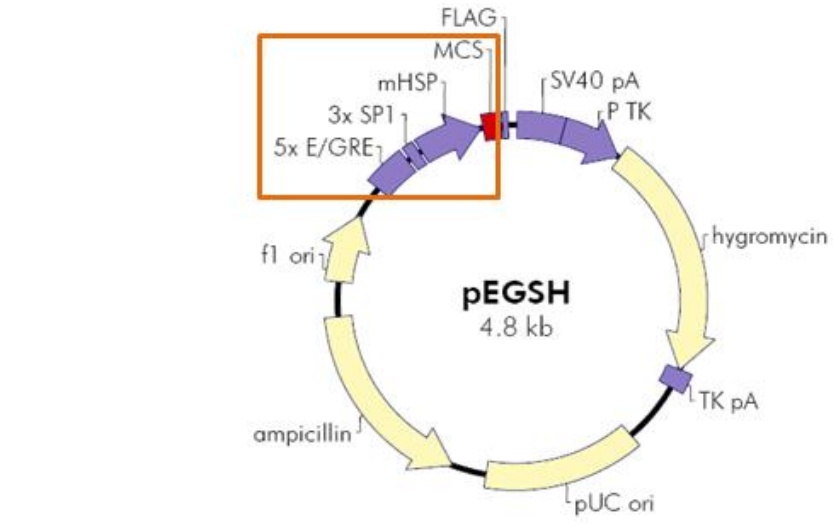
FLAG
MCS
mHSP
SV40 pA
3x SP1
P TK
5x E/GRE
hygromycin
f1 ori
pEGSH
4.8 kb
TK pA
ampicillin
pUC ori

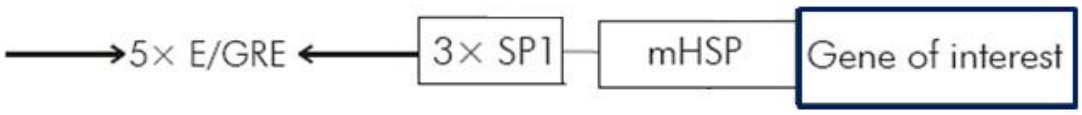
5× E/GRE
3× SP1
mHSP
Gene of interest

Appendix figure 3. Maps of the pERV3 vector and pEGSH vector

(A) The pERV3 vector includes VgEcR and RXR domains which could form heterodimer and control the downstream gene expression in pEGSH construct by the presence or absence of ponA. The neomycin antibiotic site could supply G418 resistant selection. **(B)** The pEGSH vector contains a ponA-inducible expression cassette and MCS for interest gene insertion. It has two antibiotics site for selection and flag as an epitope.

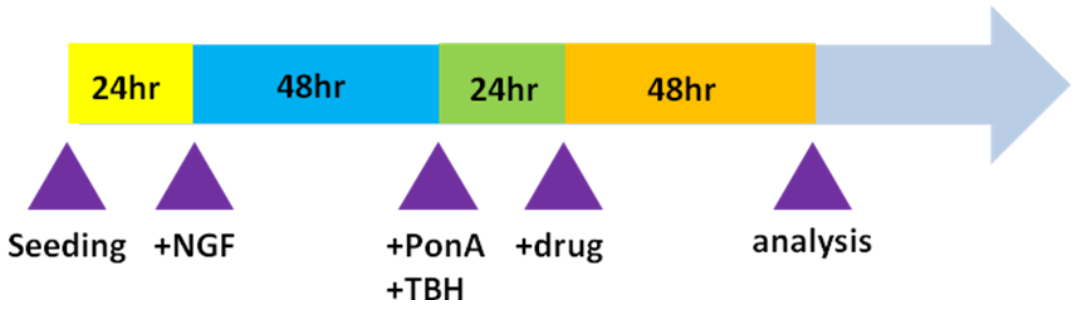

Figure 1. The experimental timeline used for potential therapeutic drug screening.

We first seeded SCA3 cells in 6-cm dishes or 12-well plates. 24 hr later, NGF was added to the medium for cell differentiation. After 48 hr, ponA and TBH were added for AT3 protein induction and creating an oxidative stress environment. The drugs to be screened were applied to the stressed cells 24 hr later. Cells were then analyzed after treated drugs for 48 hr.

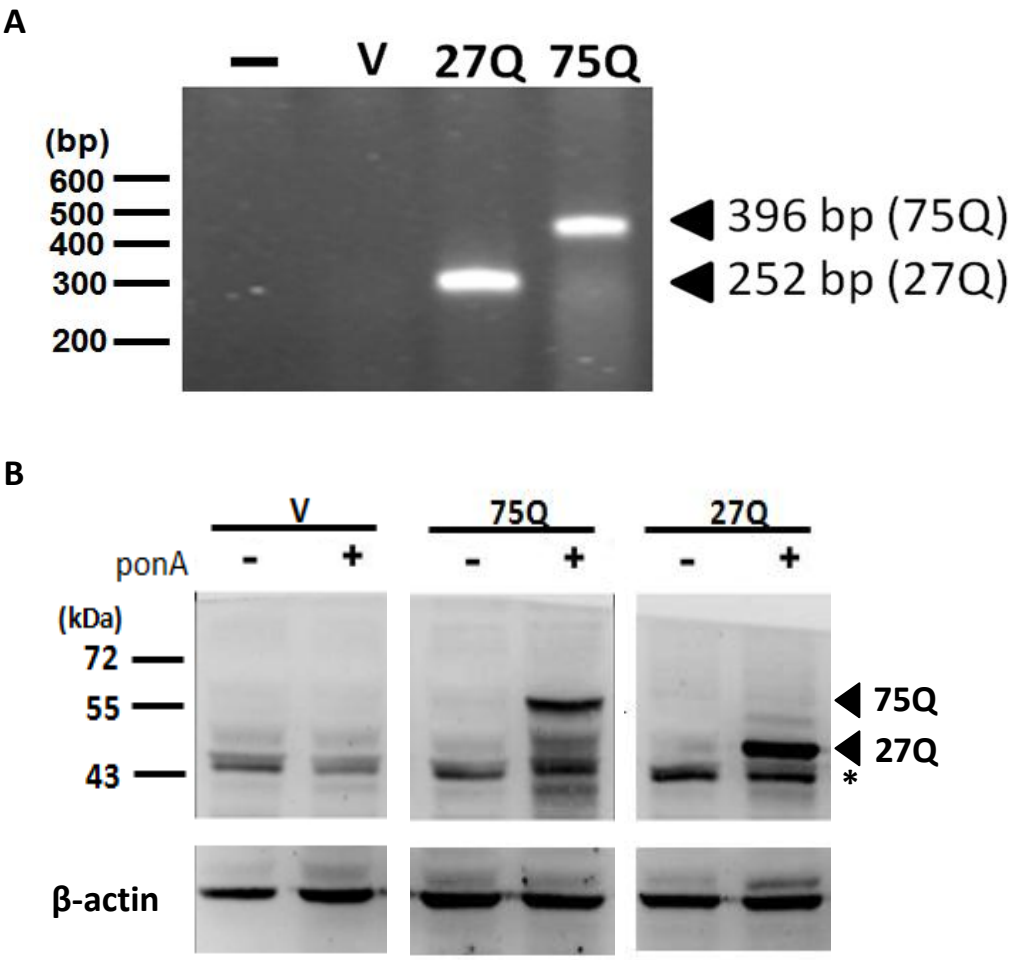

Figure 2.Maintaining of SCA3 cell lines.

(A) Genotyping of SCA3 cell lines. Fragments of transfected human SCA3 cDNA in cell lines were amplified by PCR. Products with 27Q and 75Q cDNA are 252 bp and 396 bp (arrow head), respectively.

－, negative control; V, pEGSH vector.

(B) Analysis of the AT3 proteins in the SCA3 cell lines by western blot. We used Ataxin-3 antibody to detect the AT3 expression in the SCA3 cells after ponA induction. 27Q and 75Q AT3 proteins detected are 48 KD and 60 KD respectively. There was no leaky in our 27Q and 75Q cell models. β-actin was used as an internal control. V, vector only-bearing cells. *, rat endogenous AT3.

A

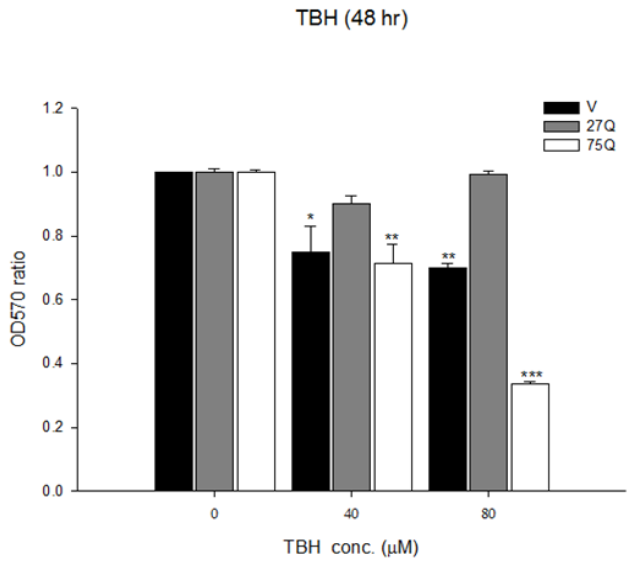
TBH (48 hr)
V
27Q
75Q
OD570 ratio
1.2
1.0
0.8
0.6
0.4
0.2
0.0
*
**
**
***
0
40
80
TBH conc. (μM)

B

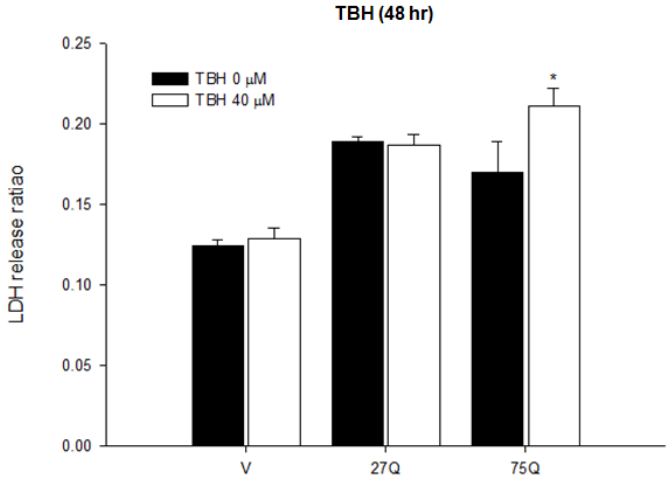
TBH (48 hr)
TBH 0 μM
TBH 40 μM
LDH release ratiao
0.25
0.20
0.15
0.10
0.05
0.00
*
V
27Q
75Q

C

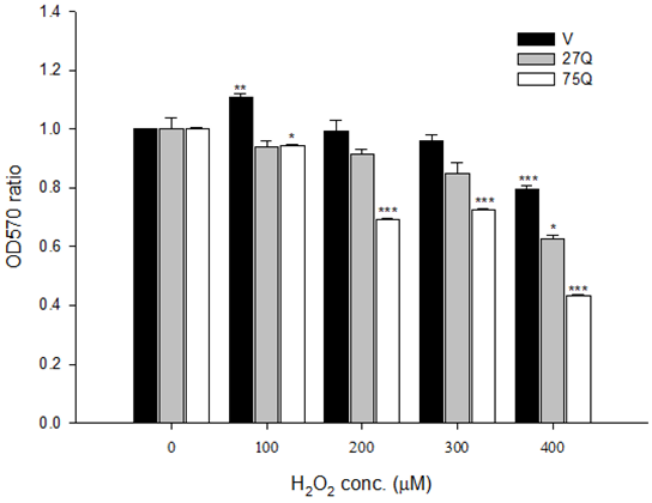
H2O2 (8 hr)
V
27Q
75Q
OD570 ratio
1.4
1.2
1.0
0.8
0.6
0.4
0.2
0.0
**
*
***
***
***
*
***
0
100
200
300
400
H2O2 conc. (μM)

Figure 3. SCA3 75Q cells showed lass tolerance to oxidative environment

SCA3 cells were treated with TBH or H_2O_2 and analyzed by MTT and LDH assay. **(A)** MTT assay of the viability of SCA3 cells after exposed to different concentrations of TBH. 75Q cells showed decreased cell viability related to TBH concentration. **(B)** LDH assay of the death of SCA3cells after exposed to 40 μM of TBH. SCA3 75Q cells released higher LDH than 27Q and vector cells. **(C)** MTT assay of SCA3 cell survival after H_2O_2 treatment. SCA3 75Q cells showed significant reduction in their cell viability after H_2O_2 treatment. Statistic analysis was performed by one way ANOVA and compared to 0 μM data. *, $p < 0.05$; **, $p < 0.001$; ***, $p < 0.0001$. (post hoc: Scheffe)

A

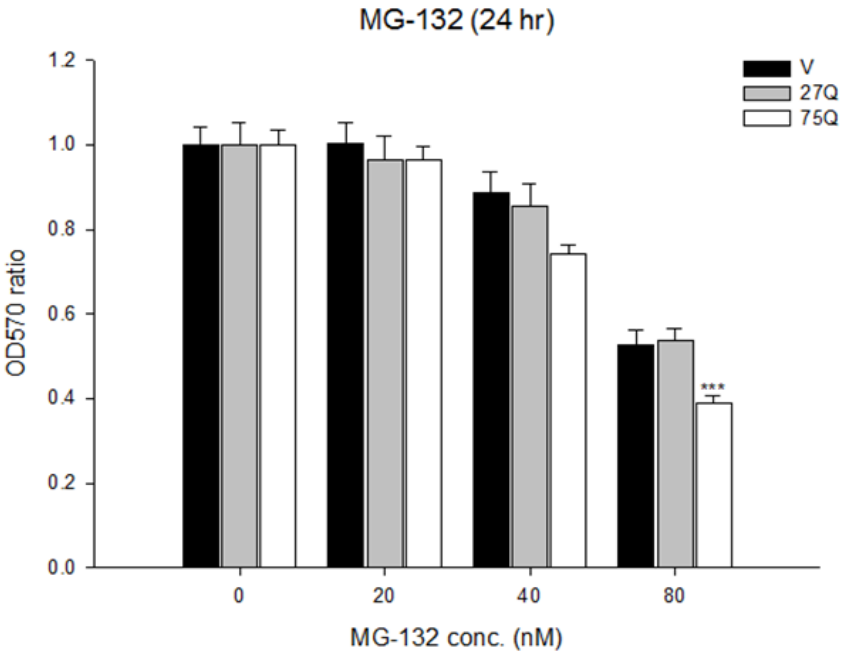
MG-132 (24 hr)
V
27Q
75Q
OD570 ratio
1.2
1.0
0.8
0.6
0.4
0.2
0.0
***
0
20
40
80
MG-132 conc. (nM)

B

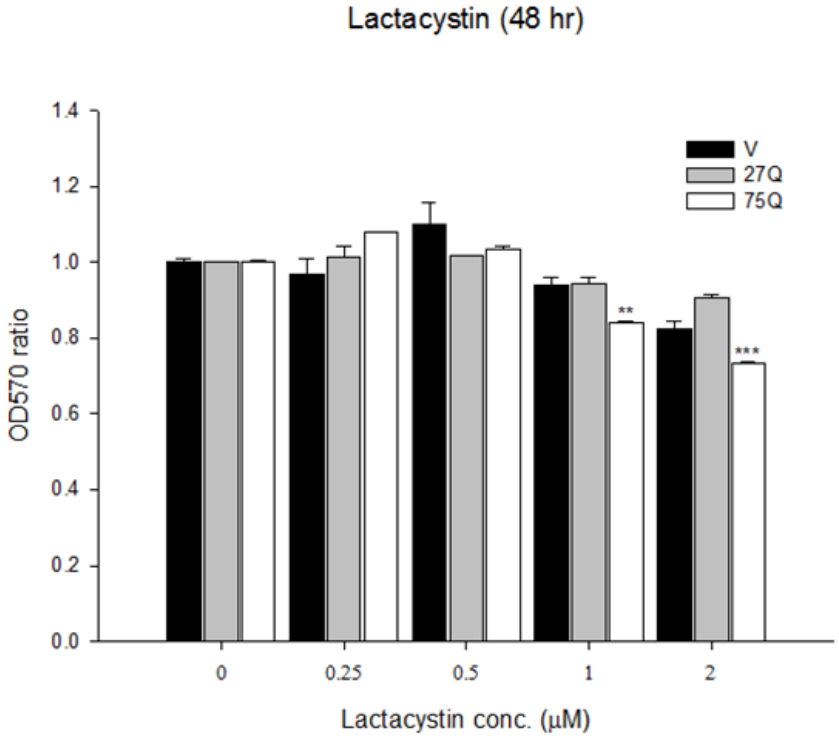
Lactacystin (48 hr)
V
27Q
75Q
OD570 ratio
1.4
1.2
1.0
0.8
0.6
0.4
0.2
0.0
**
***
0
0.25
0.5
1
2
Lactacystin conc. (μM)

Figure 4. SCA3 75Q cells show less tolerance to proteasomal stress. **(A)** MTT assay of the viability of SCA3 cells after treatment with different concentrations of MG-132 for 24 hr. SCA3 cells showed dose dependent decrement in cell viability after MG-132 treatment. SCA3 75Q cells showed significantly lower cell survival rate than 27Q and vector. **(B)** MTT assay of the cell survival rate of SCA3 cells after Lactacystin treatment for 24 hr. Statistical analysis was performed by one way ANOVA and compared to 0 μM data. **, $p < 0.001$; ***, $p < 0.0001$. (post hoc: Scheffe)

A

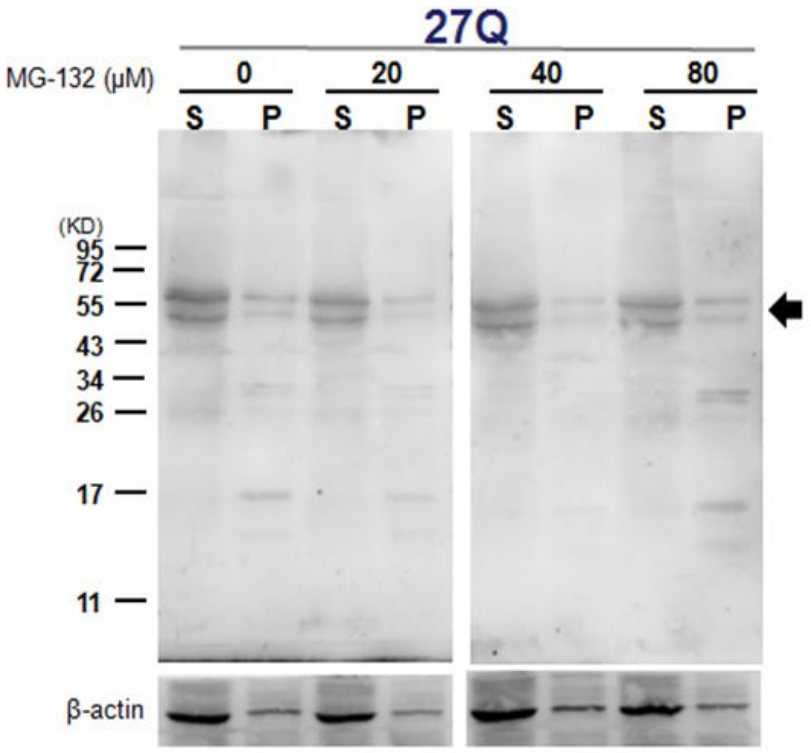
27Q
MG-132 (μM)
0
20
40
80
S P S P S P S P
(KD)
95
72
55
43
34
26
17
11
β-actin

B

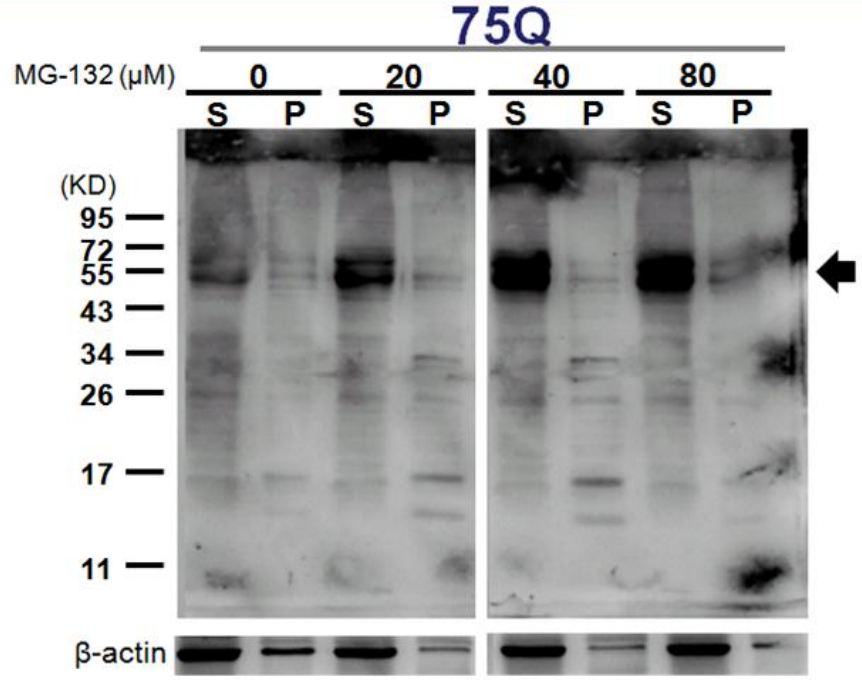
75Q
MG-132 (μM)
0
20
40
80
S P S P S P S P
(KD)
95
72
55
43
34
26
17
11
β-actin

Figure 5. 75Q cells are more polyubiquitinated after MG-132 treatment.

(A) Analysis of protein polyubiquitination of SCA3 27Q cell after MG-132 treatment. **(B)** Analysis of protein polyubiquitination of SCA3 75Q cell after exposed to MG-132 for 24 hr. Arrows represent for polyubiquitination protein. Cells with 75Q showed MG-132 dose-dependent polyubiquitination after treatment. β-actin was used as internal control. S, proteins in supernatant fraction; P, proteins in pellet fraction.

A

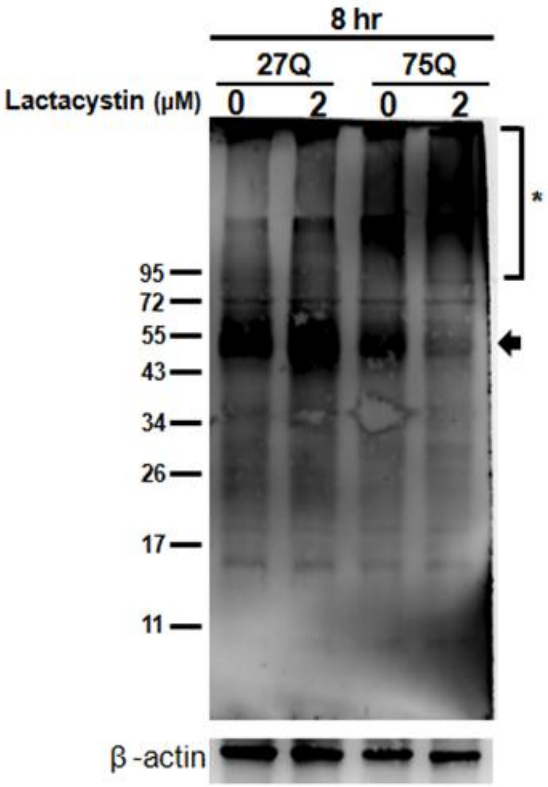
8 hr
27Q
75Q
Lactacystin (μM)
0
2
0
2
*
95
72
55
43
34
26
17
11
β-actin

B

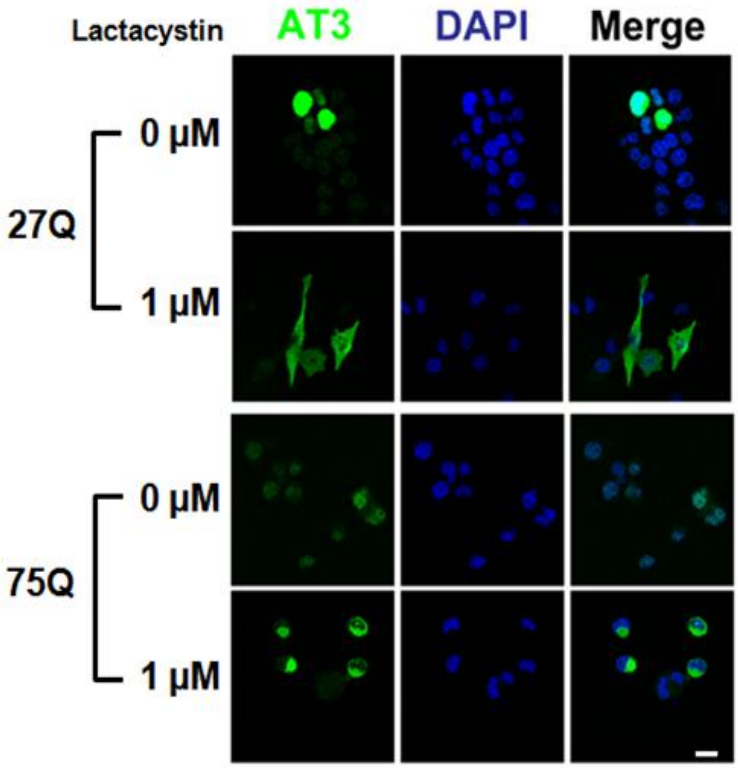
Lactacystin
AT3
DAPI
Merge
0 μM
27Q
1 μM
0 μM
75Q
1 μM

Figure 6. SCA3 75Q cells showed highly ubiquitinated aggregation after lactacystin treatment.

(A) A representative western blot of cell lysate after treated with lactacystin for 8 hr. The SDS insoluble aggregation is obviously at the stacking gel and highly polyubiquitinated (*), while the soluble ubiquitinated proteins were decreased at running gel (arrow). The SCA3 75Q cells were more sensitive than 27Q and vector cells in proteasomal stress environment. **(B)** Immunofluoresence staining of SCA3 cells after treated with lactacystin for 24 hr. 75Q cell showed perinuclear AT3 aggregation after exposed to lactacystin. Scale bar, 20 μM.

A

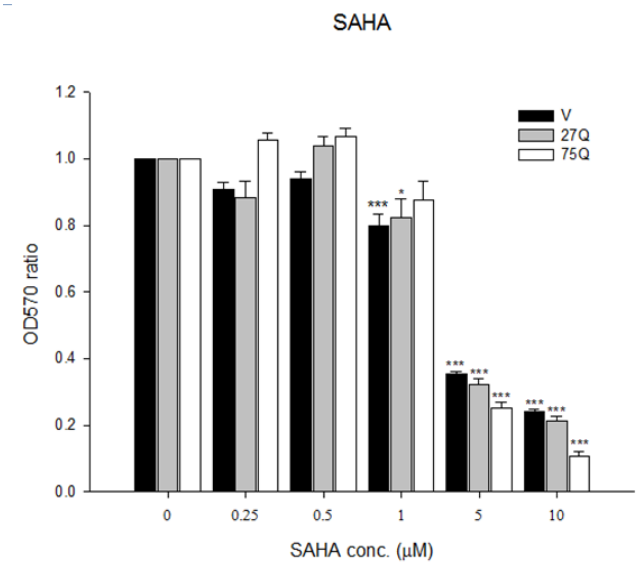
SAHA
V
27Q
75Q
OD570 ratio
SAHA conc. (μM)
0
0.25
0.5
1
5
10

B

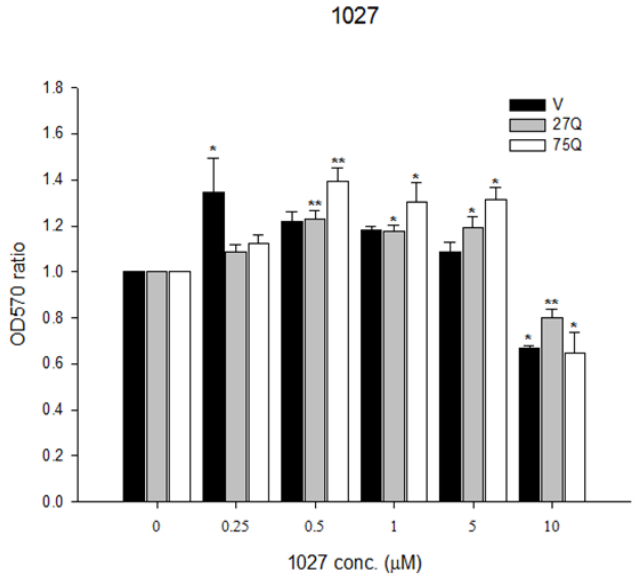
1027
V
27Q
75Q
OD570 ratio
1027 conc. (μM)
0
0.25
0.5
1
5
10

C

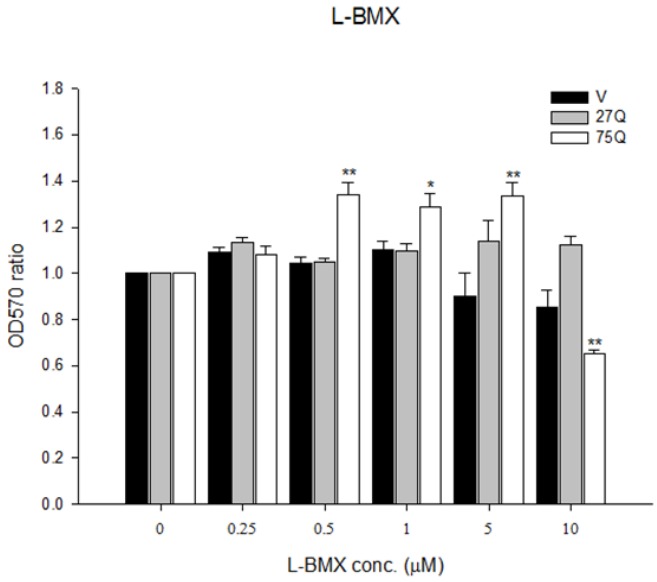
L-BMX
V
27Q
75Q
OD570 ratio
L-BMX conc. (μM)
0
0.25
0.5
1
5
10

D

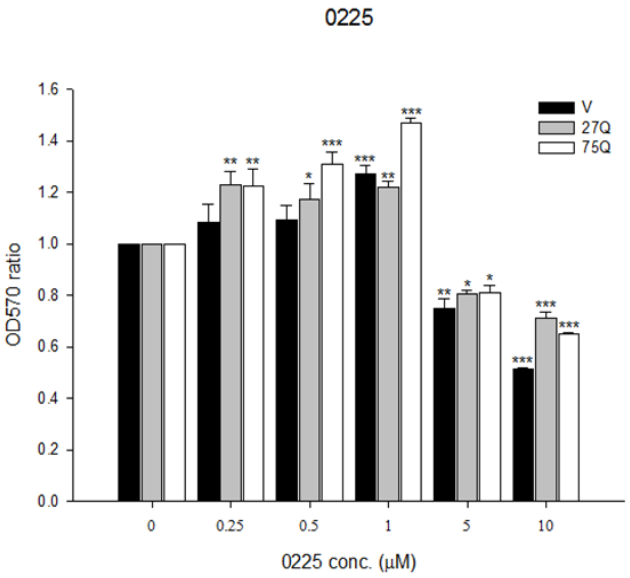
0225
V
27Q
75Q
OD570 ratio
0225 conc. (μM)

E

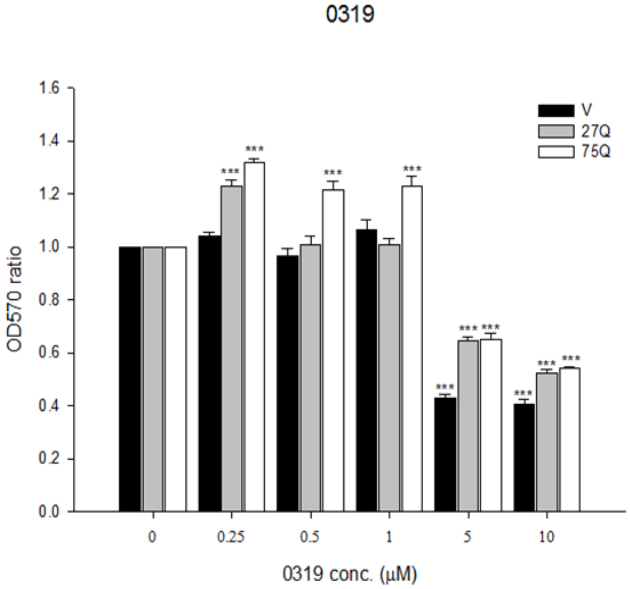
0319
V
27Q
75Q
OD570 ratio
0319 conc. (μM)

F

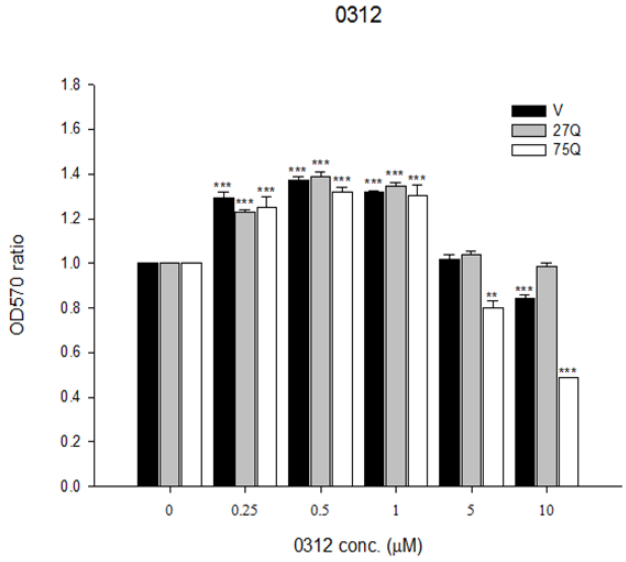
0312
V
27Q
75Q
OD570 ratio
0312 conc. (μM)

G

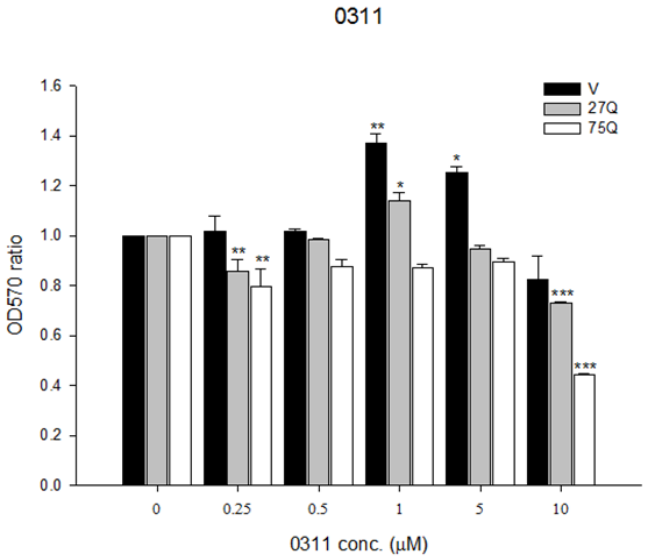
0311
V
27Q
75Q
OD570 ratio
0311 conc. (μM)

H

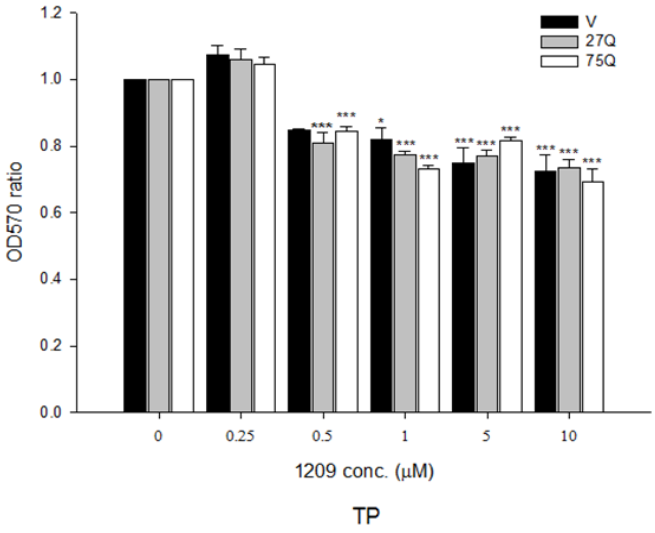
1209
V
27Q
75Q
OD570 ratio
1209 conc. (μM)

I

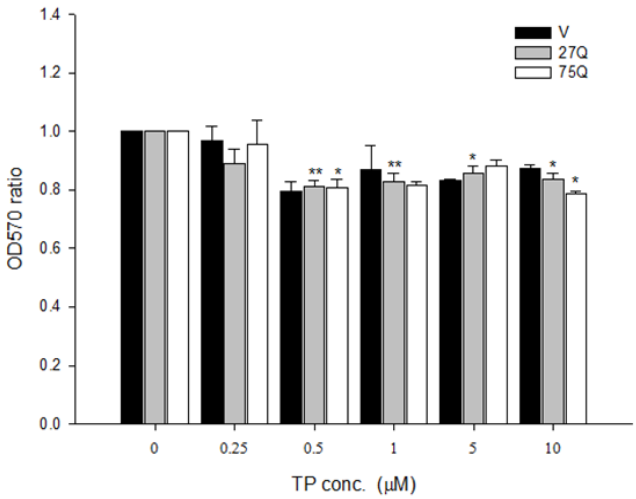
TP
V
27Q
75Q
OD570 ratio
TP conc. (μM)

Figure 7.Identification of potential HDACi for SCA3 cells.

SCA3 cells were treated with different HDACi after cells stressed by TBH for 48 hr. The results shown were cell viability determined by MTT assay. **(A)** SAHA was planned to be used as positive control, but showed limited effect to SCA3. **(B-E)** L-1027, L-BMX, 0225 and 0319 was specifically effective to 75Q cells. **(F)** 0312 generally improved all the three SCA3 cell viability. **(G-I)** 0311, 1209, and TP had limited effect to SCA3 cells. Statistical analysis was performed by one way ANOVA and compared to 0 μM data.* < 0.05; **, p < 0.001; ***, p < 0.0001. (post hoc: Scheffe)

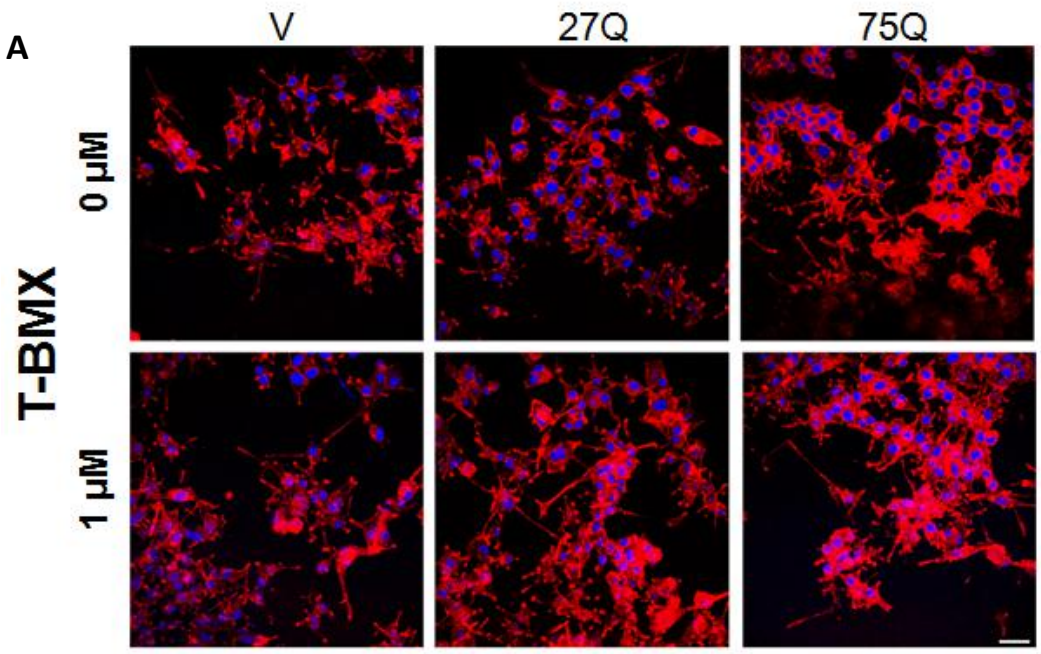
A
V
27Q
75Q
T-BMX
0 µM
1 µM

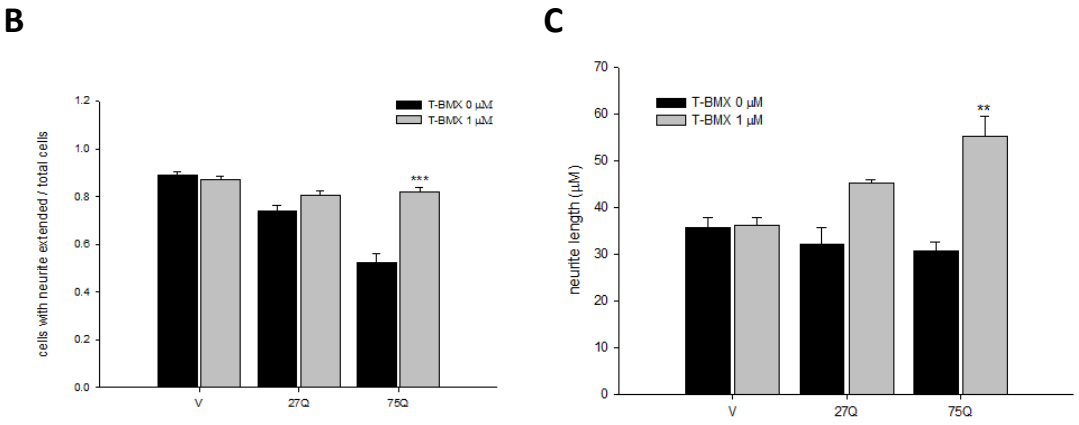
B
C
T-BMX 0 µM
T-BMX 1 µM
cells with neurite extended / total cells
neurite length (µM)
***
**
V
27Q
75Q

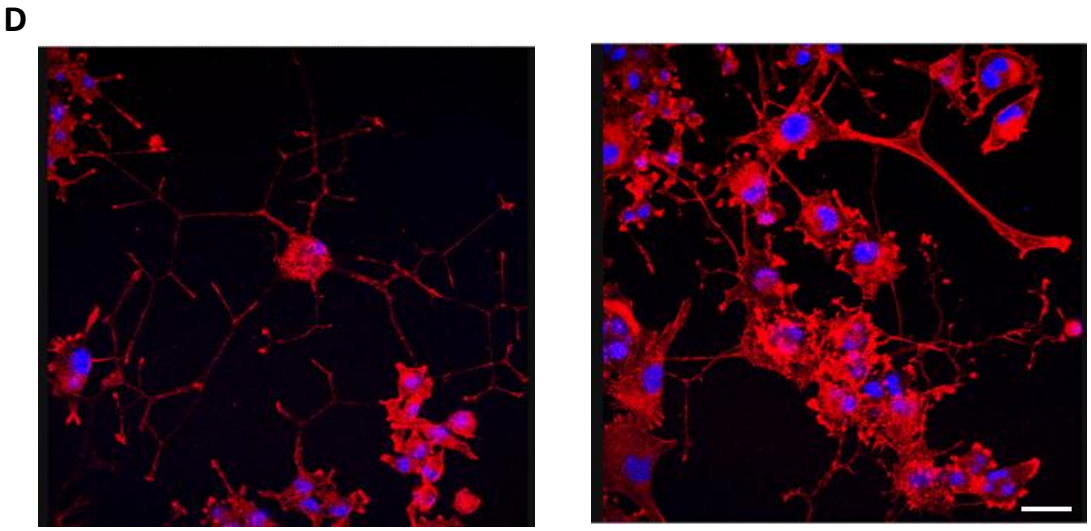
D

E

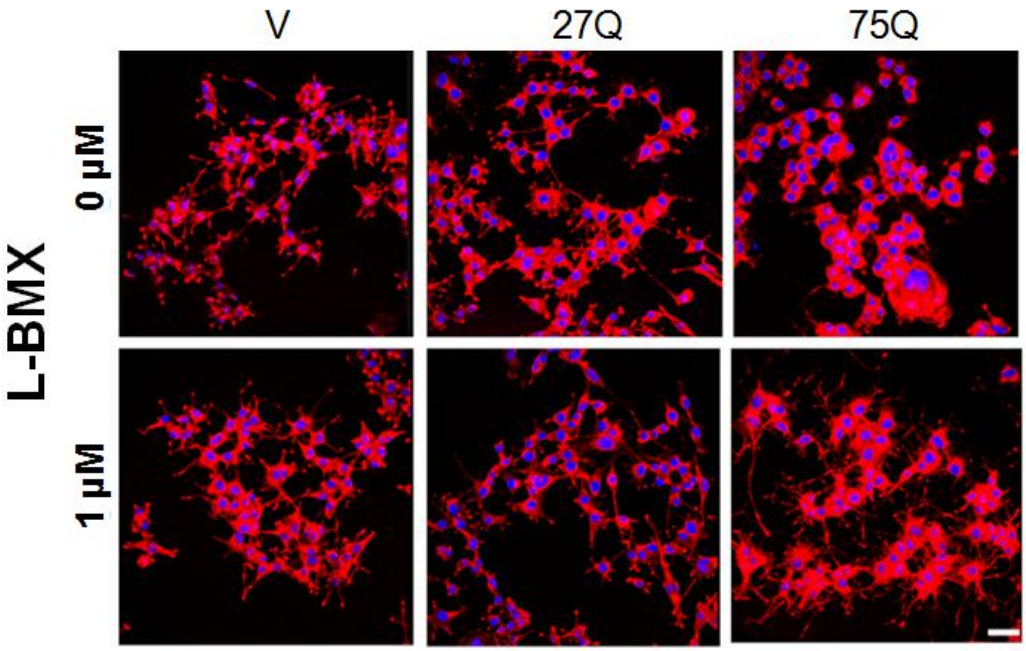
V
27Q
75Q
L-BMX
0 μM
1 μM

F

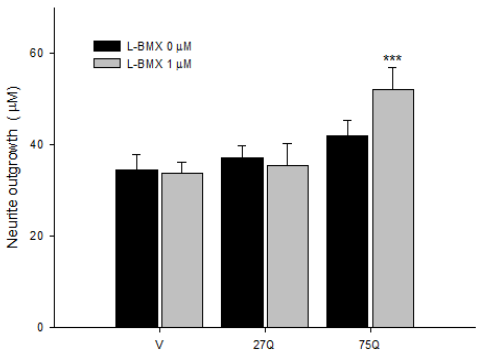
L-BMX 0 μM
L-BMX 1 μM
Neurite outgrowth (μM)
60
40
20
0
***
V
27Q
75Q

G

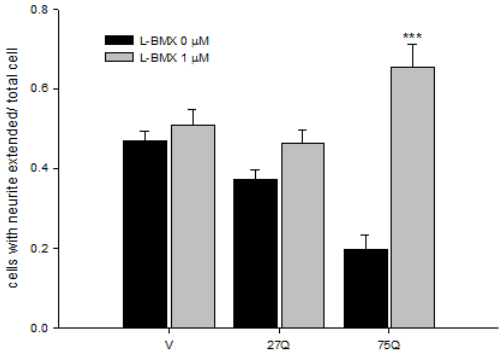
L-BMX 0 μM
L-BMX 1 μM
cells with neurite extended/ total cell
0.8
0.6
0.4
0.2
0.0
***
V
27Q
75Q

Figure 8. T-BMX and L-BMX could promote 75Q neurite outgrowth.

(A) A representative image of Rhodamine-Phalloidin staining of SCA3 cells to observe the neurite growth after T-BMX treatment. **(B)** Quantification of the cell ratio with neurite extension. 75Q cells showed elevated cell numbers with neurites after T-BMX treatment. **(C)** Quantification of SCA3 cells neurite length after T-BMX treatment.75Q cells showed significant longer neurite length than 27Q cells **(D)** Several 75Q cells showed distinguished neurite outgrowth after T-BMX treatment.**(E)**Image of Rhodamine-Phalloidin staining of SCA3 cells after L-BMX treatment. **(F)** Quantification of SCA3 cells neurite length after L-BMX treatment. L-BMX could increase 75Q neurite length.**(G)** Quantification of the neurite extension. L-BMX could significantly promote number of SCA3 75Q cells with neurite extension. Scale bar, 40 μm. Statistic analysis was performed by one way ANOVA and compared to DMSO data.* < 0.05; **, p < 0.001; ***, p < 0.0001. (post hoc: Scheffe)

A

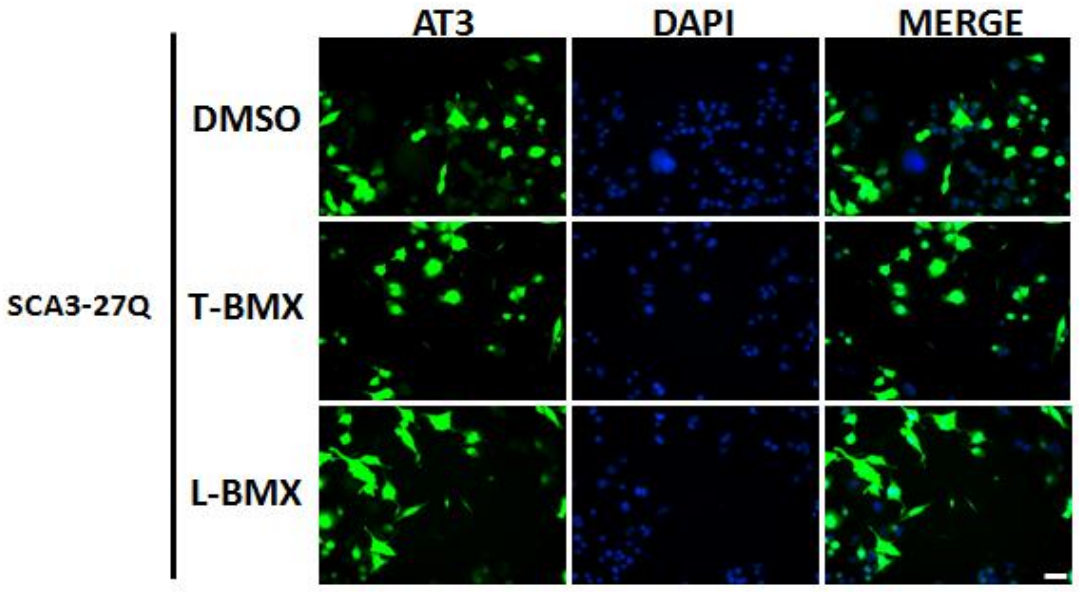
AT3
DAPI
MERGE
DMSO
T-BMX
L-BMX
SCA3-27Q

B

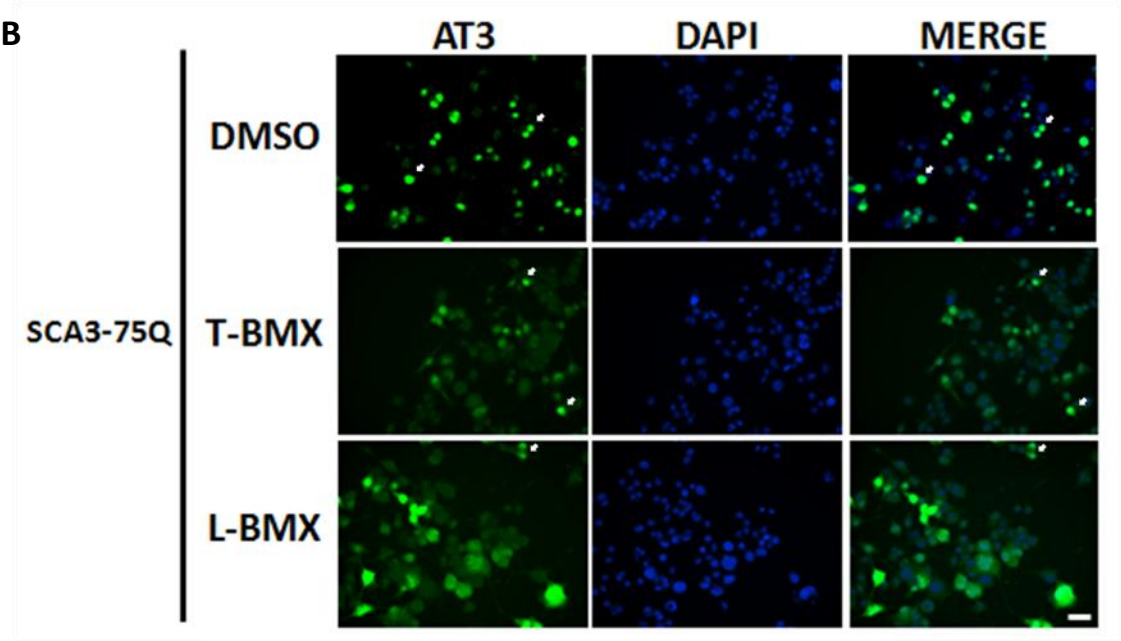
AT3
DAPI
MERGE
DMSO
T-BMX
L-BMX
SCA3-75Q

C

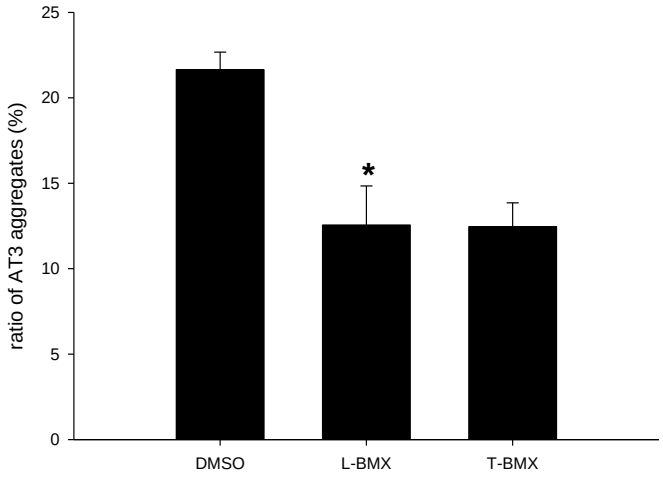
ratio of AT3 aggregates (%)
25
20
15
10
5
0
*
DMSO
L-BMX
T-BMX

Figure 9. T-BMX and L-BMX could decrease SCA3 75Q AT3 aggregation.

(A) A representative image of immunocytochemistry staining of SCA3 in 27Q cells. AT3 expression was evenly distributed in whole cells and rare aggregation found in the control and drug treatment cells. **(B)** Image of immunocytochemistry staining of SCA3 75Q cells. AT3 aggregated in peri-nuclear region in DMSO group. In L-BMX and T-BMX treatment cells, the number of AT3 aggregates (arrows) was reduced. Scale bar, 40 μm**(C)** Quantification of AT3 aggregation after T-BMX or L-BMX treatment. Both T-BMX and L-BMX could reduce AT3 aggregation. Statistic analysis was performed by one way ANOVA and compared to DMSO data.* < 0.05. (post hoc: Scheffe.)

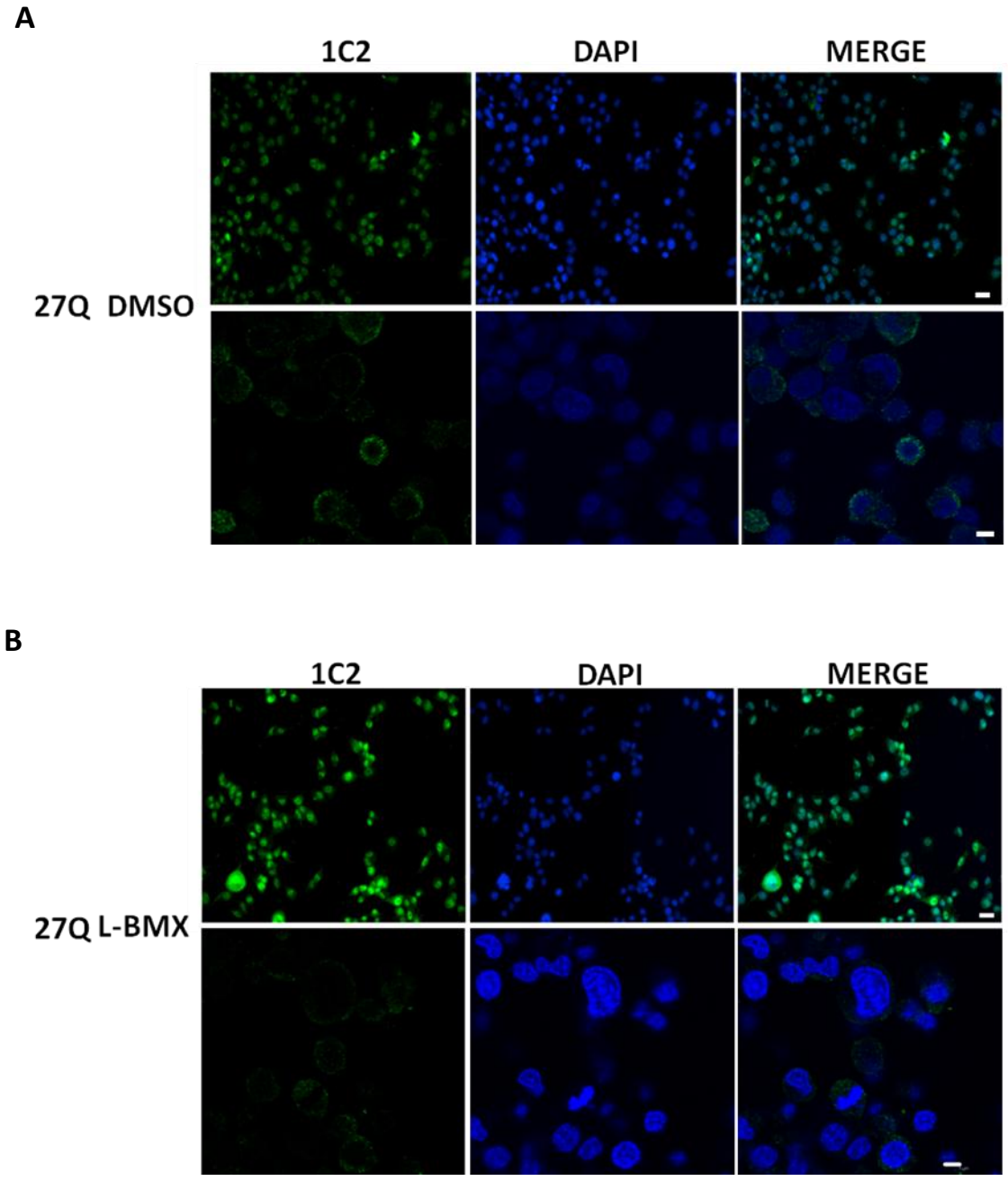
A
1C2
DAPI
MERGE
27Q DMSO
B
1C2
DAPI
MERGE
27Q L-BMX

C

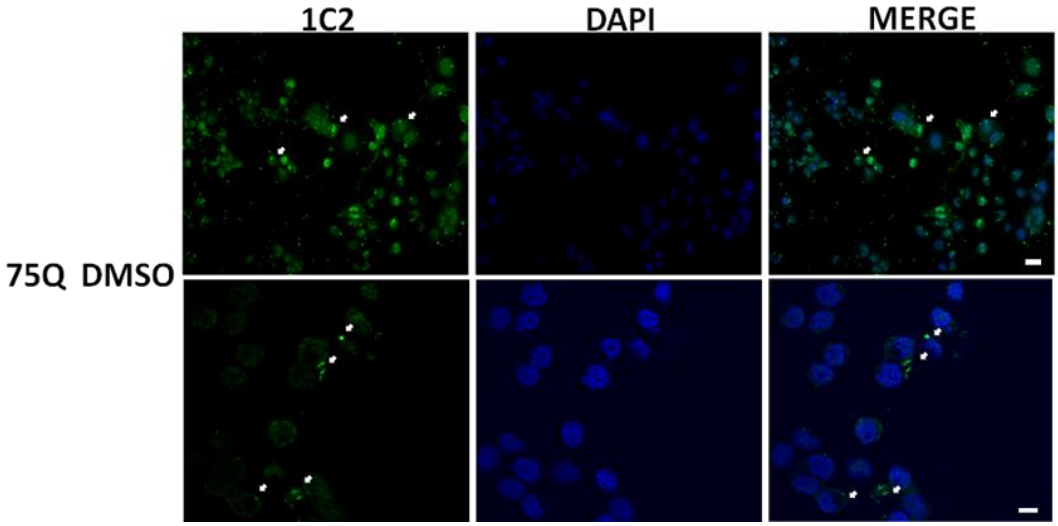
1C2
DAPI
MERGE
75Q DMSO

D

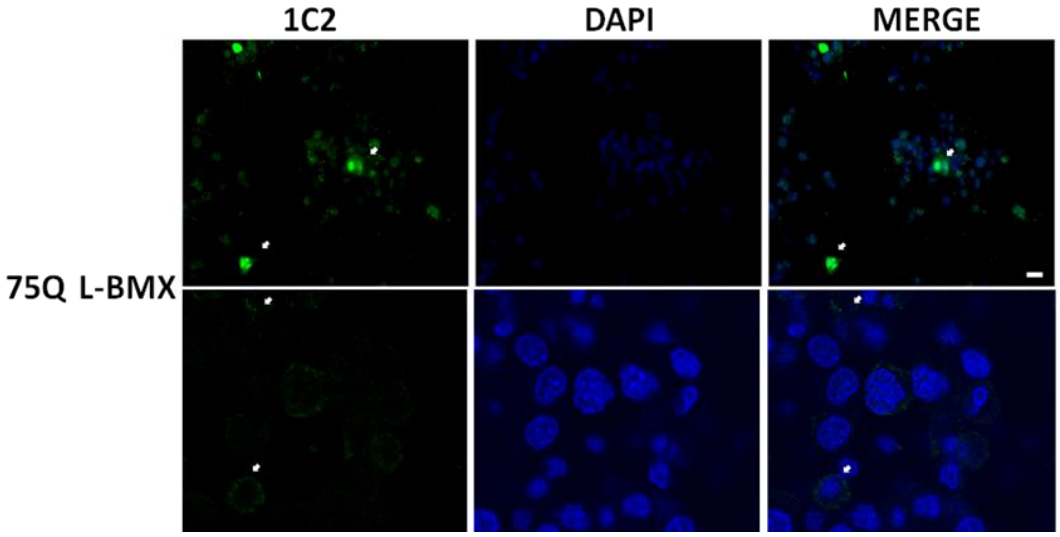
1C2
DAPI
MERGE
75Q L-BMX

E

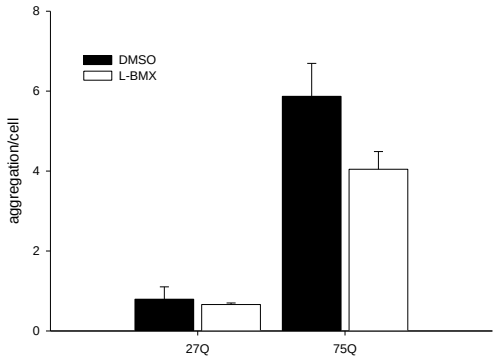
DMSO
L-BMX
aggregation/cell
0
2
4
6
8
27Q
75Q

F

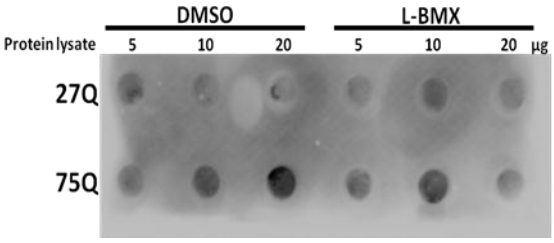
DMSO
L-BMX
Protein lysate
5
10
20
5
10
20
µg
27Q
75Q

Figure 10. L-BMX could reduce 1C2 positive aggregation in SCA3 cells.

(A-B) Representative images of 1C2 immunocytochemistry staining in SCA3 27Q cells after DMSO **(A)** and L-BMX **(B)** treatment. 1C2 staining distributed uniformly in whole cell after DMSO and L-BMX treatment. There is hardly aggregation found in SCA3 27Q cells. Scale bar in upper panel: 20 μm; in lower panel: 5 μm. **(C-D)** Representative images of 1C2 immunocytochemistry staining in SCA3 75Q cells after DMSO **(C)** and L-BMX **(D)** treatment.75Q cells showed both punctual and spherical 1C2 positive inclusion (arrows). Scale bar in upper panel: 20 μm; in lower panel: 5 μm. **(E)** Quantification of 1C2 positive signal aggregates in SCA3 cells. L-BMX could reduce aggregates in SCA3 75Q cells. **(F)** Filter trap assay of SCA3 cells, L-BMX diminished aggregation formation in 75Q cells.

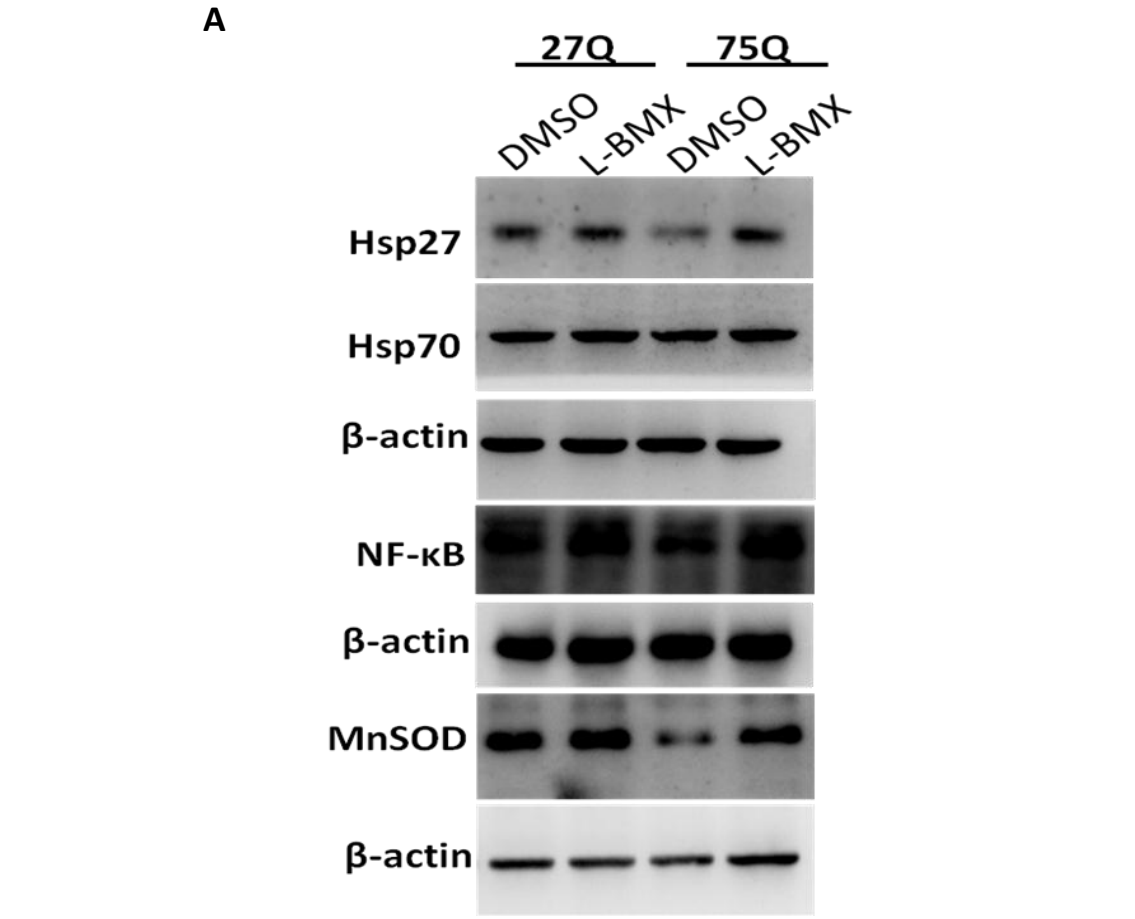
A
27Q
75Q
DMSO
L-BMX
DMSO
L-BMX
Hsp27
Hsp70
β-actin
NF-κB
β-actin
MnSOD
β-actin

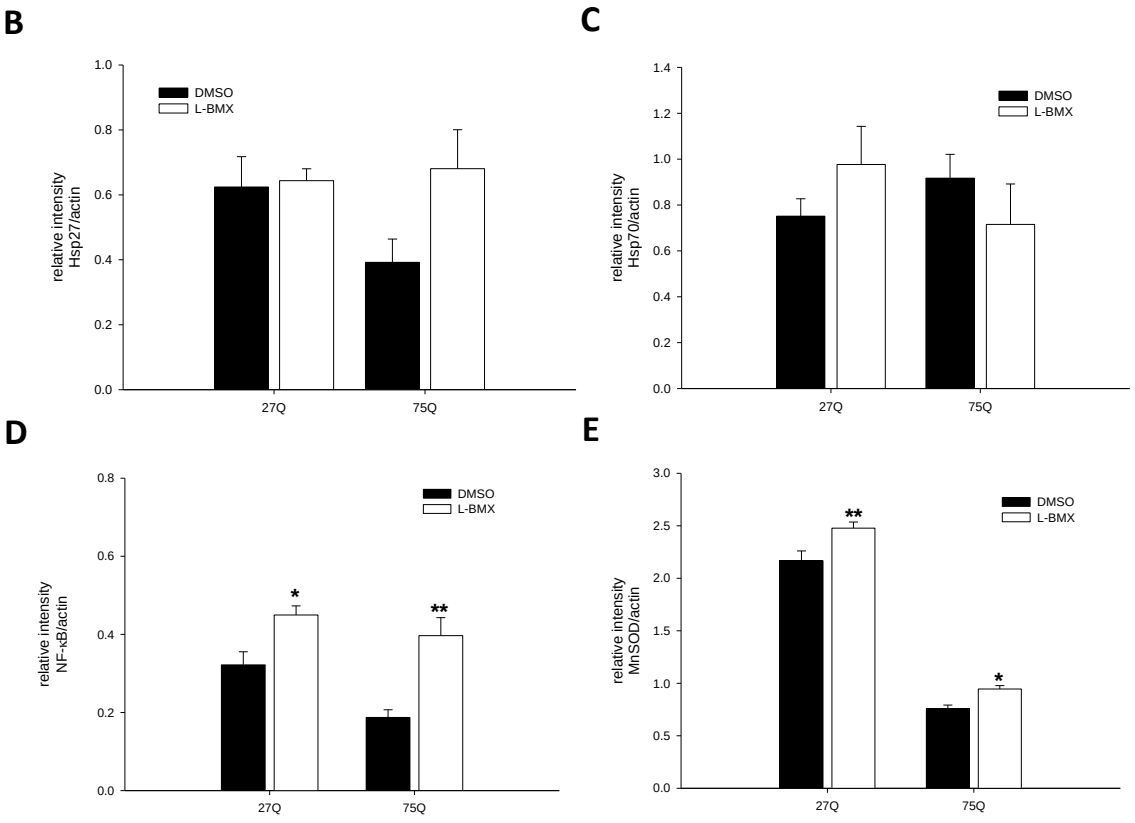
B
relative intensity Hsp27/actin
DMSO
L-BMX
27Q
75Q
C
relative intensity Hsp70/actin
DMSO
L-BMX
27Q
75Q
D
relative intensity NF-κB/actin
DMSO
L-BMX
*
**
27Q
75Q
E
relative intensity MnSOD/actin
DMSO
L-BMX
**
*
27Q
75Q

Figure 11. L-BMX could upregulate neuroprotective protein, antioxidative enzyme and rescue NF-κB downregulation.

(A) Western blot analysis of the Hsp27, Hsp70, MnSOD and NF-κBin the SCA3 cell lines after L-BMX treatment. **(B-D)** Quantification of Hsp27, Hsp70, MnSOD and NF-κB expression levels, SCA3 75Q cells could elevate Hsp27, MnSOD and NF-κB after L-BMX treatment. SCA3 27Q cells also displayed higher MnSOD and NF-κB levels after L-BMX treatment. Statistic analysis was performed by one way ANOVA and compared to DMSO data.* < 0.05; **, p < 0.001. (post hoc: Scheffe)

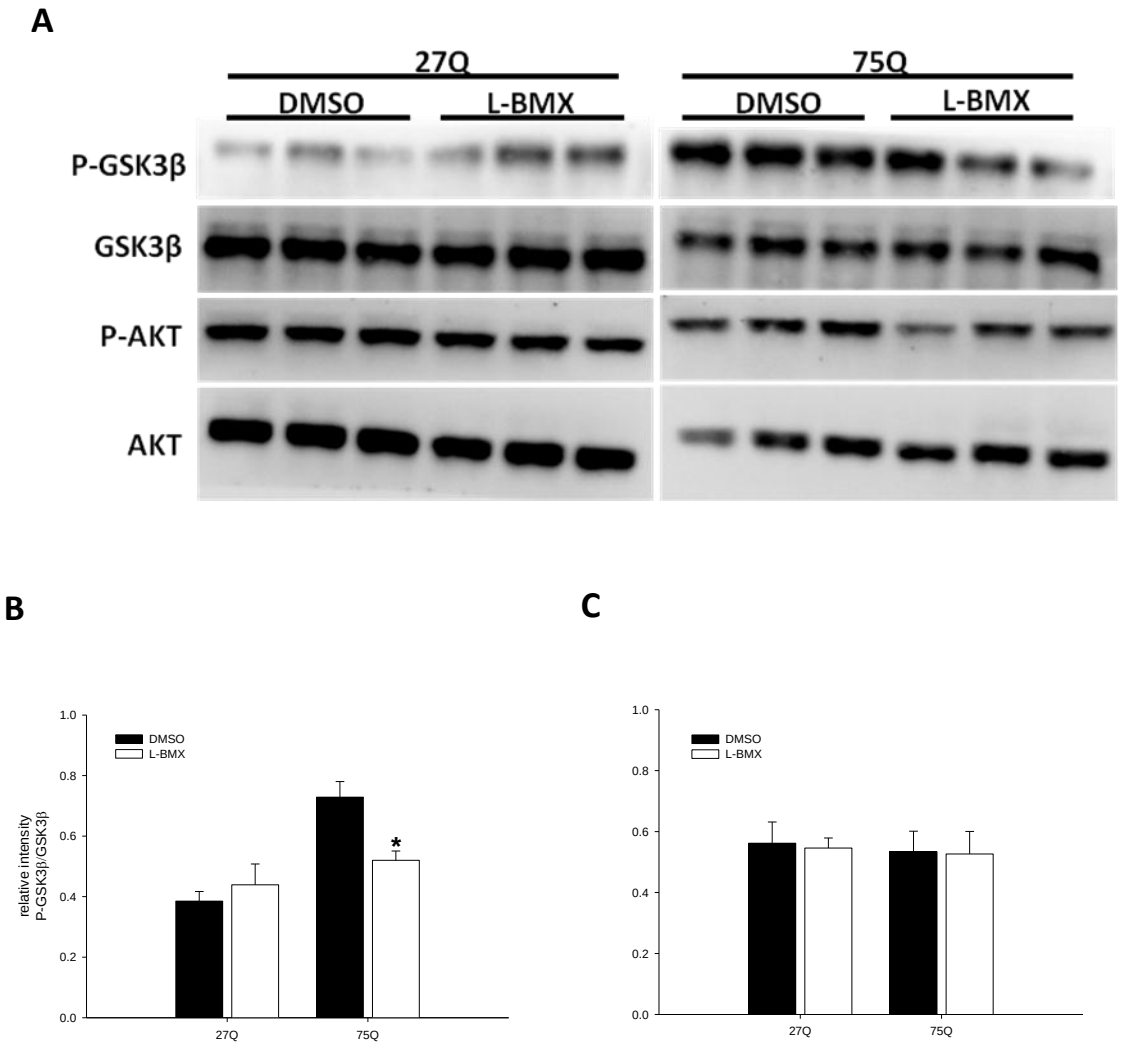

Figure 12. The expression level of P-GSK3β was reduced but P-AKT was not effected after L-BMX treatment.

(A) Western blot analysis of levels of P-GSK3β and P-AKT in SCA3 cells after L-BMX treatment. **(B)** Quantification level of P-GSK3β and P-AKT in SCA3 cells. L-BMX treatment decreased level of P-GSK3β but without effecting P-AKT level in 75Q cells. Statistic analysis was performed by one way ANOVA and compared to DMSO data.

* < 0.05. (post hoc: Scheffe)

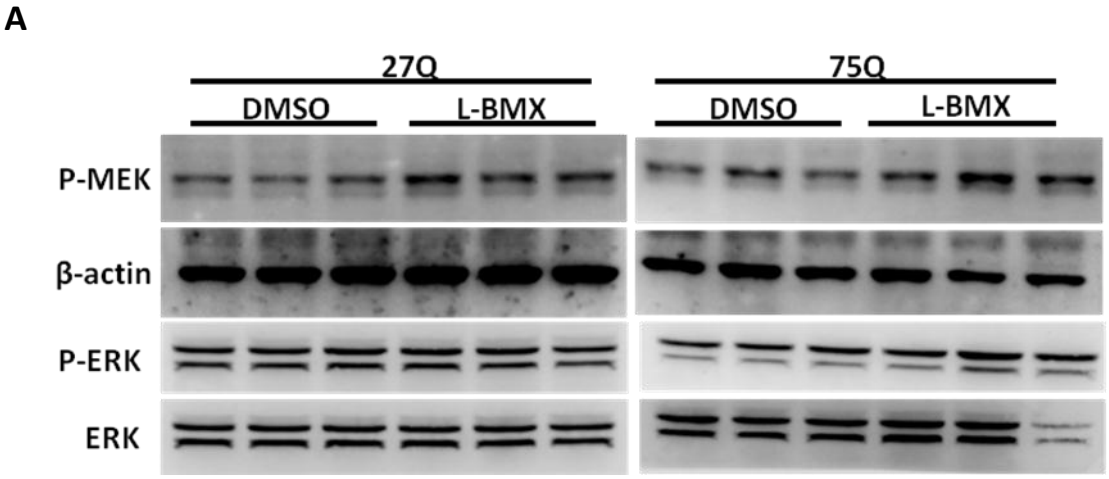
A
27Q
75Q
DMSO
L-BMX
DMSO
L-BMX
P-MEK
β-actin
P-ERK
ERK

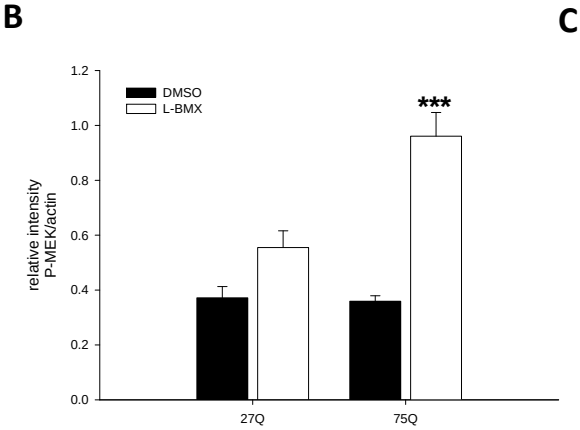
B
DMSO
L-BMX
***
relative intensity
P-MEK/actin
1.2
1.0
0.8
0.6
0.4
0.2
0.0
27Q
75Q

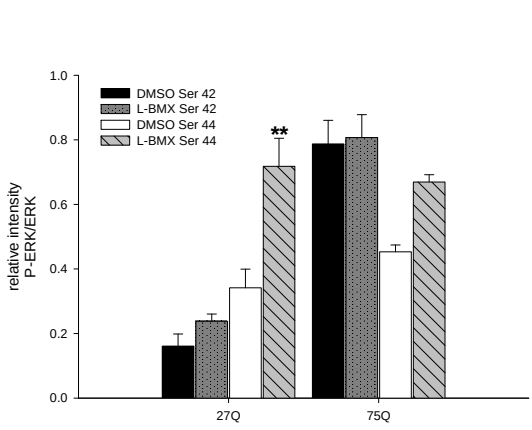
C
DMSO Ser 42
L-BMX Ser 42
DMSO Ser 44
L-BMX Ser 44
**
relative intensity
P-ERK/ERK
1.0
0.8
0.6
0.4
0.2
0.0
27Q
75Q

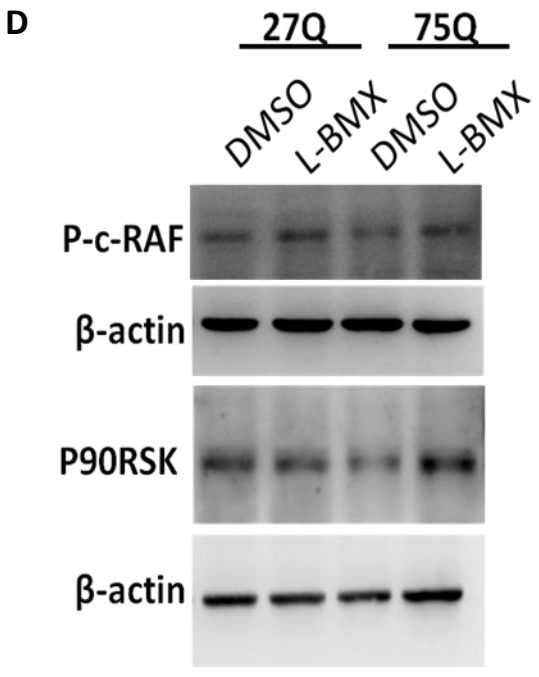
D
27Q
75Q
DMSO
L-BMX
DMSO
L-BMX
P-c-RAF
β-actin
P90RSK
β-actin

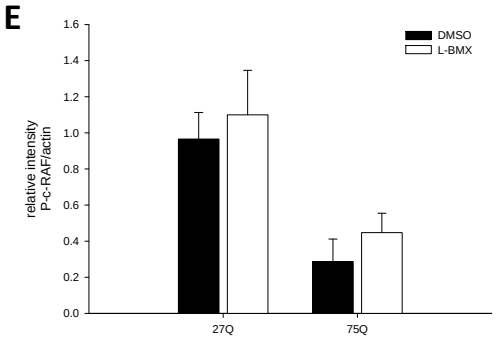
E
DMSO
L-BMX
relative intensity
P-c-RAF/actin
1.6
1.4
1.2
1.0
0.8
0.6
0.4
0.2
0.0
27Q
75Q

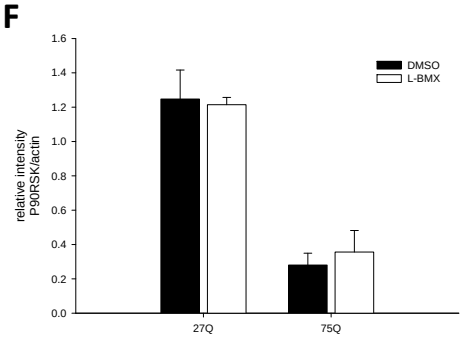
F
DMSO
L-BMX
relative intensity
P90RSK/actin
1.6
1.4
1.2
1.0
0.8
0.6
0.4
0.2
0.0
27Q
75Q

Figure 13. L-BMX could activate ERK pathway in SCA3 75Q cells. **(A)** Analysis of P-MEK and P-ERK in SCA3 cells by Western blot.**(B-C)** Quantification of P-MEK and P-ERK expression levels, SCA3 75Q cell showed lower P-MEK and P-ERK levels. L-BMX could activate P-MEK and P-ERK in SCA3 75Q cells. (D) Analysis of P-c-RAF and P90RSK in SCA3 cells by Western blot. (E-F) Quantification of P-c-RAF and P90RSK expression levels, L-BMX could elavate P-c-RAF and P90RSK in SCA3 75Q cells. Statistic analysis was performed by one way ANOVA and compared to DMSO data. **, $p < 0.001$; ***, $p < 0.0001$. (post hoc: Scheffe).

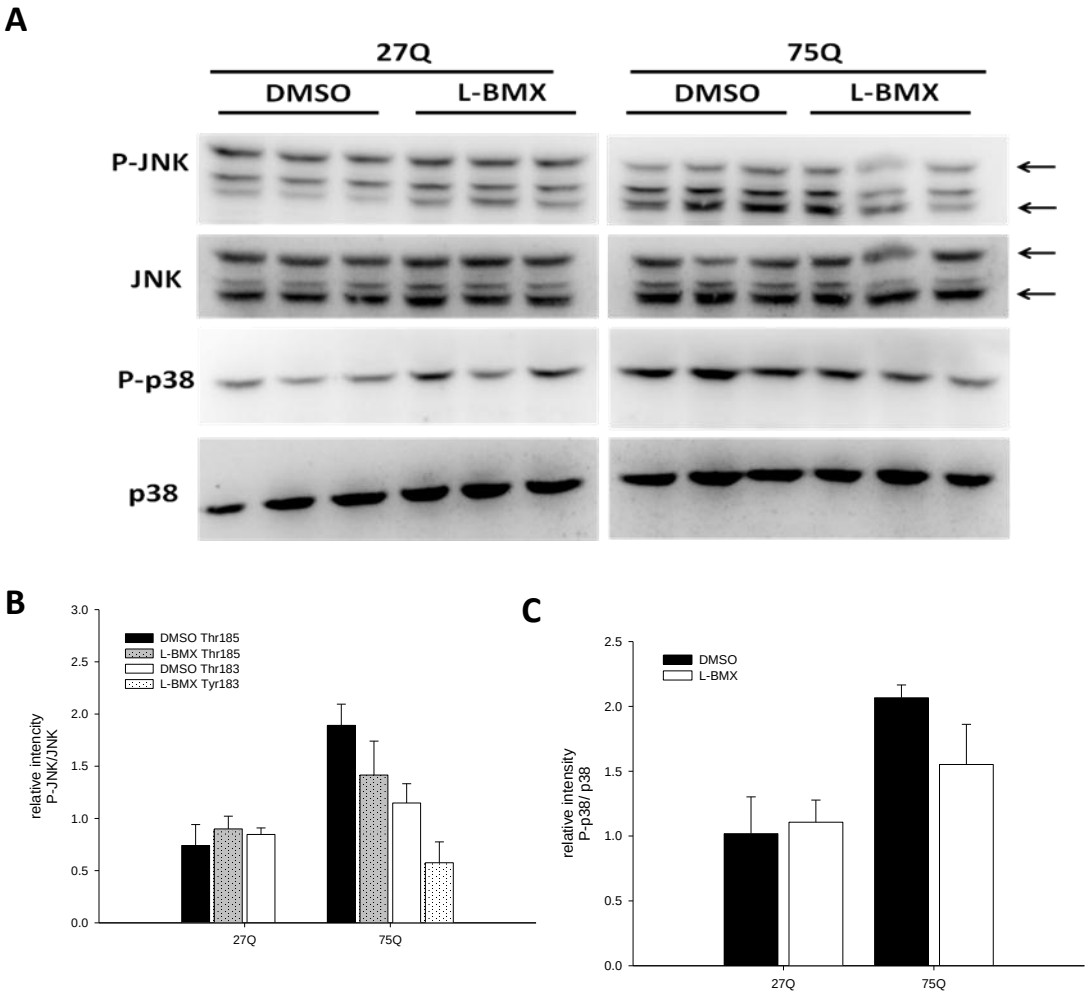

Figure 14. L-BMX treatment rescued activation of JNK signaling in SCA3 75Q cells.

(A) Analysis of P-JNK (arrows) and P-p38 in SCA3 cells by western blot. **(B)** Quantification of P-JNK expression level. 75Q cells exhibited higher expression level of P-JNK than 27Q cells. L-BMX reduced the expression level of P-JNK in 75Q cells. (C) Quantification of P-p38 expression levels. 75Q cells had higher level of P-p38 than 27Q cells. L-BMX could slightly decrease the P-p38 in 75Q cells.

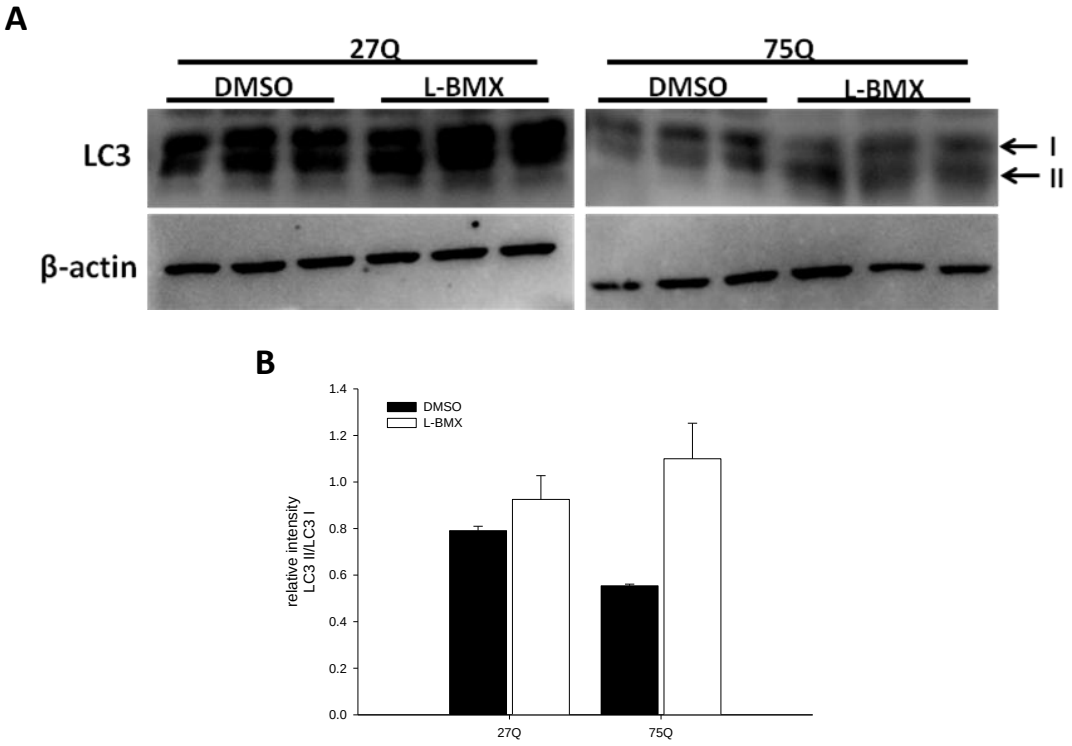

Figure 15. L-BMX treatment upregulated the autophagy associated protein, LC3 II expression level in SCA3 cells.

(A) Analysis of LC3 I and II expression levels (arrows) in SCA3 cells by Western blot.**(B)** Quantification of the ratio of LC3 I/LC3 II (autophagy induction) after L-BMX treatment in SCA3 cells. SCA3 75Q cell showed higher LC3 II level in L-BMX treatment group.

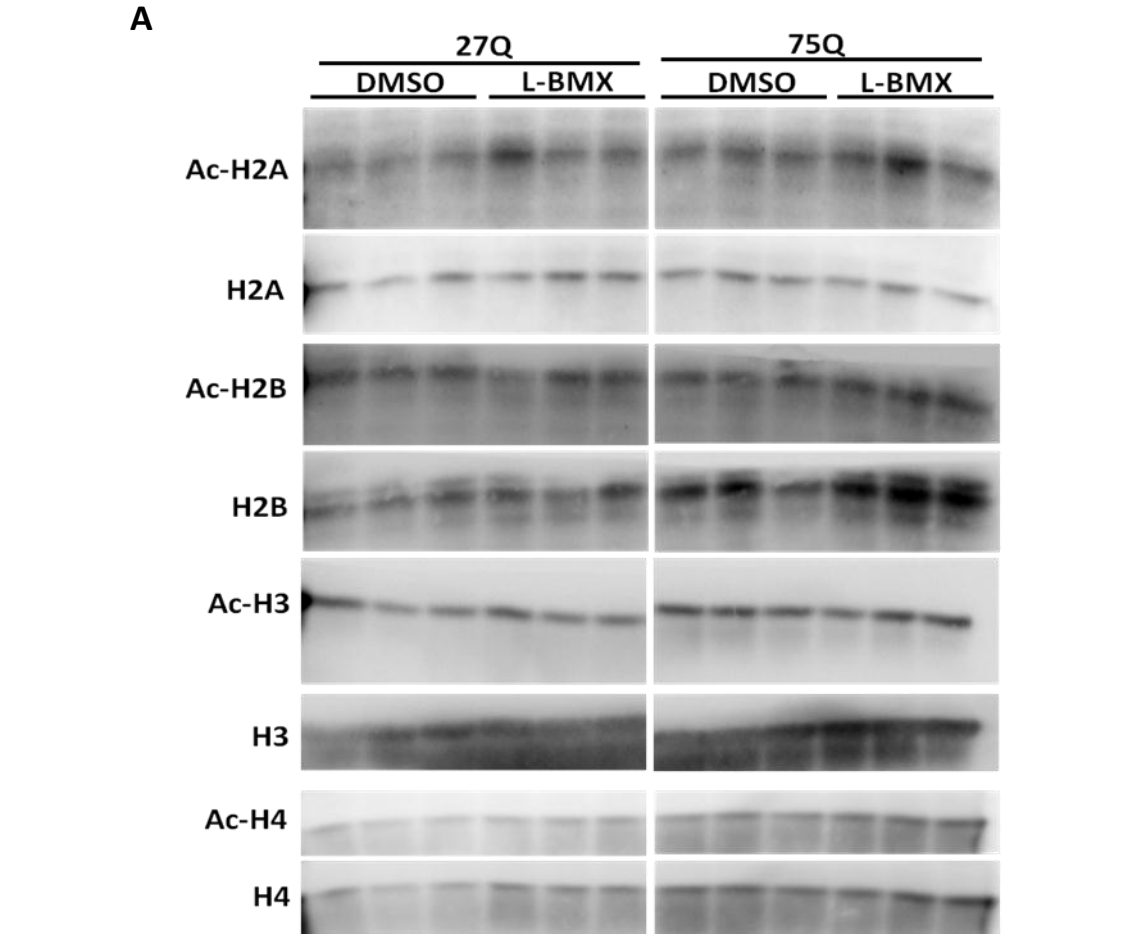
A
27Q
75Q
DMSO
L-BMX
DMSO
L-BMX
Ac-H2A
H2A
Ac-H2B
H2B
Ac-H3
H3
Ac-H4
H4

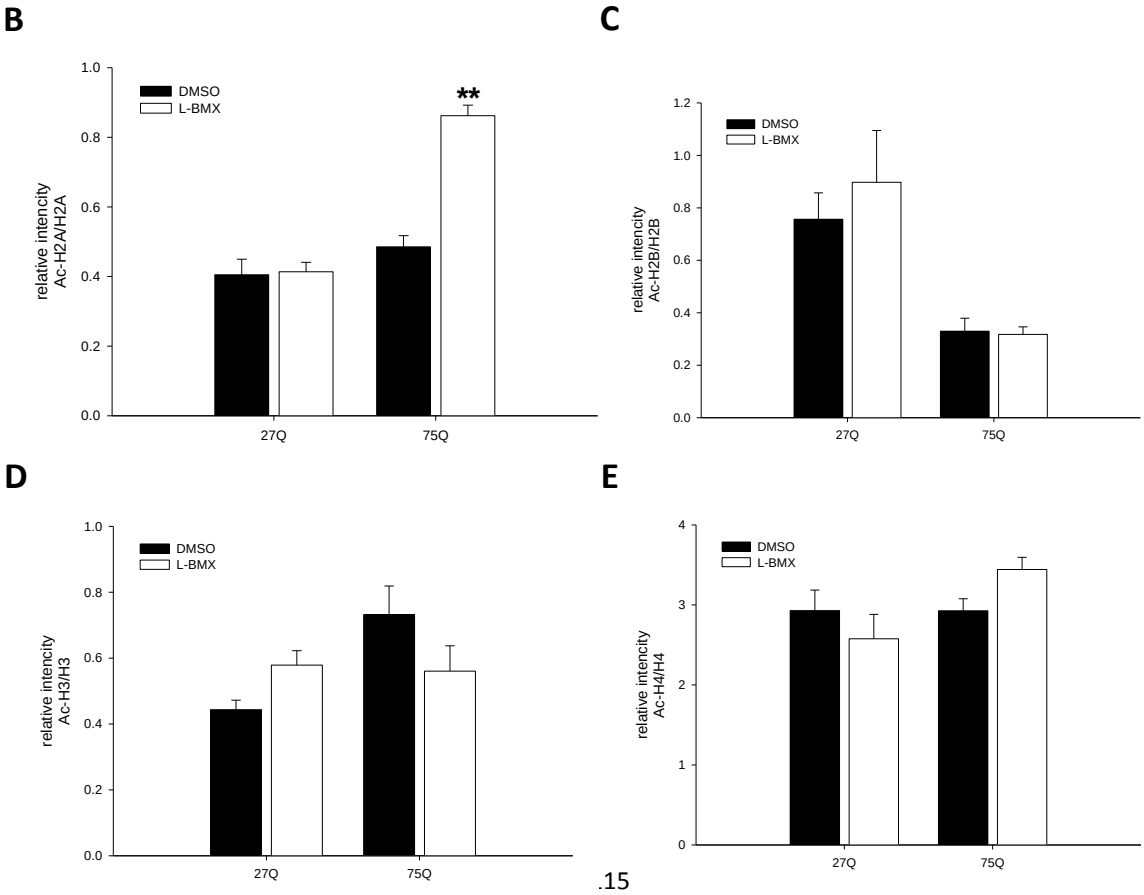
B
DMSO
L-BMX
**
relative intencity
Ac-H2A/H2A
1.0
0.8
0.6
0.4
0.2
0.0
27Q
75Q
C
DMSO
L-BMX
relative intencity
Ac-H2B/H2B
1.2
1.0
0.8
0.6
0.4
0.2
0.0
27Q
75Q
D
DMSO
L-BMX
relative intencity
Ac-H3/H3
1.0
0.8
0.6
0.4
0.2
0.0
27Q
75Q
E
DMSO
L-BMX
relative intencity
Ac-H4/H4
4
3
2
1
0
27Q
75Q

Figure 16. The acetylation of H2A was elevated after L-BMX treatment in SCA3 75Q cells.

(A) Western blots identify the effects of L-BMX on histone acetylation in SCA3 cells. **(B-E)** Quantification of the level of acetylated histones after L-BMX treatment, 75Q cells showed significant increase of the acetylation level of H2A but not the other histones after the treatment.

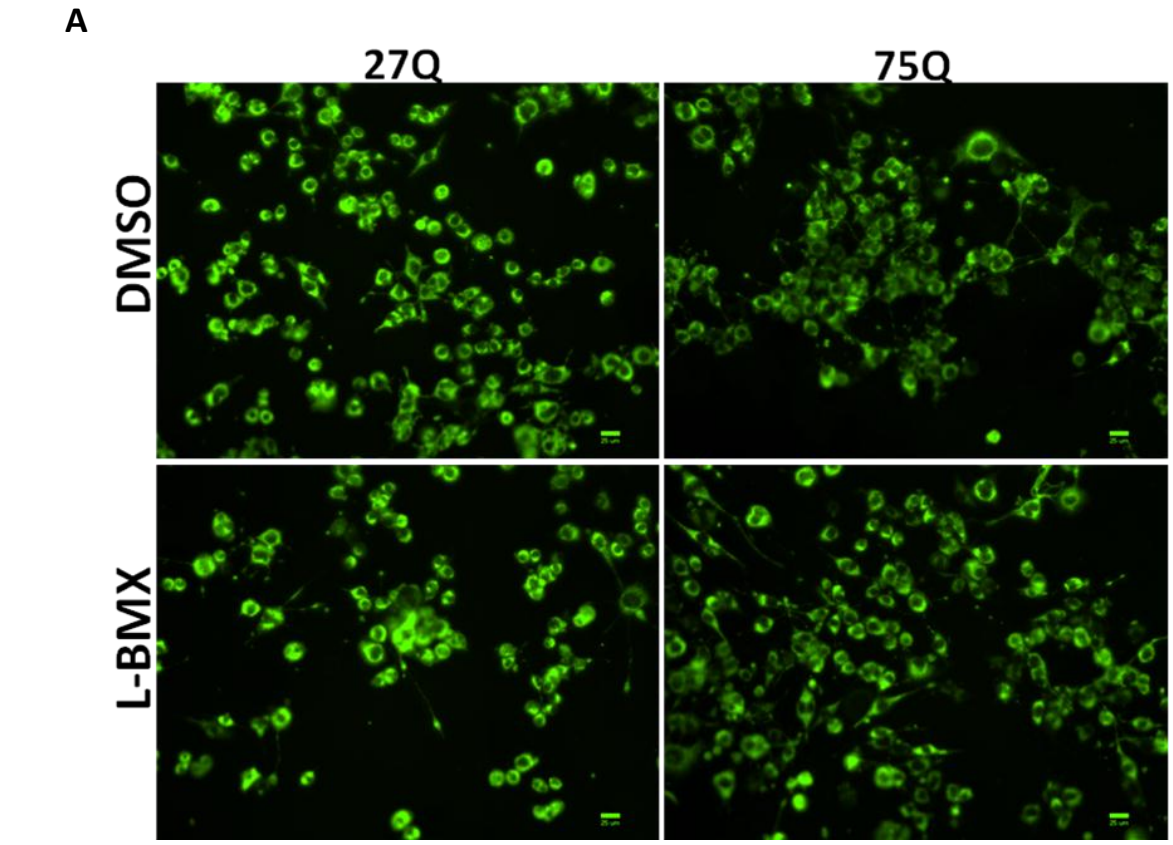
A
27Q
75Q
DMSO
L-BMX

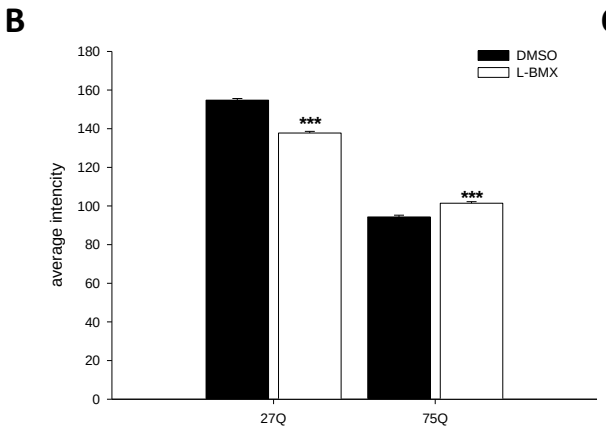
B
DMSO
L-BMX
average intencity
180
160
140
120
100
80
60
40
20
0
***
***
27Q
75Q

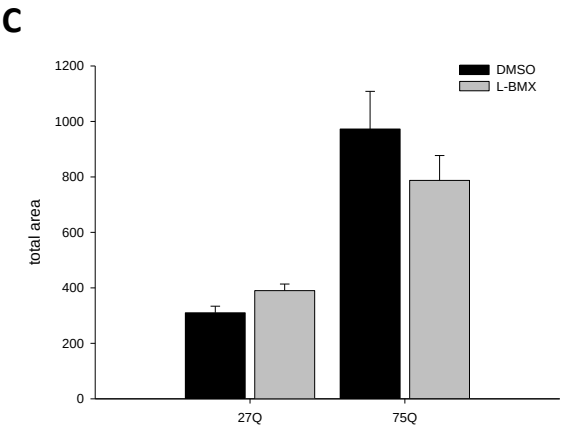
C
DMSO
L-BMX
total area
1200
1000
800
600
400
200
0
27Q
75Q

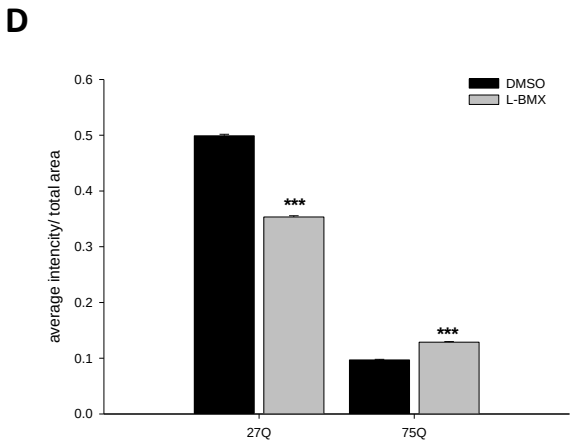
D
DMSO
L-BMX
average intencity/ total area
0.6
0.5
0.4
0.3
0.2
0.1
0.0
***
***
27Q
75Q

Figure 17. The effect on mitochondria area and Mitotracker positive signal was improved after L-BMX treatment.

(A) Representative life cell image of the Mitotracker staining in SCA3 cells. The Mitotracker signal distribution in 27Q cell appeared around nuclear uniformly. The Mitotracker signals showed diffused and weaker intensity in 75Q cells. Scale: 25 μm. **(B-D)** Quantification of Mitotracker fluorescence intensity and distribution area in SCA3 cells. In 27Q cell, the Mitotracker intensity was reduced after L-BMX treatment, but the distribution area was not affected. The distribution and intensity were improved in 75Q cell after L-BMX treatment. Statistic analysis was performed by one way ANOVA and compared to DMSO data. ***, $p < 0.0001$. (post hoc: Scheffe)

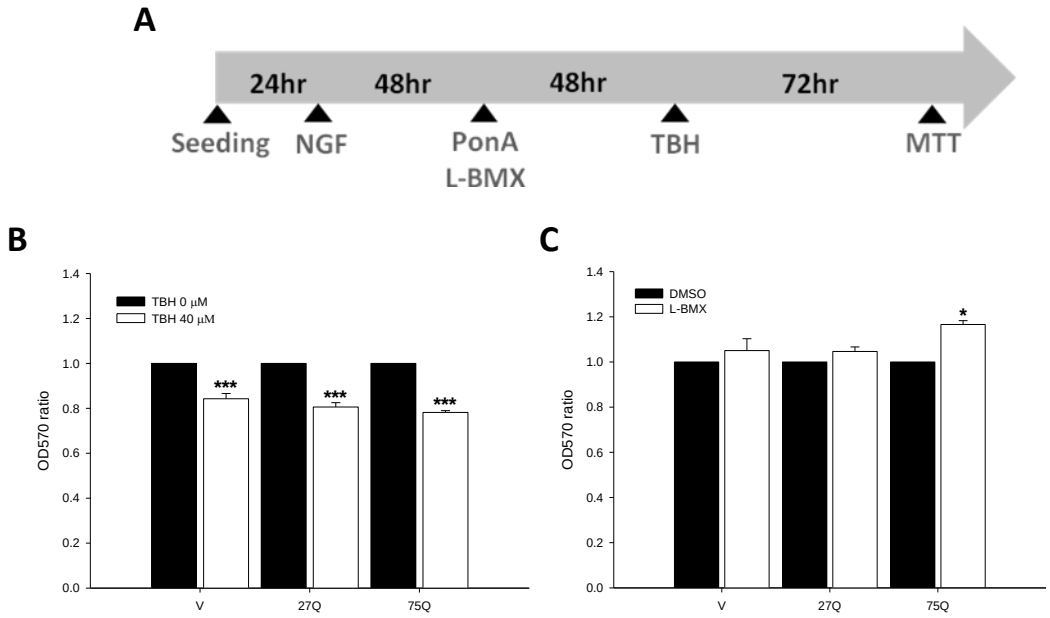

Figure 18. Prevention of TBH induced oxidative cell death by L-BMX pretreatment.

(A) A sketch representing the experiment timeline. **(B)** MTT assay of the viability of SCA3 cells after exposed to 40 μM of TBH without L-BMX pretreatment. All SCA3 cells showed decreased cell viability significantly. **(C)** MTT assay of the cell viability of SCA3 cells after L-BMX pretreatment for 48 hr and challenged with 40 μM of TBH for 72 hr. All three SCA3 cell lines were rescued from TBH induced oxidative cell death by L-TMX, and especially significantly in 75Q cells.

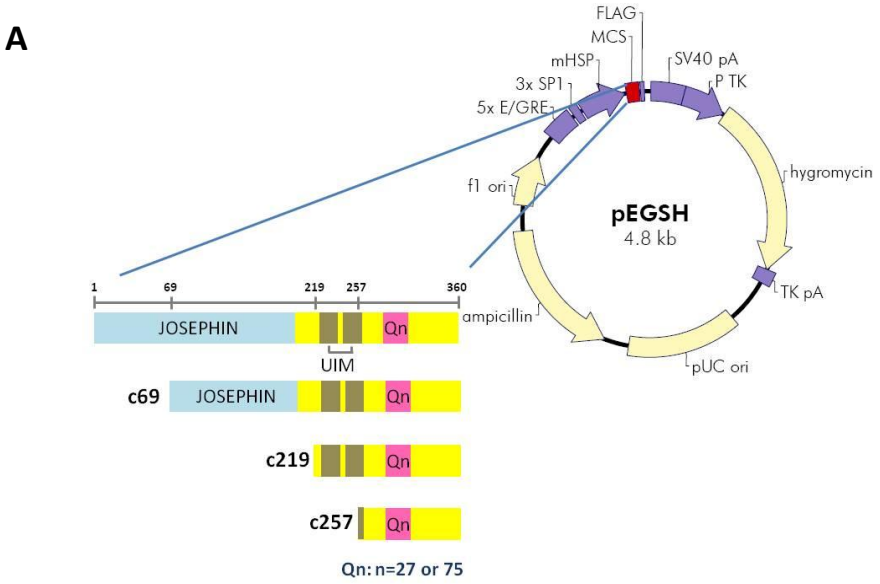
A
FLAG
MCS
mHSP
SV40 pA
3x SP1
P TK
5x E/GRE
hygromycin
f1 ori
pEGSH
4.8 kb
TK pA
ampicillin
pUC ori
1
69
219
257
360
JOSEPHIN
Qn
UIM
c69
c219
c257
Qn: n=27 or 75

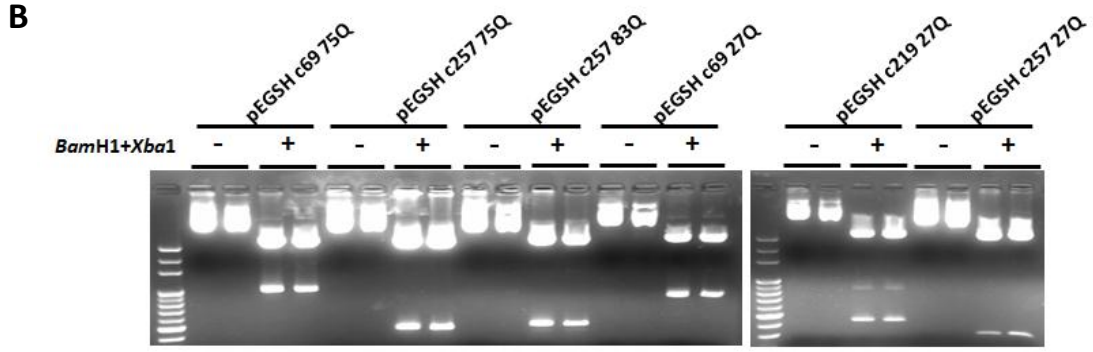
B
pEGSH c69 75Q
pEGSH c257 75Q
pEGSH c257 83Q
pEGSH c69 27Q
pEGSH c219 27Q
pEGSH c257 27Q
BamH1+Xba1
-
+

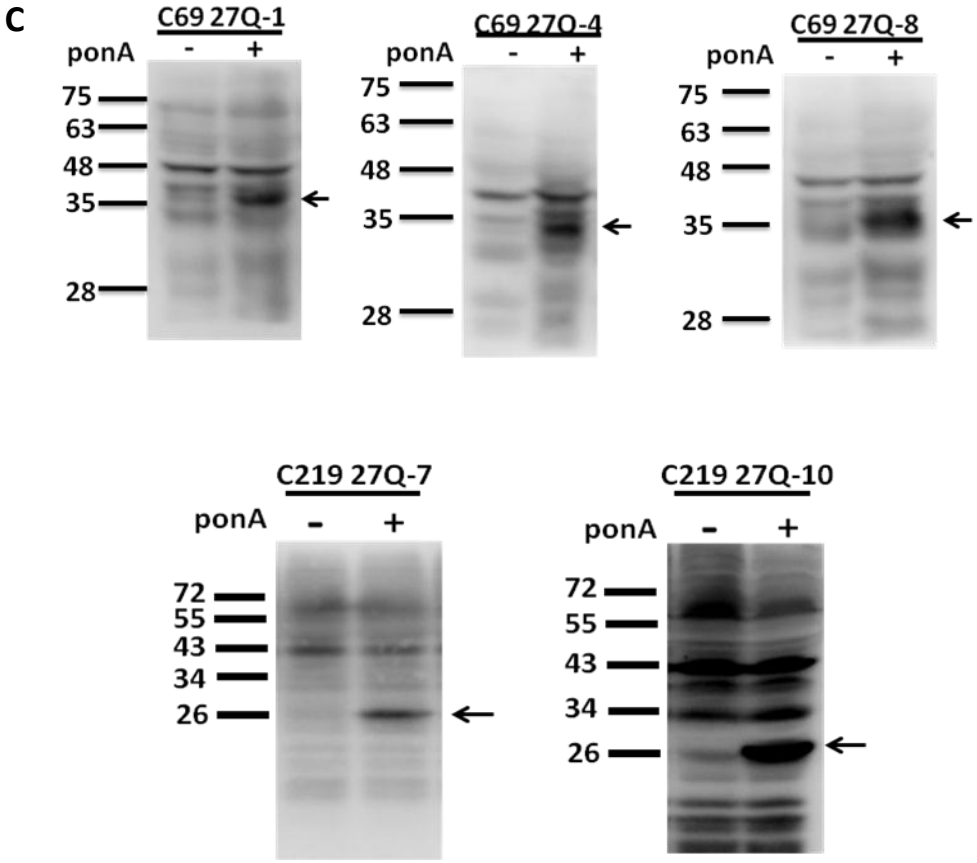
C
C69 27Q-1
C69 27Q-4
C69 27Q-8
ponA
75
63
48
35
28
C219 27Q-7
C219 27Q-10
72
55
43
34
26

Figure 19.Establishment of difference length AT-3 inducible expression in PC12.

(A) Schematic representation of functional domains on full length and three truncated human AT3, which were subcloned into the pEGSH vector. Blue: the Josephin domain; yellow: the poly-ubiquitin binding domain; brown: the ubiquitin interactive motif (UIM); pink: the polyQ domain. Our constructs contain normal 27Q and mutant expansion 75Q for each length of AT3, respectively. **(B)** Digestion map of truncated AT3 constructs.pEGSH plasmids containing difference length AT3 constructs were double-digested with *Bam*HI and *Xba*I. **(C)** Analysis of the truncate AT3 protein expression in the SCA3 cell lines by western blot. We used Ataxin-3 antibody to detect the AT3 expression in the SCA3 cells after ponA induction. The truncate AT3 protein was expressed after ponA induction (arrow).